Anthropogenic impacts on high-latitude ecosystems: Shrubs will grow. Will nitrogen flow?

A DISSERTATION
SUBMITTED TO THE FACULTY OF
UNIVERSITY OF MINNESOTA
BY

Daniel E. Ackerman

IN PARTIAL FULFILLMENT OF THE REQUIREMENTS
FOR THE DEGREE OF
DOCTOR OF PHILOSOPHY

College of Biological Sciences

Dr. Jacques Finlay, Adviser
Dr. Daniel Griffin, Co-Adviser

May 2019

Acknowledgements

This dissertation is not an individual accomplishment. I am grateful to many people, both within the University of Minnesota and beyond, who have supported me throughout my PhD program.

I thank my co-advisers, Jacques Finlay and Dan Griffin, for indulging my wildly disparate interests in high-latitude ecology and for pushing me to develop as a scientist, writer, presenter, and person. Jacques' passion for and deep knowledge of biogeogemical cycling, from the arctic tundra to his St. Paul backyard, were both instructional and inspirational. Dan taught me how to read climate history in a tree trunk, and kept me from going crazy and cross-eyed in the midst of measuring 19,624 microscopic shrub rings.

I also thank my committee members, Sarah Hobbie and Jim Cotner, for providing invaluable feedback on my scientific thinking and writing. The rest of the EEB department, especially the 2014 cohort and the members of the Finlay lab, have helped me grow both intellectually and socially during my time here. I will miss playing in the weekly EEB pick-up basketball game.

Many brilliant and kind scientists outside the EEB department also served as informal mentors. Their wisdom improved the quality of my work and often enabled projects I was not equipped to complete on my own. In particular, I thank Gus Shaver, Ken Tape, Heidi Golden, Ben Jones, Breck Bowden, Laura Gough, Isla Myers-Smith, Scott St. George, Ingibjörg Svala Jónsdóttir, Dylan Millet, and Xin Chen.

I have many institutions to thank for vital funding and logistical support for my research: National Science Foundation, Bell Museum of Natural History, Explorers Club,

UMN EEB Department, Marine Biological Laboratory, Toolik Field Station, US Geological Survey, and the Long Term Ecological Research network.

In the past five years, a number of housemates have put up with my (often strange) schedule, respected my need for quiet when I was cramming to meet a deadline, and supported me through times of stress. These wonderful beings include Karl Snyder, Justin Carlson, Robert Hest, Emily Houser, and Wizard the cat.

My parents, Jerry Ackerman and Beth Goldbaum, provided me guidance, support, and love, long before I knew what an ecologist was. Thank you for encouraging me to find and follow my passion. My earliest explorations of nature happened under the wing of my big sister, Rachel Ackerman Morrow, among the trees and dirt of our family's backyard, which seemed a vast wilderness to small children. Now from the verdant mountains of Kauai, she continues to inspire me to enjoy nature every day.

My wife, Sarah Nalven, has provided more love and support than I could ever express here. Thank you.

Table of contents

List of Tables

List of Figures

Introduction

Human activity is a dominant force shaping the structure and function of Earth's ecosystems. Some of these impacts are direct and local: phosphorus-rich runoff from urban landscapes causes excessive siltation, eutrophication, and biodiversity reduction in waterways (Carpenter *et al*. 1998, Paul and Meyer 2001). Other impacts are indirect and regional: ozone precursors released from vehicles in cities can travel downwind and form ozone harmful to plants, animals, and people (Keiser *et al*. 2018). Still other anthropogenic impacts have profound consequences worldwide, namely fossil fuel combustion and the release of carbon dioxide, a greenhouse gas, into a globally-mixed troposphere (Hayhoe *et al*. 2018).

Due to these teleconnections between human action and environmental impact, ecosystems that appear remote from direct human modification are still molded by our societal behavior. This is particularly true of northern high-latitude ecosystems, including arctic tundra and boreal forest. Cold temperatures and nitrogen limitation of terrestrial primary productivity make these biomes highly sensitive to warming and atmospheric nitrogen deposition, two widespread impacts of fossil fuel combustion (Elser *et al*. 2007, LeBauer and Treseder *et al*. 2008, Elmendorf *et al*. 2012a, Shaver *et al*. 2014).

Background on anthropogenic changes

This dissertation will examine high-latitude ecosystem responses to warming and atmospheric nitrogen deposition. The following two subsections provides background on these topics.

High latitude warming

The arctic tundra biome is warming twice as fast as the global average (Cohen *et al*. 2012). Paleoclimate proxies indicate that such polar amplification has been a reliable response to rising temperatures for at least the last three million years of Earth's climate history (Miller *et al*. 2010). This phenomenon is largely caused by the ice-albedo feedback, but other contributing factors include changes in oceanic and atmospheric heat transfer, increased near-surface cloud cover and atmospheric water vapor, and soot deposition (Serreze and Barry, 2011).

A rapidly warming arctic is a source of considerable uncertainty in climate projections due to poorly constrained biophysical carbon cycle feedbacks. Soils of high-latitude permafrost regions contain nearly 1,700 Pg of organic carbon, equivalent to roughly double the global atmospheric carbon pool (Tarnocai *et al*. 2009). As permafrost thaws, much of the permafrost organic carbon pool will be metabolized by microbes into atmospheric methane (in wet environments) or carbon dioxide (in dry environments). The magnitude and rate of change in land-to-atmosphere carbon fluxes from permafrost remains a topic of vigorous debate—"Methane bomb" media headlines may be too sensationalized (Petrenko *et al*. 2017), but a gradual and sustained carbon release (Schuur *et al*. 2015) may be too optimistic.

In addition to permafrost carbon feedbacks, high-latitude vegetation changes could trigger both positive and negative feedbacks to climate change. For example, the expansion of woody deciduous shrubs in circumarctic tundra could accelerate climate change through positive feedback mechanisms including albedo reduction, competitive exclusion of permafrost-insulating *Sphagnum spp*., and the capture of deep snowpacks that increase microbial respiration through elevated winter soil temperatures (Sturm *et al*.

2001, Cornelissen *et al.* 2001, Blok *et al*. 2011a, Chapin *et al.* 2005, Lawrence and Swenson 2011). Alternatively, shrub expansion could mitigate climate change through negative feedback mechanisms including increased primary productivity, woody stem production, recalcitrant litter chemistry, and shading of carbon-rich permafrost soils in summer (Shaver 1986, Sweet *et al.* 2015, Cornelissen *et al*. 2007, Blok *et al*. 2011a, Nauta *et al*. 2015). While the balance of such positive and negative feedbacks remains an area of active research, integrating these feedbacks into earth systems models will ultimately require accurate predictions of shrub expansion rates across space. In other words, shrub expansion has not and will not proceed at a uniform pace throughout the tundra. Chapters 1 and 2 of this dissertation seek to determine which factors underlie the variable rates of shrub expansion across environmental gradients in arctic tundra.

Nitrogen deposition

Humans have doubled the amount of bio-reactive nitrogen entering the biosphere in the industrial era through fertilization, biomass and fossil fuel combustion, and volatilization from agricultural materials such as manure (Galloway *et al*. 2004, Galloway *et al.* 2008). Despite major improvements in agricultural production, the rapid increase in nitrogen availability has wide-ranging consequences for human health, ecosystem function, and community structure. For example, nitrate-loading in groundwater aquifers in highly fertilized agricultural regions is linked to methemoglobinemia (blue-baby syndrome) and is believed to be a risk factor for certain cancers and birth defects (Spalding and Exner 1993, Weyer *et al*. 2008, Brender *et al.* 2013). In nitrogen-limited terrestrial ecosystems, increased availability boosts primary productivity, often causing community shifts toward dominance by species with low nitrogen-use efficiencies (Stevens *et al*. 2004, Clark and

Tilman 2008). Elevated delivery of nitrogen to nitrogen-limited (or nitrogen and phosphorus co-limited) freshwater and marine ecosystems can fuel algae blooms that harm plants and animals through light attenuation and oxygen depletion (Howarth and Marino 2006, Conley *et al*. 2009, Finlay *et al.* 2013). There is an urgent need to assess the capability of global ecosystems to buffer this nitrogen cycle intensification through nitrogen uptake by organisms and denitrification.

Understanding ecosystem response to elevated nitrogen deposition is particularly crucial at high latitudes, where nitrogen limitation is widespread across the boreal forest and arctic tundra biomes (Elser *et al*. 2007, LeBauer and Treseder *et al*. 2008, Shaver *et al*. 2014). Primary productivity and community composition in these systems is highly sensitive to changes in nitrogen availability (Wookey *et al*. 1994, Chapin and Shaver 1996, Van Wijk *et al*. 2004, Hobbie *et al.* 2005). Therefore, future changes in atmospheric nitrogen deposition, which tend to be regional in scale, could restructure ecosystem function and community composition in some areas.

Strategies for studying ecosystem response to anthropogenic changes

The following two subsections review methods used to research ecosystem impacts of warming and elevated nitrogen availability. The four chapters of this dissertation will both incorporate and build upon some of these methods.

Shrub expansion

Researchers have employed a variety of experimental and observational techniques to determine environmental drivers of shrub expansion in arctic tundra. Early factorial experiments crossing nutrient addition, warming, and insolation reduction suggested that nitrogen availability was the limiting factor to primary productivity in arctic tundra

(Wookey *et al*. 1994, Chapin and Shaver 1996). This limitation was believed to be caused by low mineralization rates, despite large pools of soil organic nitrogen (Shaver and Jonasson 1999). Nitrogen addition appeared to lend a competitive advantage to species with low nitrogen-use efficiencies, such as deciduous shrubs (Bret-Harte *et al*. 2001). Subsequent experiments throughout the arctic tundra have further supported this idea (DeMarco *et al*. 2014). Additional evidence for tundra shrub expansion has been provided through observational techniques including repeat photography and remote sensing (Tape *et al*. 2006, Myers-Smith *et al*. 2011).

Dendrochronology, the study of annual growth of woody plants, is becoming an increasingly popular observational approach for studying shrub response to climate (Myers-Smith *et al*. 2015a). This technique can provide a centennial-scale growth record, longer than any experimental manipulation or remote sensing measure in the arctic (Weijers *et al*. 2010). Further, the chronology of annual ring widths or other anatomical measurements is a vast improvement in temporal resolution over previously used methods such as repeat photography (Tape *et al.* 2006). Dendrochronological studies have revealed historic relationships between climate and shrub growth in a wide range of shrub growth forms, from prostrate evergreen species, e.g. *Cassiope tetragona*, to erect deciduous species, e.g. *Alnus viridis*, *Salix pulchra*, and *Betula nana* (Weijers *et al.* 2010, Blok *et al.* 2011a, Tape *et al*. 2012).

While dendrochronology appears to be a promising method, challenges remain in connecting climate and environmental variability to individual plant response. The traditional way to analyze arctic shrub dendrochronology data is to construct a site-based, annually-resolved chronology of the central tendency of growth (usually a mean or

median of individually detrended ring-width indices) for the sample site (Cook and Pederson 2011). This approach yields a uniform growth signal shared among shrubs at a site, but it discards information related to the variability in climate response among individuals (Galván *et al*. 2014, Young *et al*. 2016). An overarching goal of chapters 1 and 2 of this dissertation is to compare microsites and use individual-based statistical modeling frameworks to examine variability in the climate-growth relationship among individual shrubs on the North Slope of Alaska.

Nitrogen cycling

Long-term measurements of atmospheric nitrogen deposition are available for some high latitude sites, but deposition estimates remain poorly constrained for many regions of the vast arctic tundra and boreal forest biomes (Vet *et al*. 2014). Spatial models of nitrogen deposition tend to have low, centennial-scale temporal resolution (Galloway *et al*. 2004). Such models are insufficient for understanding nitrogen dynamics on shorter timescales, because interannual nitrogen deposition in remote areas of the arctic can vary widely based on stochastic weather and atmospheric transport events (Choudhary *et al*. 2016). This uncertainty complicates the construction of nitrogen budgets for high-latitude watersheds. Chapter 3 attempts to resolve this uncertainty by creating a spatially explicit model of global nitrogen deposition with annual- to decadal-scale temporal resolution.

Little is known about the drivers of variability in nitrogen retention among watersheds at a circumpolar scale. Studies on nitrogen retention rates often focus on individual water bodies, rather than whole watersheds (Kankaala *et al*. 2002). Those that do examine whole watershed-scale retention at large spatial scales are limited to lower latitudes (Schaefer and Alber 2007, Howarth *et al*. 2012). An improved accounting of

environmental controls on nitrogen retention across boreal forest and arctic tundra watersheds, the aim of chapter 4, will shed light on the fate of atmospheric nitrogen inputs to high latitude systems—how much is retained in inland systems, and how much is exported, potentially fueling algal blooms in downstream systems?

Outline of the remaining chapters of this dissertation

In chapter 1 I use dendrochronology to examine how hillslope position (dry upland versus moist riparian site) influences shrub climate response of the deciduous shrub *Salix pulchra* on the North Slope of Alaska. I build upon prior research in this field in two ways. First, I allow my calculated climate-growth relationship to vary based on second-order coefficients, as is predicted by ecological theory on diminishing returns to increases in a single growth-limiting factor. Second, I use my dendrochronology data on retrospective growth in combination with established shrub allometry models to predict changes in shrub aboveground primary production under a 2-degree celcius warming scenario. I find that both upland and riparian shrubs respond positively to June temperature, but marginal growth response to temperature is diminishing at the dry upland site, possibly indicative of temperature-induced moisture limitation in particularly warm years. Further, I find that 2 degrees of warming will increase shrub biomass by about 36% at the riparian site, but only by about 19% at the upland site, emphasizing the importance of microsite variability in understanding ecosystem response to climate.

In chapter 2 I construct an individual-based linear mixed effects model that incorporates *Salix pulchra* dendrochronology data from sites across the North Slope that vary not only in hillslope position, but also in glacial landscape age (a proxy for soil nutrient availability). I find that ring growth is remarkably coherent among individuals

and sites, responding strongly to June temperature. The strength of this climate response is not systematically related to glacial landscape age. This result indicates a regionally-coherent shrub growth response to early season temperature, with local soil properties exerting only a minor influence on the climate-growth relationship.

In chapter 3 I use a global Chemical Transport Model to estimate historic rates of atmospheric nitrogen deposition in the late 20th and early 21st century. From 1984 to 2016, I find that global inorganic nitrogen deposition increased by 8%, but trends varied regionally. For example, deposition declined in the European boreal and sub-arctic zones, while deposition increased in Western Canada and Eastern Siberia. Quantifying these spatially-explicit trajectories of change at high latitudes can help us predict how recent and future trends in nitrogen deposition impact ecosystem processes like primary productivity, species turnover, and nitrogen retention.

In chapter 4 I use the model results from the preceding chapter to conduct a systematized review of the environmental factors influencing nitrogen retention in watersheds throughout the circumpolar north. I find that mean annual air temperature is positively related to the proportion of atmospherically deposited nitrogen retained. Other variables including watershed area, annual runoff, and watershed soil properties did not have an apparent effect on retention rates. This outcome suggests that future warming could raise the proportion of nitrogen retained in boreal and tundra watersheds, favoring plant species with low nitrogen-use efficiencies while reducing nitrogen export. However, this effect may be reversed by rapid permafrost thaw, which could mobilize and export large stores of soil nitrogen.

Chapter 1

Arctic shrub growth trajectories differ across soil moisture levels

Summary

The circumpolar expansion of woody deciduous shrubs in arctic tundra alters key ecosystem properties including carbon balance and hydrology. However, landscape-scale patterns and drivers of shrub expansion remain poorly understood, inhibiting accurate incorporation of shrub effects into climate models. Here, we use dendroecology to elucidate the role of soil moisture in modifying the relationship between climate and growth for a dominant deciduous shrub, *Salix pulchra*, on the North Slope of Alaska, USA. We improve upon previous modeling approaches by using ecological theory to guide model selection for the relationship between climate and shrub growth. Finally, we present novel dendroecology-based estimates of shrub biomass change under a future climate regime, made possible by recently developed shrub allometry models. We find that *S. pulchra* growth has responded positively to mean June temperature over the past 2.5 decades at both a dry upland tundra site and an adjacent mesic riparian site. For the upland site, including a negative second-order term in the climate-growth model significantly improved explanatory power, matching theoretical predictions of diminishing growth returns to increasing temperature. A first-order linear model fit best at the riparian site, indicating consistent growth increases in response to sustained warming, possibly due to a lack of temperature-induced moisture limitation in mesic habitats. These contrasting results indicate that *S. pulchra* in mesic habitats may respond positively to a wider range of temperature increase than *S. pulchra* in dry habitats. Lastly, we estimate that a 2°C increase in current mean June temperature will yield a 19% increase in aboveground *S. pulchra* biomass at the upland site and a 36% increase at the

riparian site. Our method of biomass estimation provides an important link toward incorporating dendroecology data into coupled vegetation and climate models.

Background

Rapid warming at high latitudes is linked to expansion and accelerated growth of woody shrubs in arctic tundra, yielding feedbacks to global climate (Tape *et al*., 2006; Myers-Smith *et al*. 2011, Elmendorf *et al*., 2012b). Such feedbacks, occurring through litter chemistry, snow-shrub interactions, land surface reflectance, and shading of carbon-rich permafrost soils, have been intensively studied through plot-level experimentation (Hobbie 1996, Sturm *et al*., 2001; Schimel *et al*., 2004; Chapin *et al*., 2005; Blok *et al*., 2010; Nauta *et al*., 2015, Gough *et al*., 2016). However, a relative scarcity of landscape-scale investigation has made it difficult to connect plot-level experimentation to regional greening trends (Hobbie & Kling 2014). Landscape factors like topography, disturbance, and biotic interactions may modulate rates of shrub expansion (Schuur *et al*., 2007; Olofsson *et al.*, 2009; Christie *et al*., 2015; Ropars *et al*., 2015; Ackerman & Breen, 2016). A poor understanding of the heterogeneity of shrub expansion across arctic landscapes inhibits accurate incorporation of shrub feedbacks into mechanistic climate models such as dynamic global vegetation models (e.g. Sitch *et al*., 2003). Therefore, an improved understanding of the interaction between edaphic factors and climate in determining rates of shrub expansion is urgently needed.

By creating long-term, annually-resolved growth records, dendroecology has proven useful in understanding how shrubs respond to interannual variability in climate (Rayback & Henry, 2005; Bär *et al*., 2006; Forbes *et al*., 2010; Weijers *et al.*, 2010;

Buchwal *et al.*, 2013; Hollesen *et al*., 2015; Young *et al*., 2016). For erect deciduous shrubs in the rapidly expanding genera *Salix*, *Betula*, and *Alnus* (respectively willow, birch, and alder), secondary growth quantified by annual ring width in stem cross sections can provide an uninterrupted record of over a century of shrub growth that may be correlated with climate variables (Blok *et al.*, 2011; Tape *et al*., 2012; Jørgensen *et al.*, 2015).

A recent meta-analysis of arctic shrub dendroecology research hypothesizes that soil moisture is a key variable in determining climate sensitivity of arctic shrub growth (hereafter the Soil Moisture Hypothesis; Myers-Smith *et al*., 2015a). The Soil Moisture Hypothesis states that climate sensitivity of shrubs, defined as the magnitude of the slope (i.e. first-order coefficient) relating growth and summer temperature, is positively correlated with moisture (Myers-Smith *et al*., 2015a). However, the studies included in this meta-analysis were largely single-site investigations not designed to test for heterogeneity of shrub response to climate across levels of soil moisture. As of yet, there is no landscape-scale empirical test of the Soil Moisture Hypothesis.

Previous arctic shrub dendroecology work has assumed a first-order linear relationship between shrub growth and the controlling climate variable(s) of interest. This assumption of first-order linearity across the domain of observed temperatures does not consider a large body of ecological work on co-limitation theory and plant physiology, which predicts a decelerating relationship: marginal growth should diminish with increases in temperature or any other limiting factor (Bloom *et al*., 1985; Gleeson & Tilman, 1992). At the extreme, high temperatures or excessive nutrient concentrations of course may harm growth.

The functional form of the climate-growth relationship, first-order linear or decelerating, has major implications for ecosystem response to climate change. For example, if we find a decelerating relationship, it follows that a modest temperature increase may have highly variable effects on shrub growth, depending on the exact location of initial temperature along the climate axis (Figure 1.1). Using ecological theory to inform model selection in dendroecology is necessary to generate robust predictions of shrub response to future climate (Fritts, 1976).

Prior shrub dendroecology work has also been limited in its scope of inference to growth indices such as ring width index or stem elongation, which are of lesser utility that biomass estimates for climate and carbon cycle models. A poor understanding of shrub architecture and growth form variability has prevented dendroecology studies from making direct inference about biomass change. However, recent advances in arctic shrub allometry (Berner *et al*., 2015) have opened the door for using growth ring data to predict how total shrub biomass in a given landscape may respond to a change in climate.

In this study, we combine empirical data collection with ecological theory and modeling to fill the aforementioned knowledge gaps through three research questions:

(1) Is there empirical support for the Soil Moisture Hypothesis in a landscape-scale analysis of climate response in a dominant shrub at two levels of soil moisture on the North Slope of Alaska?

(2) What is the functional form of the climate-growth relationship at these sites?

(3) How will shrub biomass respond to future warming at these sites?

Methods

Site description and chronology development

In July 2015 we sampled *Salix pulchra* (Cham.) stems at two sites, riparian and upland, separated by 100 m adjacent to the Upper Kuparuk River (68.67°N, -149.44°W), a 4th order stream fed by surface runoff on the North Slope of Alaska, USA. The sites receive 312 mm of precipitation annually, with 60% falling during the summer months (Cherry *et al*., 2014). Mean annual air temperature is -8.5°C, with temperatures averaging above freezing for June, July, and August (Cherry *et al*., 2014).

These low-arctic sites fall within subzone E of the Circumpolar Arctic vegetation map (Walker *et al.*, 2005). We selected the erect deciduous shrub *S. pulchra* for our study because it is frequently the canopy dominant plant in shrub tundra, including both riparian and upland areas. We delimited the riparian site as the vegetated area within the bankfull width of the Kuparuk River, generally 3-10 meters from the edge of the river during summer baseflow conditions (Slavik *et al*., 2004). The riparian site had greater soil moisture, thaw depth, and average shrub size and growth rate than the upland site (Table 1.1). Riparian vegetation was dominated by woody shrubs (*Salix spp.* and *Betula nana*) with a sparse understory including *Sphagnum spp*., while the upland site had vegetation typical of moist-acidic tundra in the region (Gough *et al.*, 2000), including woody shrubs (*Salix spp.* and *Betula nana*), *Eriophorum vaginatum, and Sphagnum spp.*

To ensure our resulting chronologies were representative of the 140 km^2 Upper Kuparuk watershed, we used transect-based sampling covering a larger area and a greater number of individuals than is typical for shrub dendroecology studies (Blok *et al*., 2011; Buchwal *et al.*, 2013; Holleson *et al.*, 2015; Young *et al.*, 2016). Specimens were cut every 10 meters along the transects to avoid stem size bias and resampling of genetically identical clones. We collected specimens from 27 riparian and 35 upland individuals by

cutting the stem at the root collar. Serially sectioned disks (Myers-Smith *et al*. 2015b) were subsampled from the root collar and 10 centimeters further up the stem. Thin sections were cut to 15 μm with a microtome and stained with a safranin and astra-blue mixture to enhance optical contrast, following Gärtner *et al*. (2015). Ring widths along two radii per disk were measured using CooRecorder (Larsson, 2013). Calendar year dating of the microscopic growth increments was determined through the classical method of crossdating, with pairwise comparison of ring width time series within and between shrubs (Stokes & Smiley, 1968). The four radii measured per individual were averaged to obtain a single series of annual growth per individual. In total, 7,228 (3304 riparian, 3924 upland) annual growth increments along 248 radii (108 riparian, 140 upland) from 62 individuals (27 riparian, 35 upland) were measured for this study.

Growth increment time series were standardized with methods typical to dendroecology (Cook & Kairiukstis, 1990) using the program ARSTAN (Cook, 1985). Time series were detrended to remove age-related trends, consistent across shrubs at both sites, of rapidly declining ring width in the first 5-10 years of stem growth. We selected a flexible 20-year cubic smoothing spline for detrending (Cook & Peters, 1981), which is equivalent to 2/3 of the mean length of our ring width time series, though we additionally attempted a less flexible negative exponential function to minimize the impact of the chosen detrending function on our results. Ring width indices were calculated as the ratio of the measurement value to the detrending curve fitted value for each year, yielding a dimensionless ring width index (RWI) with a mean of one, so that individuals could be integrated into a site-level chronology (Larsson, 2013). Low order autocorrelation was assessed and removed if determined to be statistically significant (Cook, 1985). Site level

chronologies were calculated as the median RWI value for each year. Chronology statistics including mean interseries correlation (rbar), expressed population signal (EPS), mean sensitivity, and mean first-order autocorrelation, were calculated in ARSTAN to validate our mean chronology estimates (Cook, 1985; Briffa & Jones, 1990).

Climate sensitivity comparison

We calculated correlation coefficients between RWI and monthly mean temperature and total precipitation, including both current- and previous-year temperature and precipitation, using *treeclim* (Zang & Biodi, 2015). Correlations were deemed statistically significant for a site if they achieved alpha = 0.05 across both detrending strategies. Slopes of significant relationships produced by *treeclim* were compared between the upland and riparian sites. To improve temporal precision of the climate signal being expressed by the shrubs, we conducted a moving-window analysis (*sensu* Fonti *et al.*, 2006) during a three month interval centered on the month found to be significant from the *treeclim* analysis. Variable window sizes of 5, 10, 20, 30, and 40 days were tested. Climate data for the site has been continuously collected at Toolik Field Station since 1989 (Environmental Data Center Team, 2016).

Climate-growth model

Using the significant monthly relationships indicated by the climate sensitivity analysis above, we used multiple linear regression to test for negative second-order (i.e. decelerating) relationships between climate and shrub growth. We used model explanatory power, quantified by adjusted R^2, as the basis of comparison between our decelerating models and the first-order models typically used in dendroecology analysis. A likelihood ratio test was conducted to determine whether the decelerating model

provided a better goodness-of-fit at the alpha = 0.05 level. If the decelerating model was preferred at a given site, we compared this model with a sigmoidal model to test for asymptotic behavior. We used model difference in Akaike information criterion (ΔAIC) of 2 as a cutoff for selecting the sigmoidal model over the decelerating model. Finally, we used individual-based hierarchical mixed model analysis to confirm that the detected deceleration was consistent across all (or most) shrubs at the site by preserving individual-level variability and maximizing temporal replication (Pinheiro *et al*., 2014; Myers-Smith *et al*., 2015a; Young *et al.*, 2016). Year and individual shrub were treated as random effects in individual-based the model.

Biomass simulation

We estimated aboveground *S. pulchra* biomass at our sites for both the current temperature regime and a +2°C warming scenario using output from our climate-growth model and shrub allometry equations. From our climate-growth model, we determined the percent increase in basal diameter expected for a 2°C increase in mean temperature. We then constructed normal distributions for stem basal diameter and stem density using the means and standard deviations of these variables from our on-site measurements. Variable estimates were randomly selected from these distributions 1,000 times and used in the allometric equation modified from Berner *et al*. (2015; Equation 1) to estimate total aboveground biomass per square meter. This simulation was repeated three times using low, medium, and high parameter estimates (Berner *et al*., 2015).

Results

Chronology development

RWI chronologies for both sites (Figure 1.2) showed high inter-series correlations and EPS ≥ 0.85 for the 1989-2014 period in common between the chronologies and the local climate data (Table 1.2). Neither site showed significant low-order autocorrelation.

Climate sensitivity comparison

Climate sensitivity (slope of the relationship between RWI and its strongest climate correlate, mean June temperature) was not significantly different between sites (Figure 1.3), but climate sensitivity was more robust to detrending strategy at the upland site than at the riparian site. Analysis with *treeclim* revealed significant climate sensitivity at the upland site, with current year mean June temperature controlling RWI (slope estimate = 0.49, $p<.05$). This result remained significant across both detrending strategies (see Supplemental Material Tables S1.1-S1.4 for full *treeclim* output). For the riparian site, June temperature was a significant predictor of RWI for the 20-year cubic spline chronology (slope estimate = 0.28, $p<.05$), but this result was not significant for the less flexibly detrended chronology (Table 1.3). Neither monthly, nor seasonal, nor annual precipitation significantly predicted RWI at either site.

Our moving window analysis (Figure 1.4) confirmed that June is the key period for *S. pulchra* growth at the upland site, as effect size of mean temperature peaked for 30- and 40-day windows centered in mid-June (day of year = 166). Effect sizes for the riparian site peaked in late June (day of year = 179).

Climate-growth model

Regression tests for the upland site (Figure 1.5a, top) revealed a decelerating relationship between RWI and current-year mean June temperature. This decelerating model, employing a negative second-order temperature term as predicted by ecological theory,

showed greater explanatory power (adjusted R^2=0.45, p<.001) than the first-order relationship (adjusted R^2=0.33, p =0.001) typically used in dendroecology models. The likelihood ratio test revealed that the decelerating model was preferred at the upland site (p = 0.02). The sigmoidal model did not meet our ΔAIC cutoff (ΔAIC = 1.06), so we proceeded with the decelerating model for the remainder of our analysis. Results from the individual-based hierarchical mixed model were consistent with the decelerating trend, estimating a significant negative coefficient for the second-order temperature term (p = 0.03, see Supplemental Material Tables S1.5 and S1.6 for model output and Figure S1.1 for individual curve fits).

For the riparian site (Figure 1.5a, bottom), the second-order model (adjusted R^2=0.27, p=0.01) performed similarly to the first-order model (adjusted R^2=0.30, p=0.002). Including a negative second-order temperature term did not improve explanatory power at the riparian site, and the likelihood ratio test revealed that the two models were equivalent (p = 0.75). Slopes of the first-order regression models for the two sites were not significantly different (0.085 ± 0.024 standard error of the mean for upland, and 0.104 ± 0.031 for riparian).

The second-order relationship between June temperature and upland RWI predicted that a 2°C increase in temperature, from the present-day June mean of 8.77°C to 10.77°C, would increase RWI from 1.029 to 1.111, representing an 8% increase in basal diameter growth. The first-order relationship for the riparian site predicted than an identical temperature increase would yield a RWI increase from 0.981 to 1.190, a 21% increase in basal diameter growth.

Biomass simulation

Our simulations predicted that the 8% growth increase at the upland site in response to 2°C of warming would yield a mean aboveground biomass increase of 19%, from 939 to 1121 grams dry weight per m^2, using mean parameter estimates from Berner *et al*. (2015). At the riparian site, a 21% growth increase would yield a 36% biomass increase, from 5,455 to 8,502 grams dry weight per m^2. Within each site, the use of low and high parameter estimates yielded similar percent increases in biomass (Figure 1.6).

Discussion

Climate sensitivity comparison and climate-growth relationship

Contrary to our expectation outlined in the Soil Moisture Hypothesis, the mesic riparian site did not show greater climate sensitivity as defined by the slope of the relationship between RWI and mean June temperature. Slopes were nearly identical for the riparian and upland sites (Figure 1.3). While the moving window analysis confirmed June as the key period for shrub growth, the overall June climate signal may result from a "smearing" of two shorter term peaks in effect size, especially apparent for 5- and 10-day windows at the upland site (Figure 1.4). These peaks, centered on the final days of May and the second half of June, respectively align with bud break and leaf out for *S. pulchra* in this region (Sweet *et al*., 2014).

Our finding of similar first-order slope coefficients for the two sites does not imply that soil moisture plays no role in modulating shrub response to temperature. Rather, our use of ecologically-based models to explore the functional form of the climate-growth relationship suggests that soil moisture may become increasingly important in determining whether shrubs will take advantage of sustained increases in June temperature (Figure 1.7). Upland *S. pulchra* growth was explained better by a

decelerating model, incorporating a negative second-order term for mean June temperature, than by the first-order model. In contrast, a first-order linear model fit best at the riparian site. A potential explanation for these distinct results is that riparian shrubs growing in mesic soils are not subject to temperature-induced moisture limitation that could affect shrubs growing in the drier, upland site during warm growing seasons (Wilmking *et al*. 2005; D'Arrigo *et al*., 2008; D'Arrigo *et al*., 2009; Myers-Smith *et al*., 2015a). Therefore, while modest warming may affect riparian and upland shrubs similarly, sustained warming (e.g. greater than 2°C above present mean) may have positive effects on riparian shrub growth, with negligible to negative effects on upland shrub growth. This combination of effects represents a new definition of climate sensitivity, where contrasting responses to climate may be detected by examining the functional form of climate response.

It is possible that a functional relationship besides quadratic, such as sigmoidal, may usefully describe the climate response of shrubs at sites similar to our upland *S. pulchra*. We could not distinguish here between the quadratic and sigmoidal functions using ΔAIC. Still, our comparison of the first-order linear and quadratic functions demonstrates that moving beyond estimates of first-order linearity may provide a more realistic representation of shrub growth dynamics. We believe this approach will improve predictive power of dendroecology models and produce outcomes that are more useful for climate and carbon cycle models.

Our finding that June mean temperature is the primary driver of *S. pulchra* growth is of particular importance given the disproportionately rapid warming for this month. June mean temperature has increased by .49°C per decade since 1965 ($p<.001$; NOAA

North Slope divisional climate data), faster than any other month of the growing season. At this rate, the conservative 2°C temperature increase used in our biomass simulation will be exceeded within the next 50 years (IPCC, 2013).

Biomass simulation

Our biomass simulation predicted that a 2°C increase in mean June temperature will increase *S. pulchra* biomass by 19% at our upland site and by 36% at our riparian site. These are conservative estimates that account only for accelerated individual growth, not the proliferation of new shrub stems across the landscape. However, we emphasize that factors besides soil moisture, such as topography, biotic interactions, or disturbance, may modify shrub growth trajectories (Schuur *et al*., 2007; Olofsson *et al.*, 2009; Christie *et al*., 2015; Ropars *et al*., 2015; Ackerman & Breen, 2016). As reviewed by Myers-Smith *et al*. (2011), biomass increases like those predicted here will likely have significant impacts on surface energy balance, primary productivity, and soil temperature and gas exchanges. Suitable nesting habitat for birds, as well as food quantity and quality for herbivores, may also be altered (Ehrich *et al*., 2012; Boelman *et al*., 2015; Tape *et al*., 2016). These effects will be particularly strong at the riparian site, where predicted percent increase in biomass is nearly double that of the upland site. In the context of Equation 1, this doubling may be largely attributed to greater stem basal diameter at the riparian site (Table 1.1). Increases in transpiration at the riparian site may have the potential to alter local hydrologic regimes.

Summer mean temperature commonly drives growth in arctic shrubs, often indirectly via elevated nitrogen mineralization rates (e.g. Hobbie & Chapin, 1998; Zamin & Grogan, 2012), so biomass increases similar in magnitude to those described here are

likely to be pan-Arctic. Direct estimates of shrub biomass increases on this scale may be possible using our biomass simulation method, which connects dendroecology analysis to allometric biomass equations. To accomplish this goal, we call for the coupling of allometry measurements with future dendroecology studies, as well as improved spatial coverage of such investigations. This would facilitate the inclusion of growth ring data into dynamic vegetation models and carbon cycle models.

Future directions

We have demonstrated that *S. pulchra* at a dry upland and a mesic riparian site have similar sensitivities to modest temperature increases based on first-order coefficient estimates, an unexpected outcome given the Soil Moisture Hypothesis. However, our examination of the functional form of the climate-growth relationship revealed that site-level growth responses diverged with more sustained temperature increase (e.g. >2° C increase in mean June temperature), with riparian shrubs responding positively over a wider range of temperatures. Finally, we used results of our climate-growth model coupled with allometric equations to simulate a greater percent increase in biomass at the riparian site than at the upland site, given a +2°C temperature increase.

We believe that dendroecology will continue to yield unique insight into the dynamics of arctic shrub growth by providing long-term, annually resolved growth chronologies that can be compared to climate records. The functional form analysis developed here could usefully be applied to existing chronologies of tree and shrub growth at sites with different climate histories and edaphic conditions. To maximize the applicability of such research for global dynamic vegetation modeling, we advocate the use of ecologically-based model selection in dendroecology, as well as the coupling of

growth ring studies with allometric measurements. This way, dendroecology data collected across landscape gradients of circumpolar north may be the key to accurately incorporating shrub expansion into predictions of future shifts in climate and wildlife habitat structure.

Acknowledgements

We thank the Arctic LTER for logistics support and valuable guidance for this project. Climate datasets were provided by the Toolik Field Station Environmental Data Center; this material is based upon work supported by the National Science Foundation (NSF) under grants #455541 and #1048361. Financial support was generously provided by the Dayton Fund from the Bell Museum of Natural History, Explorers Club, NSF Graduate Research Fellowships Program (grant #00039202), and the University of Minnesota Department of Ecology, Evolution, and Behavior. Kelly Popham, Erin Jones, Melissa Markay, and Lucas Veitch helped process shrub samples. We thank Dr. Isla Myers-Smith, Sandra Angers-Blondin, and an anonymous reviewer for insightful feedback on this manuscript.

Equation 1. Aboveground biomass (AGB, grams of dry weight m^{-2}) estimation adapted from Berner *et al.* (2015), where: SD = stem density (stems m^{-2}); BD = stem basal diameter (cm); PI = % increase in growth based on the climate-growth model (PI=0 for present-day temperature regime); *a* and *b* are fitted parameters.

$$AGB = SD(a(BD(1 + PI))^b)$$

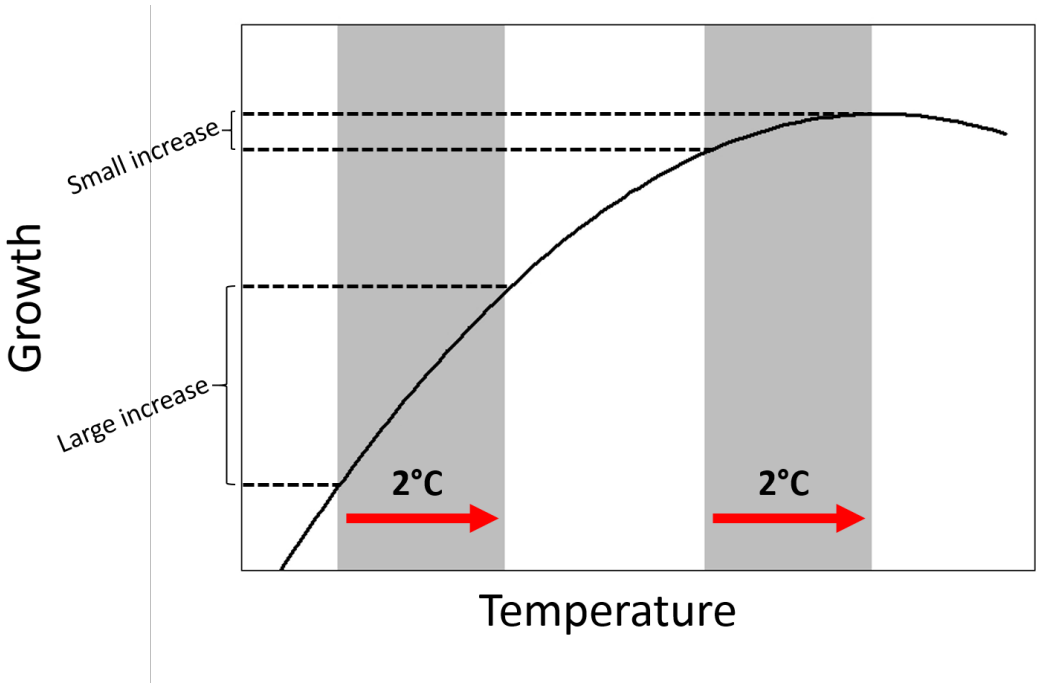

Figure 1.1 Diminishing growth returns to increasing temperature. A 2°C increase in temperature may have highly variable effects on plant growth, depending on the location of current mean temperature along the x-axis.

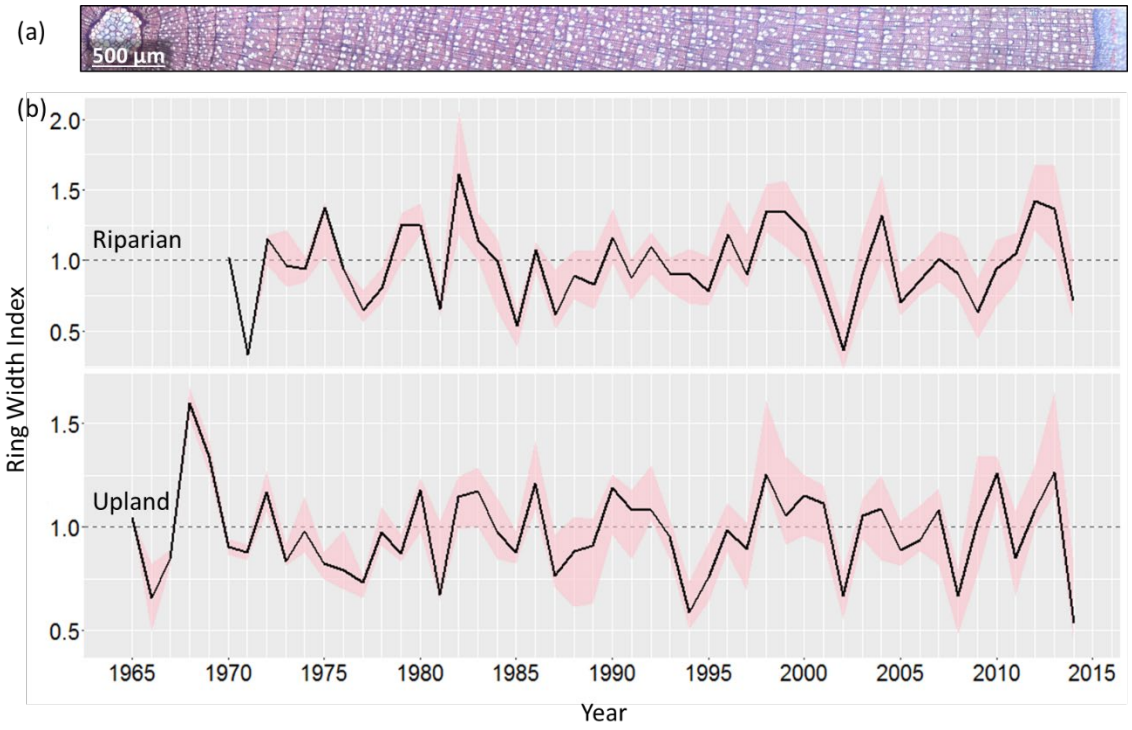

Figure 1.2 (a) Example of *S. pulchra* radius, with growth increments from 1964 to 2014. (b) Ring width index chronologies for riparian (top) and upland (bottom) sites. Median chronology is shown in black, and the interval bounding the 25-75 percentile is shown by the red band.

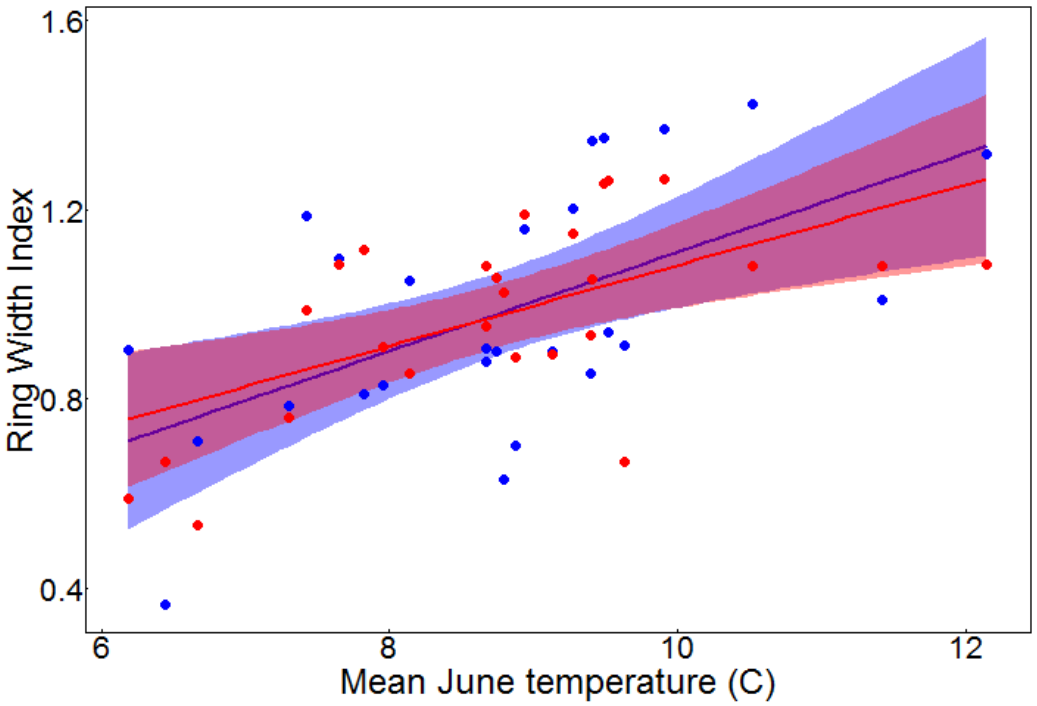

Figure 1.3 First-order linear relationship between ring width index and mean June temperature does not differ significantly between the upland (red) and riparian (blue) site. Mean RWI estimates are bounded by 95% confidence intervals.

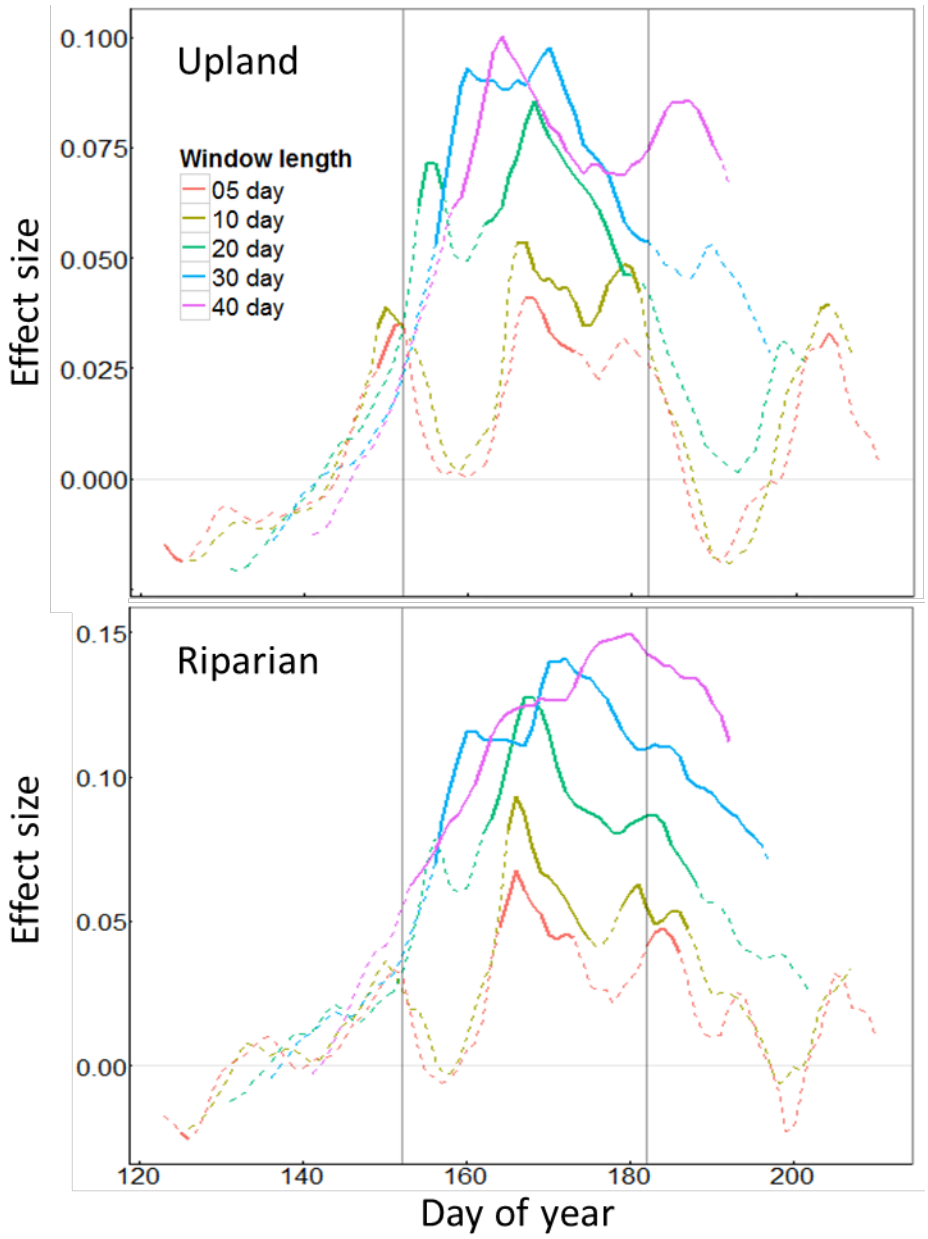

Figure 1.4. Moving window analysis for upland (top) and riparian (bottom) sites. Effect sizes are defined as the coefficient relating RWI to mean temperature for variable-length time windows (represented by line color) centered on each day of year (x-axis) between May 1 and July 31. Solid line portions represent significant effect sizes at the alpha = 0.05 level, while dashed line portions are not significant.

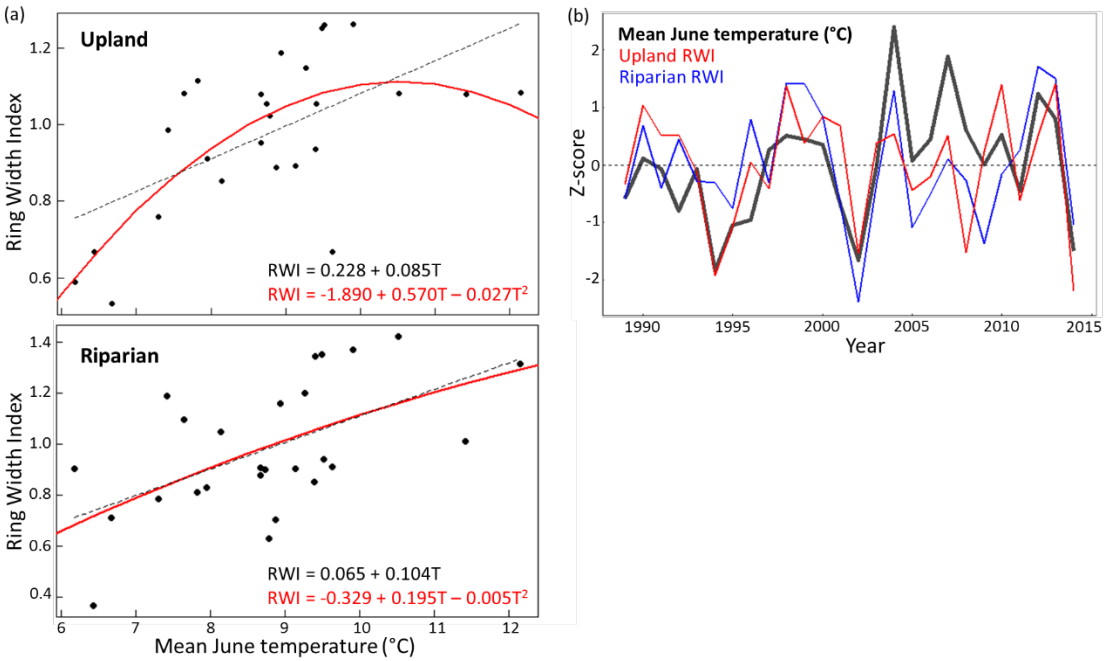

Figure 1.5 (a) Scatterplots relating ring width index (RWI) to mean June temperature (T) for upland (top) and riparian (bottom) sites. First-order linear and quadratic fits are shown respectively by the black dashed and solid red lines. Quadratic model best explains variation in upland RWI, while models perform similarly for the riparian site. (b) Time series of scaled RWI for upland (red) and riparian (blue) cohere with mean June temperature (black).

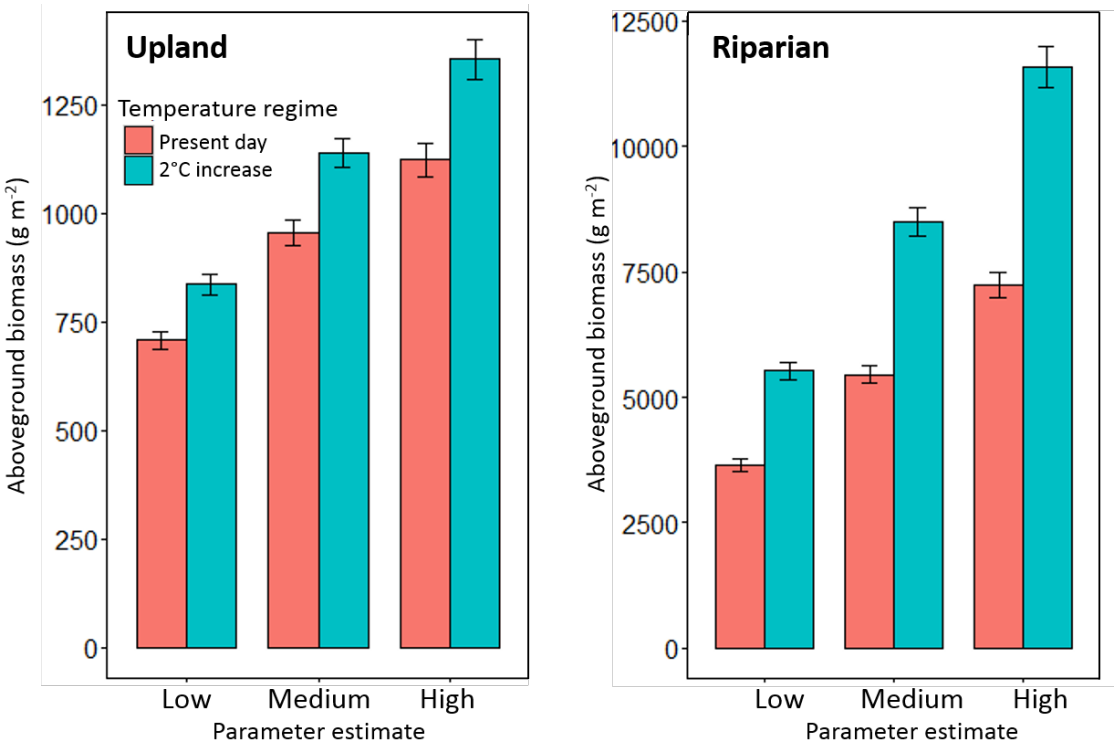

Figure 1.6 Aboveground *S. pulchra* biomass for present-day temperature regime and +2°C increase in mean June temperature at upland and riparian sites. Three bar groups represent variable parameter estimates from allometric equations provided by Berner *et al*. (2015).

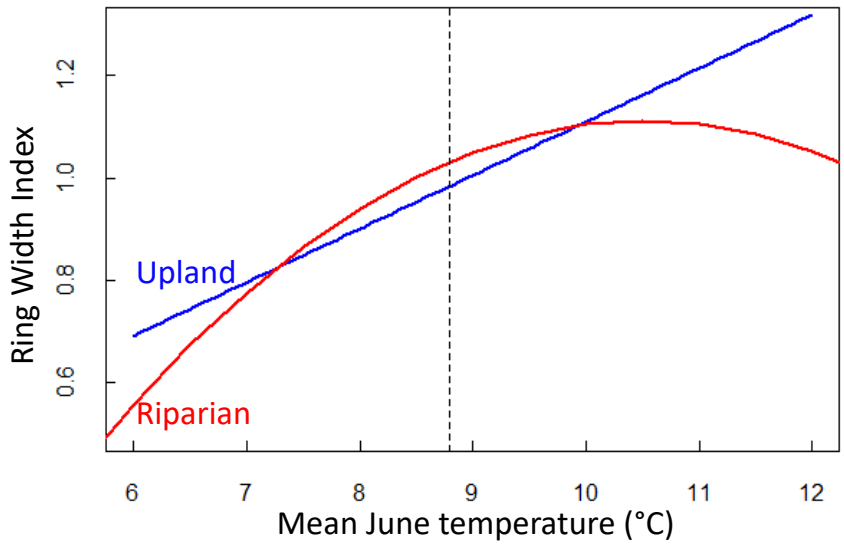

Figure 1.7 Overlay of best-fit models relating ring width index to mean June temperature for upland (red) and riparian (blue) sites over the domain of observed temperatures during the last 2.5 decades. Growth responses for the two sites are similar for present-day mean June temperature (8.8°C, vertical dashed line), but responses are likely to diverge as temperature increases beyond +2°C.

Table 1.1. Site characteristics (standard error of mean). Asterisks in Significance column indicate difference between sites at an alpha = 0.05 level in a two-tailed t-test with 30 samples per site.

Site characteristic	Upland	Riparian	Significance
Soil moisture (% volumetric water content)	9.05 (2.01)	27.54 (4.23)	*
Thaw depth (cm)	32.50 (1.09)	57.65 (2.20)	*
Stem height (cm)	48.51 (1.95)	114.93 (5.44)	*
Stem length (cm)	67.50 (3.38)	162.87 (6.74)	*
Stem basal diameter (cm)	1.45 (.08)	3.01 (0.21)	*
Stem age (years)	28.03 (1.83)	30.59 (2.40)	

Table 1.2. Chronology statistics. Mean age and ring width are measured respectively in years and mm. Parenthetical values represent standard error of the mean. EPS = Expressed population signal; rbar = mean interseries correlation; MS = mean sensitivity; 1r = first-order autocorrelation; snr = signal/noise ratio

Site	Mean age	Mean ring width	EPS	rbar	MS	1r	snr
Upslope	28.03 (1.83)	.197 (0.014)	0.85	0.356	0.260	0.018	5.536
Riparian	30.59 (2.40)	.403 (0.030)	0.87	0.367	0.329	0.058	6.949

Table 1.3. Summary of climate sensitivity and climate-growth relationship analyses. Climate sensitivity values (95% confidence interval) are based on June mean temperature and derived from *treeclim* analysis (Zang & Biondi, 2015) using two detrending strategies for each site chronology. Asterisks indicate climate sensitivities are significantly different from zero at an alpha = 0.05 value.

Site	Climate sensitivity		Climate-growth adjusted R^2	
	20-year cubic spline	Negative exponential	1^{st}-order model	2^{nd}-order model
Upslope	0.492 (0.075, 0.736)*	0.390 (0.035, 0.653)*	0.33	0.45
Riparian	0.276 (0.029, 0.547)*	0.292 (-0.033, .632)	0.30	0.27

Chapter 2

Uniform shrub growth response to June temperature across the North Slope of Alaska

Summary

The expansion of woody shrubs in arctic tundra alters many aspects of high-latitude ecosystems, including carbon cycling and wildlife habitat. Dendroecology, the study of annual growth increments in woody plants, has shown promise in revealing how climate and environmental conditions interact with shrub growth to affect these key ecosystem properties. However, a predictive understanding of how shrub growth response to climate varies across the heterogeneous landscape remains elusive. Here we use individual-based mixed effects modeling to analyze 19,624 annual growth ring measurements in the stems of *Salix pulchra* (Cham.), a rapidly expanding deciduous shrub. Stem samples were collected at six sites throughout the North Slope of Alaska. Sites spanned four landscapes that varied in time since glaciation and hence in soil properties, such as nutrient availability, that we expected would modulate shrub growth response to climate. Ring growth was remarkably coherent among sites and responded positively to mean June temperature. The strength of this climate response varied slightly among glacial landscapes, but in contrast to expectations, this variability was not systematically correlated with landscape age. Additionally, shrubs at all sites exhibited diminishing marginal growth gains in response to increasing temperatures, indicative of alternative growth limiting mechanisms in particularly warm years, such as temperature-induced moisture limitation. Our results reveal a regionally-coherent and robust shrub growth response to early season growing temperature, with local soil properties contributing only a minor influence on shrub growth. Our conclusions strengthen predictions of changes to

wildlife habitat and improve the representation of tundra vegetation dynamics in earth systems models in response to future arctic warming.

Background

Woody shrubs are expanding in arctic tundra, with cascading effects on terrestrial carbon balance and wildlife habitat (Tape *et al.* 2006, Myers-Smith *et al.* 2011). Establishing the drivers of shrub expansion is therefore key to predicting future shifts in both ecosystem and community processes at high latitudes, where half of Earth's terrestrial organic carbon is stored (Tarnocai *et al.* 2009, Hugelius *et al.* 2014). Recent meta-analyses (Myers-Smith *et al.* 2015a, Martin *et al.* 2017) suggest that shrub growth variability is driven by temperature and precipitation, and modified by ecosystem properties like soil moisture and nutrient status. However, very few empirical studies have tested these ideas by measuring shrub growth on decadal timescales across landscapes with varying ecosystem properties.

One over-arching "master" variable controlling ecosystem properties in arctic Alaska is the time since last glaciation. Due to the heterogeneous nature of glacial advance and retreat in this region, adjacent watersheds can vary in landscape age by more than an order of magnitude (Hamilton 2003). This patchwork of glacial histories gives rise to spatial variation in ecosystem properties among landscapes. Older glacial landscapes have greater plant biomass, cation exchange capacity, soil acidity, and net nitrogen mineralization (Hobbie and Gough 2002, Hobbie *et al.* 2002, Walker *et al.* 2014). Because of these legacy effects of glaciation, Oswald *et al.* (2014) argue that glacial history is a key regional control on vegetation response to future climate changes. Nitrogen availability, the strongest limiting factor to plant growth in the region, varies

widely among landscapes of different ages. For example, Hobbie and Gough (2002) found 10 times greater rates of annual net nitrogen mineralization in an older landscape (120,000-60,000 years since glaciation) compared to an adjacent younger landscape (25,00-11,500 years since glaciation). Therefore, it may be expected that shrub growth is more responsive to climate variability in older glacial landscapes where nitrogen limitation is less severe (Chapin 1983, Chapin *et al.* 1995, Whittinghill and Hobbie 2011, Walker *et al.* 2014, Shaver *et al.* 2014).

Within glacial landscapes, variability in local soil conditions has further consequences for vegetation response to climate. For example, while shrub growth often responds positively to growing season temperature, temperature-induced moisture limitation may constrain growth during particularly hot years at drier locations such as uplands (Ackerman *et al.* 2017, Gamm *et al.* 2017). Such local variability in soil conditions interacts with regional glacial geology and broad-scale climate patterns to create a hierarchical structure of controls on tundra vegetation growth (Myers-Smith *et al.* 2015a). This hierarchy poses a major challenge to building a predictive understanding of arctic shrub growth.

Dendroecology, the study of annual growth increments in woody plants, has become a popular method within the last two decades for analyzing climate response of arctic vegetation (See studies included in Myers-Smith *et al.* 2015a, Young *et al.* 2016, Ackerman *et al.* 2017, Gamm *et al.* 2017). This method is particularly well-suited for arctic tundra, since many plant species are long-lived and interannual climate is highly variable. Further, the use of individual-based mixed effects models in the analysis of dendroecological data yields estimates of the strength of controls on shrub growth across

all levels of the aforementioned hierarchy (Myers-Smith *et al.* 2015a, Myers-Smith *et al.* 2015b). In contrast to the traditional site-level standardization approach that extracts a uniform growth signal shared among individuals at a site, the mixed-modeling approach maintains information related to the variability in climate response among individuals (Galván *et al.* 2014). Therefore, this method is ideal for comparing individualistic climate responses of shrubs sampled from distinct glacial landscapes and from multiple microsites within those landscapes (Galván *et al.* 2014, Myers-Smith *et al.* 2015b).

In this study, we present results of dendroecological analysis from six populations of *Salix pulchra* (diamond-leaf willow), a rapidly expanding deciduous shrub, growing across four landscapes of different glacial ages on the North Slope of Alaska. This work builds on a prior study by Ackerman *et al.* (2017) that revealed shrub growth sensitivity to mean June temperature at upland and riparian sites within a single glacial landscape. Diminishing marginal growth gains to increasing temperature were evident only at the upland site, a potential indicator of temperature-induced moisture limitation during particularly warm years. Here we explore whether such patterns hold at a regional scale encompassing four landscapes ranging in age from 14,000 to over 900,000 years since glaciation. We use individual-based mixed modeling to test two hypotheses:

1. Shrub growth on older glacial landscapes will respond more strongly to climate variability, because older landscapes are less nitrogen-limited.

2. In upland areas (but not in riparian areas), shrubs will show diminishing marginal growth gains in response to increasing temperature, because fewer soil resources such as moisture are available in upland areas to facilitate elevated growth in warm years.

Methods

During the summers of 2015 and 2016, we sampled six populations of *Salix pulchra* (cham.) on the North Slope of Alaska across four landscapes of different glacial ages, ranging between 14,000 and >900,000 years old (Figure 2.1). Within two of the landscapes, Kuparuk and Inigok, we replicated our sampling of 40 stems at both upland and streamside riparian sites. Within the other two landscapes, Itkillik and Roche Moutonee in the Brooks Range, we sampled only from upland sites. Detailed description of the geologic histories of the sampling sites can be found in the references in Table 2.1. At each site, shrub sampling protocol (including serial sectioning along the stem), microscope slide preparation, image-based ring width measurements, and cross-dating were conducted following methods described by Ackerman *et al.* (2017). In total, we cross-dated 19,624 annual ring (i.e. secondary stem growth) measurements across 184 individuals to assemble the ring width dataset. Measurements from the Kuparuk landscape have been previously published (Ackerman *et al.* 2017), while data from the rest of the landscapes are presented here for the first time. For visualization purposes, traditional dendroecological standardization (following Ackerman *et al.* 2017) was used to calculate time-stable ring width indices for each individual, and site-level chronologies were calculated as the median of all ring-width index values available in a given year (Figure 2.2). We ran a principal component analysis of the six site-level chronologies to assess coherence in the growth signal among the sites.

Expanding on the more traditional dendroecological standardization approaches used in Ackerman *et al.* (2017), we used linear mixed effects modeling to analyze the raw, unstandardized ring width data of individual shrubs. Compared with traditional

methods, mixed effects modeling is more effective in preserving individual-level variation in shrub growth while accounting for the influence of intrinsic factors, such as stem age, on ring width (Galván *et al.* 2014, Myers-Smith *et al.* 2015b). We used the R package *nlme* (Pinheiro *et al.* 2014) to run our models, with ring width (log transformed to achieve normality of residuals) as the response variable, individual shrub as a random effect, and a first-order autocorrelation structure.

To determine which climate variables to test as fixed effects in our model, we used the R package *treeclim* (Zang and Biondi 2015) to correlate growth chronologies from each site with monthly climate variables including precipitation and minimum, mean, and maximum temperatures. Climate data for Kuparuk, Itkillik, and the Brooks Range landscapes come from Toolik Field Station (Environmental Data Center Team 2017), which is within 50 km of each of these sites and has continuously monitored climate conditions since 1989. Climate data for Inigok come from the NOAA Climate Divisional Dataset for the North Slope of Alaska (NOAA, Vose *et al.* 2014), a regional climate monitoring product, as no individual meteorological station has a continuous multi-decadal record of climate near Inigok. Monthly climate variables found to be significant predictors of shrub growth across multiple sites were selected for inclusion as fixed effects. The other fixed effects were stem length, glacial landscape (categorical, 4 levels), and position (categorical, 2-levels: upland or riparian). We included a term for the interaction between climate variables and glacial landscape, to test whether shrub response to climate varied among landscapes (Hypothesis 1). We also tested for second-order relationships between significant climate variables and shrub growth, to account for potential decreasing marginal growth gains in response to increasing temperature. A

negative second-order relationship between temperature and ring width would be consistent with temperature-induced moisture limitation during warm growing seasons (Ackerman *et al.* 2017). Finally, we tested for an interaction between this second-order relationship and position, to determine whether temperature-induced moisture limitation was stronger at the upland sites (Hypothesis 2). We ran the model for ring width measurements from 1989 to 2014, the common period between the shrub growth measurements and the instrumental record across all sites.

After running the full model described above, we tested a more parsimonious model that excluded terms not found to be statistically significant at alpha = 0.05. To compare the full model with the parsimonious model, we used both the Akaike Information Criterion (AIC) and the Bayesian Information Criterion (BIC), which imposes a stronger penalty for increasing model complexity.

Results

Climate correlation analysis in *treeclim* revealed strong positive correlations between standardized ring-width index and June mean temperature (hereafter June T) across all sites (Figures 2.2 and 2.3). May minimum temperature had a weak negative correlation with ring-width index. Shrub growth was highly coherent among the six sites, as the first principal component captured 72.4% of the total variance in ring-width indices. Ring-width measurements are available from the International Tree Ring Data Bank (http://www.ncdc.noaa.gov/paleo/treering.html).

In our individual-based mixed modeling analysis of the raw ring width measurements, the parsimonious model (AIC = 5568, BIC = 5562) was preferred over the full model (AIC = 5584, BIC = 5691). Both models explained 45% of the variability in

ring width, using Nakagawa and Schielzeth's (2013) calculation of conditional R^2. Therefore, we focus on results of the parsimonious model, but we present complete output for both models in Table 2.2.

June T was the climate variable with the greatest effect size on ring width. Further, there was a statistically significant interaction between June T and glacial landscape. However, in contrast to our prediction arising from Hypothesis 1, the strength of this interaction did not vary systematically with landscape age. For example, shrub growth was most sensitive to climate in the youngest landscape, Brooks Range, while shrub growth was least sensitive to climate the second youngest landscape, Itkillik. Shrub growth sensitivities to June T at the two oldest landscapes were intermediate. There was also a negative second-order relationship between ring width and June T, which is consistent with temperature-induced moisture limitation of growth in warm growing seasons. However, in contrast to our expectation in Hypothesis 2, the strength of this temperature-induced moisture limitation did not vary by position within the landscape (upland versus riparian), because position itself was not a significant term in the model.

Longer stems were positively associated with ring width, while stem age was negatively associated with ring width (Table 2.2). Though position was not included as a significant term in the parsimonious model, it should be noted that position was correlated with stem length, which was a significant predictor of ring width (Figure 2.4; Table 2.3). Riparian shrubs had greater mean ring widths than upland shrubs. Mean annual stem elongation was also greater for riparian individuals than for upland individuals, as stem age did not differ across populations (Table 2.3).

Discussion

Our analysis revealed an overwhelming effect of June temperature on shrub growth, despite substantial variation in ecosystem properties (e.g. pH, soil moisture, nitrogen availability) associated with glacial landscape age and position (Chapin *et al.* 1988, Hobbie and Gough 2002, Hobbie *et al.* 2002, Walker *et al.* 2014, Ackerman *et al.* 2017). Contrary to our expectation in Hypothesis 1, shrubs growing on older glacial landscapes were not more sensitive to climate variability, though shrub response to climate did vary slightly among landscapes. Contrary to our expectation in Hypothesis 2, within-landscape shrub response to climate did not vary based on position (upland versus riparian). Temperature-induced moisture limitation (as indicated by a negative, second-order relationship between temperature and ring width) was evident across our entire set of samples, regardless of position. At the site level, interannual shrub growth was remarkably coherent across the North Slope (Figure 2.2), likely driven by the strength of the June temperature signal.

Mean June temperature was the only climate variable to significantly affect individual shrub growth in all six populations sampled, and in all cases it provided the strongest growth signal of any climate variable (Figure 2.2). This coherence in climate response across the North Slope contrasts with a meta-analysis (Myers-Smith *et al.* 2015a) that found significant variability in shrub response to climate at both regional and local scales. However, the studies included in this meta-analysis are largely single-site investigations with varied methodologies not designed to test for uniformity-versus-heterogeneity in climate response among sites. The uniform climate response we found in shrubs across the North Slope emphasizes the importance of consistency in sampling and measurement protocols, as outcomes of shrub dendroecological analyses vary based on

the specific measurement techniques used (Myers-Smith *et al.* 2015b). For example, climate sensitivity of shrub growth appears greater when ring measurements are taken at the root collar compared with higher up the stem (Ropars *et al.* 2017). In our analysis, we used serial sectioning (Myers-Smith 2015b) to ensure that the June temperature signal in the shrubs we sampled was indicative of secondary growth throughout the stem, not just in a specific part of the stem (e.g. the root collar).

Shrub climate response varied among glacial landscapes, indicated by a significant interaction between landscape and June T. However, the strength of this interaction was not systematically related to landscape age. Shrubs in older landscapes reported to have greater nitrogen availability did not respond more strongly to June T than shrubs in younger landscapes reported to have lower nitrogen availability (Hobbie and Whittinghill 2011). This outcome did not support Hypothesis 1, perhaps due to the difficulty of measuring nitrogen availability for plants in tundra soils. Although older landscapes have greater net nitrogen mineralization rates (Hobbie *et al.* 2002), this may not be the best indication of nitrogen availability, as some tundra plant species can use organic forms of nitrogen (Schimel and Chapin 1996, Schimel and Bennet 2004). Additionally, other factors associated with landscape properties (e.g. pH, herbivory rates, disturbance regimes, availability of other nutrients, etc.) may impact shrub climate response more than nitrogen availability or landscape age *per se*.

Within-landscape variability in position (upland versus riparian) did not alter shrub climate response, nor was its main effect a significant predictor of ring width. However, stem length, which was partially determined by position, was positively correlated with ring width. Favorable landscape positions such as riparian zones tend to

host taller shrubs with greater growth rates (Ackerman *et al.* 2017). In turn, taller shrubs have stronger climate responses (Myers-Smith *et al.* 2015a), perhaps due to release from competition with shorter conspecific neighbors (Saccone *et al.* 2017). Therefore, while position was not directly useful in modeling shrub growth, stem length, often an indirect effect of position, was a highly significant predictor of secondary growth. Separating the often correlated effects of shrub size and position within the landscape would not have been possible using a traditional site-based chronology approach to the analysis of our ring width data, as individual (within-site) variability in stem size would have been lost. Our mixed modeling approach thus provided unique ecological insight on the importance of shrub size and competition in growth variability (Myers-Smith *et al.* 2015a, Myers-Smith *et al.* 2015b, Young *et al.* 2016).

We found evidence supporting temperature-induced moisture limitation of shrub growth, indicated by the negative second-order relationship between ring width and June T. In other words, shrubs across the North Slope showed decreasing marginal growth gains in response to increasing June T. This second-order relationship did not depend on shrub position within the landscape. This result differs from findings by Ackerman *et al.* (2017), who found temperature-induced moisture limitation at a dry upland site, but not at a nearby moist riparian site. The contrasting results described in the present study may be due either to greater individual replication, or to the difference in model specification, which here includes more individual-level information (e.g. stem length). Alternatively, the standardization procedure used by Ackerman *et al.* (2017) may have removed low- to medium-frequency variability in ring-width index that would be diagnostic of temperature-induced moisture limitation at both sites, given the monotonic increase in

mean June air temperature on the North Slope in recent decades (NOAA). In this study, we avoided this potential issue by analyzing raw ring width data using an individual-based model, which preserved growth variability at all temporal frequencies and maintained shrub-level information in the model (Galván *et al.* 2014, Myers-Smith *et al.* 2015a, Myers-Smith *et al.* 2015b). Regardless of the exact cause of the discrepancy, our results further support the idea that greater temperatures do not always lead to consistent increases in shrub growth, due to interactions with other limiting resources such as moisture (Ackerman *et al.* 2017, Gamm *et al.* 2017). We cannot rule out that another variable besides moisture might become a limiting factor to shrub growth at high temperatures.

The early season response in secondary stem growth across all our sites is consistent with the findings of Chapin and Shaver (1989), who showed that biomass accumulation in the leaves and twigs of deciduous shrubs was restricted to the early growing season. Shaver (1986) found that secondary growth accounts for half of aboveground net primary productivity in *Salix* shrubs from the region (the other half being stem elongation and leaf growth). Therefore, we can infer that almost all aboveground net primary productivity in *Salix* occurs early in the growing season. Radville *et al.* (2016) also documented early season peaks in belowground productivity of tundra communities near Kangerlussuaq, Greenland, though phenology of deciduous shrub roots in particular were not reported.

Our results suggest that as June temperatures continue to warm, shrub growth will increase across all glacial landscapes of the North Slope. Based on allometric relationships between secondary stem growth and aboveground biomass, large shrubs

with high growth rates will add proportionally more biomass in response to increased temperatures than smaller shrubs (Berner *et al.* 2015, Ackerman *et al.* 2017). Consequently, areas favorable for large shrubs, such as riparian zones and water tracks, may continue to yield improved habitat quality for shrub-reliant species such as moose and ptarmigan (Tape *et al.* 2010, Tape *et al.* 2016). Greater aboveground shrub biomass in these areas may also impact rates of soil carbon turnover, and increased secondary stem growth in particular affects water balance (Bret-Harte *et al.* 2002). Across both riparian and upland habitats, biomass increase may be limited by soil moisture in particularly warm growing seasons.

The robust and highly coherent shrub growth response to temperature early in the growing season raises prospects for climate reconstruction using a multi-proxy approach. Otolith growth in long-lived fish of tundra lakes has been introduced as an effective annually-resolved climate proxy beyond latitudinal treeline (Black *et al.* 2013, Torvinen 2017). In contrast to the June signal embedded in the shrub rings, otolith growth in lake trout (*Salvelinus namaycush*) on the North Slope of Alaska responds positively to mean August air temperature (Black *et al.* 2013, Torvinen 2017). June and August air temperatures in this region are not correlated ($R^2 = 0.02$, $p = 0.44$ for the period 1989-2014; NOAA). Therefore, reconstructing past temperature conditions over the course of entire growing seasons necessitates the use of both shrub and otolith proxies, which are each tuned to distinct, uncorrelated periods of the growing season. We believe the prospects for such a multi-proxy reconstruction are strong, given the large range overlap between *S. namaycush* and deciduous shrubs in the Arctic. Multi-proxy climate reconstruction in the Arctic would be useful because of the poorly resolved

spatiotemporal climate record during the instrumental period (Overland *et al.* 2004, Simmons and Poli 2014, Cowtan and Way 2014, Simmons *et al.* 2017). On the North Slope of Alaska, for example, the NOAA divisional dataset (NOAA) incorporates data from just a single inland meteorological station. Multi-proxy reconstructions from the North Slope could be used to evaluate spatial patterns in climate where instrumental data are lacking.

Conclusion

Our dendroecological analysis of *S. pulchra* revealed remarkable coherence in secondary growth and climate response across four glacial landscapes of the North Slope of Alaska. June mean temperature was the dominant control on annual shrub growth at all sites. Shrub response to climate varied slightly among glacial landscape, but there was no systematic correlation between landscape age and climate sensitivity of shrub growth. Position (upland versus riparian) had no direct effect on growth, though taller shrubs, more common in riparian areas, had higher growth rates. As June temperatures continue to increase, deciduous shrubs are likely to continue expanding across all glacial landscapes of the North Slope. However, this expansion may be limited by temperature-induced moisture limitation, or by another factor, in particularly warm years. Together, these outcomes highlight the preeminence of climate in controlling shrub growth variability across the North Slope. When combined with future climate scenarios, our model of shrub growth may strengthen predictions of changes to habitat structure and improve the representation of tundra communities in dynamic vegetation models.

Acknowledgments

We thank Toolik Field Station and the Arctic LTER (National Science Foundation grants #1026843 and #1637459) for valuable logistics support and guidance during this project. We also thank Dr. Benjamin Jones (U. S. Geological Survey) for generously hosting DEA at Inigok Field Facility (Bureau of Land Management) and Teshekpuk Lake Observatory to sample at Inigok. Climate datasets for Kuparuk, Brooks Range, and Itkillik landscapes were provided by the Toolik Field Station Environmental Data Center; this material is based upon work supported by the National Science Foundation grants #455541 and #1048361. Financial support was provided by the Dayton Fund from the Bell Museum of Natural History, Explorers Club, National Science Foundation Graduate Research Fellowships Program (grant #00039202), the University of Minnesota Undergraduate Research Opportunities Program, and the University of Minnesota Department of Ecology, Evolution, and Behavior. Melissa Markay and Lucas Veitch helped process shrub samples.

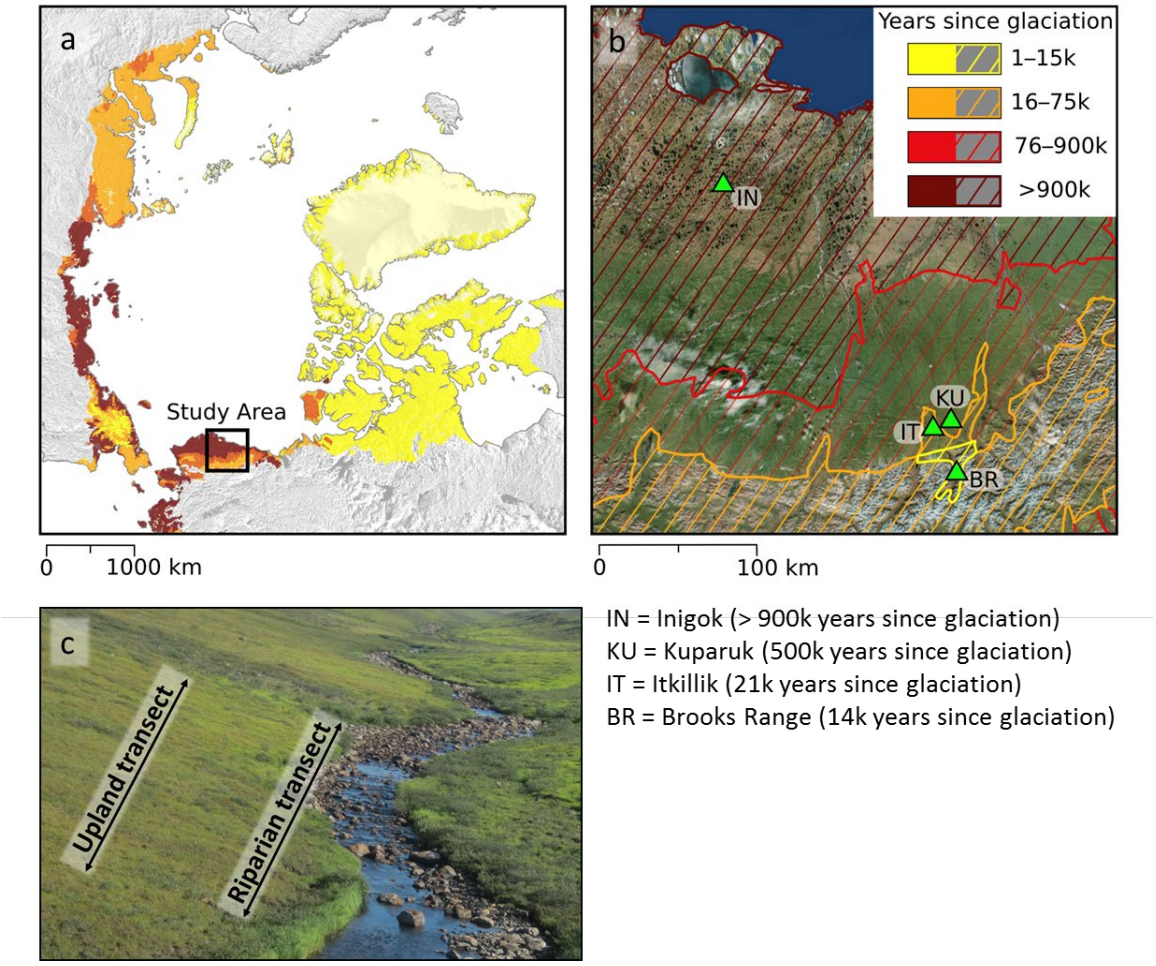

Figure 2.1. Landscape age in the circumpolar Arctic tundra (a) and on the North Slope of Alaska (b), where *Salix pulchra* were sampled across four glacial landscapes. At the Kuparuk (c) and the Inigok landscapes, *S. pulchra* were sampled from both upland and riparian positions. Only upland samples were taken at the Brooks Range and Itkillik landscapes. Landscape age data was provided by Raynolds and Walker (2009).

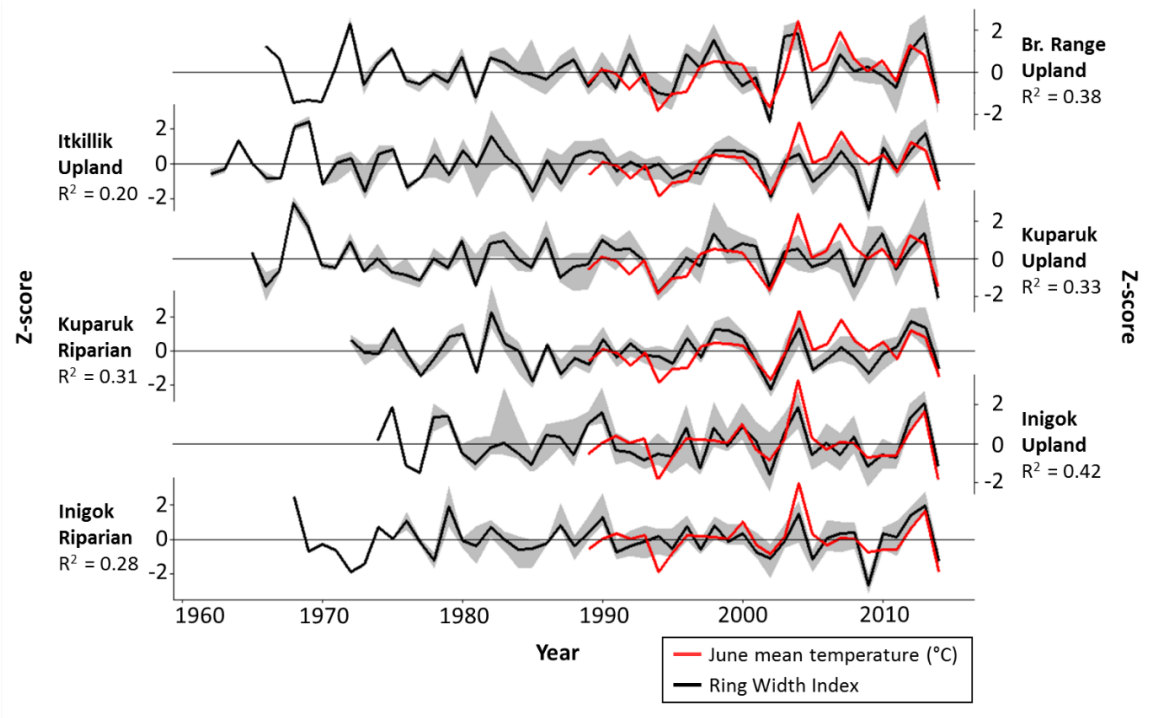

Figure 2.2. Z-scores of median ring-width index (black) correlate with mean June air temperature (red) in six *Salix pulchra* populations across the North Slope of Alaska. Gray ribbons represent 25th and 75th percentile of ring-width index at each site. Growth was strongly coherent among the six sites, as the first principal component explained 72.4% of the variance in ring width indices for the period of overlap with the climate record (1989-2014). Raw ring widths were standardized for visualization using a 20-year cubic smoothing spline following Ackerman *et al.* (2017).

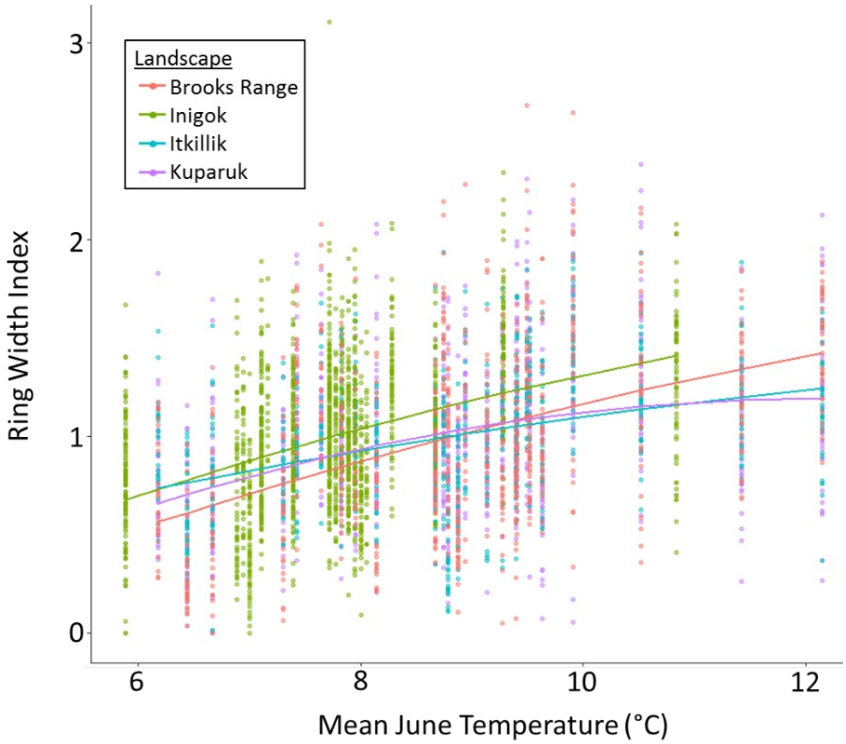

Figure 2.3. Mean June air temperature correlates positively with ring-width index in *Salix pulchra* individuals across four glacial landscapes on the North Slope of Alaska. Raw ring widths were standardized for visualization using a 20-year cubic smoothing spline following Ackerman *et al.* (2017). Calculations of best-fit curves for each landscape include both first- and second-order temperature terms, to account for potential effects of temperature-induced moisture limitation.

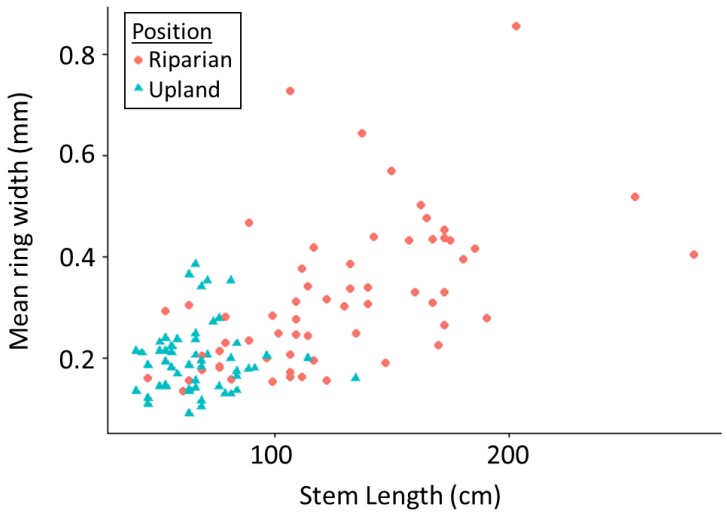

Figure 2.4. Stem length correlates with mean ring width in individuals from Inigok and Kuparuk, where both upland and riparian populations were sampled. Riparian individuals had longer stems and larger ring widths than upland individuals.

Table 2.1. Characteristics of four glacial landscapes sampled across the North Slope of Alaska for this project. Basal diameter, stem length, stem age, and stem elongation rate represent mean (standard error) values for shrub individuals sampled in each landscape. Geology reference 1 = Badding *et al.* 2013; 2 = Hamilton 2003; 3 = Walker *et al.* 2014; 4 = Hobbie and Gough 2002; 5 = Hobbie *et al.* 2002; and 6 = Carter 1981.

Site	Latitude, Longitude	Landscape age (years)	Populations sampled	Basal diameter (mm)	Stem length (cm)	Stem age (years)	Stem elongation rate (cm/year)	Geology reference
Brooks Range	68.375, -149.295	14,000	Upland	19.04 (1.62)	111.4 (9.5)	26.14 (1.38)	4.48 (0.15)	1
Itkillik	68.641, -149.614	21,000	Upland	16.13 (0.60)	82.0 (2.6)	30.52 (1.95)	3.06 (0.22)	2, 3, 4, 5
Kuparuk	68.660, -149.423	500,000	Riparian & upland	23.83 (1.90)	122.7 (8.6)	31.17 (1.68)	4.50 (0.42)	2, 3
Inigok	70.000, -153.097	> 900,000	Riparian & upland	14.06 (0.66)	82.6 (3.4)	24.31 (1.00)	3.70 (0.07)	6

Table 2.2. Fixed effect coefficient estimates for the parsimonious and full mixed models predicting *Salix pulchra* ring width (mm, log-transformed) across the North Slope of Alaska. The parsimonious model was preferred based on both AIC and BIC. Conditional R^2 (Nakagawa and Schielzeth 2013) was 0.45 for both models. Temperatures (T) are in units of °C, and stem age is measured in years.

	Parsimonious model AIC = 5568, BIC = 5562			**Full model AIC = 5584, BIC = 5691**		
Parameter	**Estimate**	**St. error**	**p-value**	**Estimate**	**St. error**	**p-value**
Intercept	-4.42	0.244	< 0.001	-4.36	0.271	< 0.001
June mean T	0.324	0.048	< 0.001	0.329	0.049	< 0.001
(June mean T)^2	-0.007	0.001	0.01	-0.006	0.003	0.028
May minimum T	-0.035	0.003	< 0.001	-0.035	0.003	< 0.001
Stem length	0.018	0.001	< 0.001	0.016	0.001	< 0.001
Landscape Inigok	0.87	0.152	< 0.001	0.88	0.169	< 0.001
Landscape Itkillik	1.064	0.165	< 0.001	1.046	0.165	< 0.001
Landscape Kuparuk	1.005	0.151	< 0.001	1.04	0.168	< 0.001
Stem age	-0.035	0.002	< 0.001	-0.035	0.002	< 0.001
June mean T*Landscape Inigok	-0.069	0.017	< 0.001	-0.079	0.019	< 0.001
June mean T*Landscape Itkillik	-0.102	0.017	< 0.001	-0.102	0.017	< 0.001
June mean T*Landscape Kuparuk	-0.086	0.016	< 0.001	-0.096	0.018	< 0.001
Position_upland		Not included		-0.028	0.082	0.73
(June mean T)^2*Position_upland		Not included		-0.001	0.001	0.21

Table 2.3. Shrub characteristics from upland and riparian populations. Shrubs included in these results were sampled from the Kuparuk and Inigok landscapes, where shrubs at both positions were sampled. Riparian shrubs were generally larger and faster growing than upland shrubs. Values are reported as means (standard errors) of individual shrub measurements. All differences between upland and riparian shrubs were significantly different at the alpha = 0.05 level, except for stem age (p = 0.18).

Position	Basal diameter (mm)	Mean ring width (mm)	Stem length (cm)	Stem age (years)	Stem elongation rate (cm/year)
Upland	12.391 (0.530)	0.182 (0.003)	66.825 (2.399)	25.626 (1.396)	2.938 (0.150)
Riparian	22.643 (1.464)	0.301 (0.005)	125.589 (5.912)	28.159 (1.271)	4.952 (0.300)

Chapter 3

Global Estimates of Inorganic Nitrogen Deposition Across Four Decades

Summary

Atmospheric deposition of inorganic nitrogen is critical to the function of ecosystems and elemental cycles. During the industrial period, humans have doubled the amount of inorganic nitrogen in the biosphere and radically altered rates of atmospheric nitrogen deposition. Despite this rapid change, estimates of global nitrogen deposition patterns generally have low, centennial-scale temporal resolution. Lack of information on annual- to decadal-scale changes in global nitrogen deposition makes it difficult for scientists researching questions on these finer timescales to contextualize their work within the global nitrogen cycle. Here we use the GEOS-Chem Chemical Transport Model to estimate wet and dry deposition of inorganic nitrogen globally at a spatial resolution of 2° × 2.5° for 12 individual years in the period from 1984 to 2016. During this time, we found an 8% increase in global inorganic nitrogen deposition from 86.6 to 93.6 Tg N/year, a trend that comprised a balance of variable regional patterns. For example, inorganic nitrogen deposition increased in areas including East Asia and Southern Brazil, while inorganic nitrogen deposition declined in areas including Europe. Further, we found a global increase in the percentage of inorganic nitrogen deposited in chemically reduced forms from 30% to 35%, and this trend was largely driven by strong regional increases in the proportion of chemically reduced nitrogen deposited over the United States. This study provides spatially explicit estimates of inorganic nitrogen deposition over the last four decades and improves our understanding of short-term human impacts on the global nitrogen cycle.

Background

Humans have doubled the amount of bio-available inorganic nitrogen (IN) in the biosphere, radically altering ecosystem structure and function across the terrestrial-aquatic-marine continuum (Fowler *et al*., 2013). Much of this anthropogenic IN enters ecosystems by atmospheric deposition of IN species following combustion and atmospheric transportation and transformation. Once deposited to land or surface water, IN may stimulate primary productivity, reduce plant species richness, acidify aquatic and terrestrial ecosystems, and alter rates of decomposition (Bobbink *et al*., 2010; Bobbink & Hicks, 2014; Grennfelt & Hultberg, 1986; Knorr *et al*., 2005; Phoenix *et al*., 2006; Stevens *et al*., 2004). Despite these effects of IN deposition on fundamental ecosystem and community processes, comprehensive inventories of global IN deposition with high spatial and temporal resolutions are lacking.

Even with considerable advances in recent decades, significant gaps remain in the monitoring of both wet and dry IN deposition. Large-scale networks measuring IN deposition in precipitation have aided in detecting regional trends in IN deposition quantity and redox state (i.e., the proportion of oxidized vs. reduced compounds). For example, Du *et al*. (2014) report that while overall IN deposition across the United States remained stable between 1985 and 2012, the proportion of chemically reduced nitrogen in wet IN deposition significantly increased. However, describing such patterns at a global scale is difficult, because the spatial coverage of IN wet deposition monitoring networks is low in many continental areas and absent in most marine areas (Dentener *et al*., 2014). Sparser still are measurements of dry IN deposition, due to the analytical challenge of measuring particle and trace gas fluxes in ambient air (Dentener *et al*., 2014).

Modeling of global IN deposition has filled some of these monitoring gaps. The spatial resolution of IN deposition models has improved in recent years due to increased computing power, though the temporal resolution of available data sets remains low (Lamarque *et al*., 2013). For example, Galloway *et al*. (2004) demonstrated the increasing human dominance of the global nitrogen cycle by modeling IN deposition at a single time point in each of the 19th, 20th, and 21st centuries. This tendency toward centennial-scale IN deposition modeling is useful for considering such long-term trends. However, ecologists, biogeochemists, and others working on annual- or decadal-scale questions are often left with few resources to contextualize their work within the broader global nitrogen cycle. For example, researchers who have conducted a 3-year experiment of plant response to nitrogen fertilization may not have access to reliable IN deposition data over the specific duration of their experiment, potentially limiting the generalizability of their results. This lack of global-scale, high-temporal resolution IN deposition data contrasts with the wide availability of other variables of ecological interest such as climate parameters, soil moisture, and primary productivity (Cook *et al*., 2007, 2010, 2015; Fan & van den Dool, 2004; Running *et al*., 2004).

Here we present a new, spatially explicit data set of global wet and dry atmospheric IN deposition spanning the last four decades. We have two primary objectives with this work:

(1) create a data product for researchers seeking estimates of IN deposition from anywhere on Earth (including both continental and oceanic locales) during the last 40 years and (2) determine recent decadal-scale trends in IN deposition across the globe, with special focus on areas with rapidly changing rates of IN deposition.

Methods

GEOS-Chem Chemical Transport Model

We applied the GEOS-Chem Chemical Transport Model (v11–01; www.geos-chem.org) to obtain global gridded estimates of annual dry and wet deposition of IN. The model includes detailed HOx-NOx-VOC-ozone-BrOx tropospheric chemistry (Mao *et al*., 2013; Millet *et al*., 2015; Parrella *et al*., 2012) and aerosol thermodynamics (Fountoukis & Nenes, 2007; Pye *et al*., 2009). Chemical species included in the wet IN deposition calculations were NH_3, NH_4, NO_3, and HNO_3. Dry IN deposition calculations included these species plus N_2O_5 and NO_2. The model also explicitly accounts for the deposition of nitrogen contained in organic nitrates. However, GEOS-Chem does not simulate certain biogenic nitrogen-bearing compounds, such as amino acids and urea, which can constitute a significant component of organic nitrogen deposition (Cornell *et al*., 2003). Therefore, our estimates of organic nitrogen deposition, reported in the supporting information, should be considered lower-bound estimates. The organic nitrates simulated by GEOS-Chem included propanone nitrate, isoprene hydroxynitrate, methyl vinyl ketone + methacrolein nitrates, ≥C4 alkylnitrates, methyl peroxy nitrate, peroxyacetylnitrate, peroxypropionylnitrate, and peroxymethacryloyl nitrate. We did not include halogen nitrates in our deposition analysis.

Our model runs used assimilated meteorological data (the Modern-Era Retrospective Analysis for Research and Applications, version 2; MERRA-2; Gelaro *et al*., 2017) from the NASA Global Modeling and Assimilation Office at a degraded horizontal resolution of 2° × 2.5° with 47 vertical layers. The MERRA-2 product begins in 1980, and it has 3-hr temporal resolution for 3-D meteorological parameters and 1-hr

resolution for surface quantities and planetary boundary layer (PBL) height. The simulation applied the TPCORE advection algorithm (Lin & Rood, 1996), convective mass fluxes from the MERRA-2 archive (Wu *et al*., 2007), and nonlocal PBL mixing (Lin & McElroy, 2010). Our simulation was configured with a 15-min time step for transport/convection/PBL mixing and a 30-min time step for emissions/dry deposition/chemistry.

Anthropogenic emissions of $NOx/NH_3/CO/SO_2$ are from the Emission Database for Global Atmospheric Research (EDGAR v4.2; edgar.jrc.ec.europa.eu/overview.php?v=42) inventory, which covers the years from 1970 to 2010. For later years, we scaled the 2010 emissions inventory for each year and grid square based on an interpolation of species-specific Representative Concentration Pathways 8.5 scenarios (Riahi *et al*., 2011) between 2010 and 2020. NOx emissions from microbial processes in soil are estimated, following Hudman *et al*. (2012). We use monthly biomass burning emissions from the Global Fire Emissions Database version 4 (GFED4s; implemented as GFED4s in GEOS-Chem; van der Werf *et al*., 2017). Because the GFED4s data are available from 1997, fire emissions simulated for prior years were set to 1997 levels. Other NOx emissions include maritime shipping (Holmes *et al*., 2014), aviation (Stettler *et al*., 2011), and lightning (Murray *et al*., 2012). Methane concentrations were prescribed based on observational data (Dlugokencky *et al*., 2018) as a meridional gradient imposed on four latitudinal bands assumed vertically uniform throughout the troposphere.

The wet deposition scheme in the GEOS-Chem simulation includes scavenging of particulate and soluble gaseous compounds in convective updrafts, in-cloud rainout

(removal of species from the atmosphere into cloud droplets and subsequent rainwater), and below-cloud washout by precipitation (Liu *et al*., 2001; Wang *et al*., 2011, 2014). Re-evaporation is not considered. Dry deposition is based on the resistance-in-series scheme implemented as described by Wang *et al*. (1998) with coupled aerosol deposition (Alexander *et al*., 2005; Fairlie *et al*., 2007; Fisher *et al*., 2011; Jaeglé *et al*., 2011; Zhang *et al*., 2001).

Due to the computational costs, we ran GEOS-Chem for 4 years per decade (1983–1986, 1993–1996, 2003–2006, and 2013–2016), treating the first year run for each decade as the model spin-up time, which was later discarded from our final data set. Thus, our model output included strings of three consecutive years in each decade, allowing us to assess both interannual and interdecadal trends in IN deposition.

The model-estimated deposition fluxes were converted to units of $kgN \cdot km^{-2} \cdot year^{-1}$ for each surface grid pixel, and species-specific deposition values were then summed to determine overall IN dry and wet deposition. This allowed us to calculate the fraction of total IN deposited through (a) wet scavenging or (b) surface uptake and gravitational settling for each model pixel. Wet deposition fluxes at Earth's surface for each model pixel were calculated by aggregating the 3-D loss rate over 47 vertical model layers.

Model Evaluation

To evaluate the performance of the GEOS-Chem model across space, we compared our results with measured values of wet and total IN deposition for the year 2006, for which measured data sets are available (Vet *et al*., 2018). We used a global data set (Vet *et al*., 2018) to evaluate wet IN deposition. To evaluate total IN deposition, we used a North

American data set (Vet *et al*., 2018), because this region hosts the only major monitoring networks that routinely estimate regionally representative dry deposition fluxes of IN (Dentener *et al*., 2014). We used linear regression to compare our modeled deposition values with the measured values at every measurement location for 2006 to determine correlation coefficients between the modeled and measured values.

In addition to the above spatial assessments, we evaluated the temporal trends in our model output against IN deposition measurements conducted by long-term monitoring programs including the United States' National Atmospheric Deposition Program (National Atmospheric Deposition Program (NADP), 2018) and the European Monitoring and Evaluation Programme (Tørseth *et al*., 2012). We selected four sites from across the spatial domain of these monitoring programs with IN deposition measurements dating back to at least 1984, the beginning of our simulation. The sites include New York (United States), Westerland (Germany), Denali (United States), and North Dakota (United States). For each site, we estimated the annual rate of change in IN deposition, and we compared these values to our modeled rate of change for the corresponding grid cell. We transformed all IN deposition time series into Z-scores before making these comparisons to account for methodological differences in quantifying IN deposition between the monitoring programs.

Regional nitrogen emissions regulate the strength of IN deposition. Therefore, we generated maps of the distribution of nitrogen emissions from the various sources (e.g., anthropogenic emissions, biomass burning, industry, natural emissions, and biomass burning) used to drive the GEOS-Chem simulation of nitrogen transport and transformation.

Analysis of Model Output

After running and evaluating the GEOS-Chem model, we used the output to calculate a rate of change in IN deposition during the last four decades. This calculation was done by dividing the difference between 2016 and 1984 IN deposition values for each grid cell by the number of intervening years (33). We then mapped these values to visualize mean annual rate of change in IN deposition across the globe. We conducted a similar analysis to visualize the proportion of IN deposited in chemically reduced molecules.

Results

Model Evaluation

The GEOS-Chem simulation reliably reproduced measured IN deposition patterns across space for both total and wet deposition (Figures 3.1a and 3.1b). For total IN deposition over North America, we found a correlation coefficient of 0.83 for modeled versus measured values, with a slope between 0.76 and 1.06 (95% confidence interval), indicating no statistically significant model bias. For the global comparison of wet IN deposition, we found a correlation coefficient of 0.77 for modeled versus measured values, with a slope between 0.43 and 0.50 (95% confidence interval), indicating a low bias in the modeled values. The spatial patterns in IN deposition produced by the GEOS-Chem simulation closely matched patterns reported in the literature for the industrialized period (Dentener *et al*., 2006; Galloway *et al*., 2004; Kanakidou *et al*., 2016; Lamarque *et al*., 2013; Vet *et al*., 2014).

In addition to these spatial patterns, the model reliably reproduced measured temporal trends at the four long-term monitoring sites across North America and Europe.

Our model estimates of annual change at these sites matched measured trends in both direction and magnitude (Figure 3.1c).

Contemporary patterns in IN deposition

Our global maps (Figure 3.2) revealed hotspots of IN deposition in eastern Asia, Europe, eastern North America, and southern Brazil. The highest modeled IN deposition rate for 2016 was 5,155.6 $kgN \cdot km^{-2} \cdot year^{-1}$ in central China (28°N, 105°E), compared to a global average of 183.5 $kgN \cdot km^{-2} \cdot year^{-1}$. In total, 93.6 TgN were deposited as IN chemical species in 2016, closely matching output from other models of contemporary IN deposition, such as Galloway *et al*. (2004), who estimated 92.3 TgN/year in the early 1990s (for direct comparison, our simulation estimated 93.8 TgN in 1994). IN deposition tended to be low over marine environments, deserts, and polar regions. At the North and South Poles, IN deposition for 2016 was, respectively, 27 and <1 $kgN \cdot km^{-2} \cdot year^{-1}$. The fraction of IN deposited by precipitation was generally greater than 50%, except in areas with low mean annual precipitation (Supplemental Material Figure S3.1). Across grid cells, nitrogen emission levels alone explained 58% of the variability in IN deposition.

Change through time

Overall, global IN deposition rose by 8%, from 86.6 TgN in 1984 to 93.6 TgN in 2016, though our change map (Figure 3.3) revealed variable regional trends during the period simulated. Major reductions in IN deposition have occurred in Europe and the Central Indo-Pacific, with the greatest reduction occurring over Borneo (2°S, 115°E), where simulated IN deposition fell by an average of 124 $kgN \cdot km^{-2} \cdot year^{-1}$, from a high flux of 5,066 $kgN \cdot km^{-2} \cdot year^{-1}$ in 1984. Modest reductions in IN deposition also occurred over the northeastern United States. Reductions in IN deposition in Europe and the

northeastern United States were associated with decreased nitrogen emissions from anthropogenic activity (Supplemental Material Figure S3.2). IN deposition in the Central Indo-Pacific was heavily influenced by biomass burning (Supplemental Material Figure S3.2), which has high interannual variability, making it difficult to infer decadal-scale trends in this source of atmospheric nitrogen.

Significant increases in IN deposition have occurred over a widespread area in eastern Asia. The greatest increase in deposition rate, 111.5 $kgN \cdot km^{-2} \cdot year^{-1}$, has occurred in central China (28°N, 105°E). Modest increases in IN deposition have also occurred over areas of northwestern Canada, southern Brazil, and eastern Siberia. Increased IN deposition in eastern Asia and southern Brazil was associated with increased nitrogen emissions from anthropogenic activity in those regions (Supplemental Material Figure S3.2). IN deposition in northwestern Canada and eastern Siberia was strongly influenced by biomass burning (Supplemental Material Figure S3.2). Changes in IN deposition rates were generally minor over oceans, where we do not expect significant change in deposition due to low nitrogen emission rates.

The rate of change in IN deposition has varied through time in some regions (Supplemental Material Figure S3.3). For example, IN deposition rate declined more slowly in Europe between 2004 and 2016 than during earlier periods of the simulation. In the eastern United States, both the magnitude and the direction of the change have varied; IN deposition increased from 1984 to 1996, remained steady from 1994 to 2006, and declined from 2004 to 2016.

During the period simulated, the percentage of IN deposited in reduced molecules (NH_3 and NH_4) increased globally from 30.3% to 35.3% ($p = 0.001$), though regional

trends varied (Figure 3.4). Increases in the percentage of IN deposited in reduced molecules were found in most continental and marine areas, though decreases occurred over Russia and the Arctic Ocean.

Discussion

Our simulation showed a global increase in IN deposition between 1984 and 2016, though trends varied strongly by region. Our simulation successfully reproduced spatial patterns reported by other authors and matched IN deposition levels at locations where it has been measured directly (Dentener *et al*., 2006; Galloway *et al*., 2004; Jia *et al*., 2014; Kanakidou *et al*., 2016; Lamarque *et al*., 2013; Vet *et al*., 2014; Zhang *et al*., 2018). This study extends upon prior work by providing a data set with high temporal replication (12 years modeled between 1984 and 2016). This focus on annual- and decadal-scale variation in IN deposition provides a more detailed understanding of how the global nitrogen cycle has changed in the last four decades.

IN deposition generally correlates with regional emissions (Tamm, 1991), a pattern evident in our model output. Our change map (Figure 3.3) shows that IN deposition has increased in regions where emissions have also grown in recent decades. For example, we found significant growth in IN deposition in east Asia, where emissions from fossil fuel combustion and excess fertilizer application have increased (Jia *et al*., 2014; Liu *et al*., 2013). Similarly, we found decreased deposition where emissions have fallen in recent decades, such as Europe, where nitrogen emissions from fossil fuel combustion have declined (Fowler *et al*., 2007). Therefore, local management of IN deposition levels will rely on local-to-regional-scale control of nitrogen emissions. This situation contrasts with management strategies for other atmospheric components that are

less chemically reactive and thus mix well globally, such as anthropogenic carbon dioxide, and require global-scale emission control.

Our finding of an increased proportion of IN deposited in chemically reduced forms (NH_3 and NH_4) between 1984 and 2016 is likely reflective of regional policies to manage nitrogen emissions. For example, the global trend appears to be strongly driven by sharp increases in the proportion of chemically reduced nitrogen deposited over the United States (Figure 3.4), in accord with reports by Du *et al*. (2014) and Li *et al*. (2016). The United States has implemented controls on the emission of oxidized nitrogen, primarily caused by combustion processes, but not on the emission of reduced nitrogen, primarily caused by volatilization from livestock waste and fertilizer (Li *et al*., 2016; Reis *et al*., 2009). The continuation of this trend toward an increased proportion of chemically reduced nitrogen in IN deposition is likely to impact the competitive balance among plants with differing affinities for various nitrogen forms (Choudhary *et al*., 2016; Kahmen *et al*., 2006; Kanakidou *et al*., 2018; Liu *et al*., 2018).

The IN deposition data product can serve the needs of ecologists, biogeochemists, and others in search of IN deposition data during the last four decades. Potential applications include completing nitrogen budgets for experimental sites or making management decisions based on recent trends in IN deposition. Moving forward, the development of a similar annually updated IN deposition data set would allow researchers to better contextualize their work within the global nitrogen cycle. Such products are already available for other variables of ecological interest (Cook *et al*., 2007, 2010, 2015; Fan & van den Dool, 2004; Running *et al*., 2004). Mapping changes to IN deposition on annual to decadal scales will improve our understanding of short-term

human impacts on global elemental cycles and improve predictions of ecosystem change across the globe.

Acknowledgments

The authors gratefully acknowledge the sources of precipitation chemistry and deposition data acknowledged on p. 92 of Vet *et al*. (2014) Atmospheric Environment, 93, https://doi-org.ezp3.lib.umn.edu/10.1016/j.atmosenv.2013.10.060. Computing resources were provided by the Minnesota Supercomputing Institute (http://www.msi.umn.edu) at the University of Minnesota. The MERRA-2 data used in this project have been provided by the Global Modeling and Assimilation Office at NASA Goddard Space Flight Center (https://gmao.gsfc.nasa.gov/reanalysis/MERRA-2). The ECCAD database (http://eccad.sedoo.fr) hosted emission inventories used in this work. The authors also thank James Cotner, Jacques Finlay, and Sarah Hobbie, who provided valuable feedback on this project. Data produced by this analysis are available through the Data Repository for the University of Minnesota (https://conservancy.umn.edu/handle/11299/197613). The authors declare no conflicts of interest.

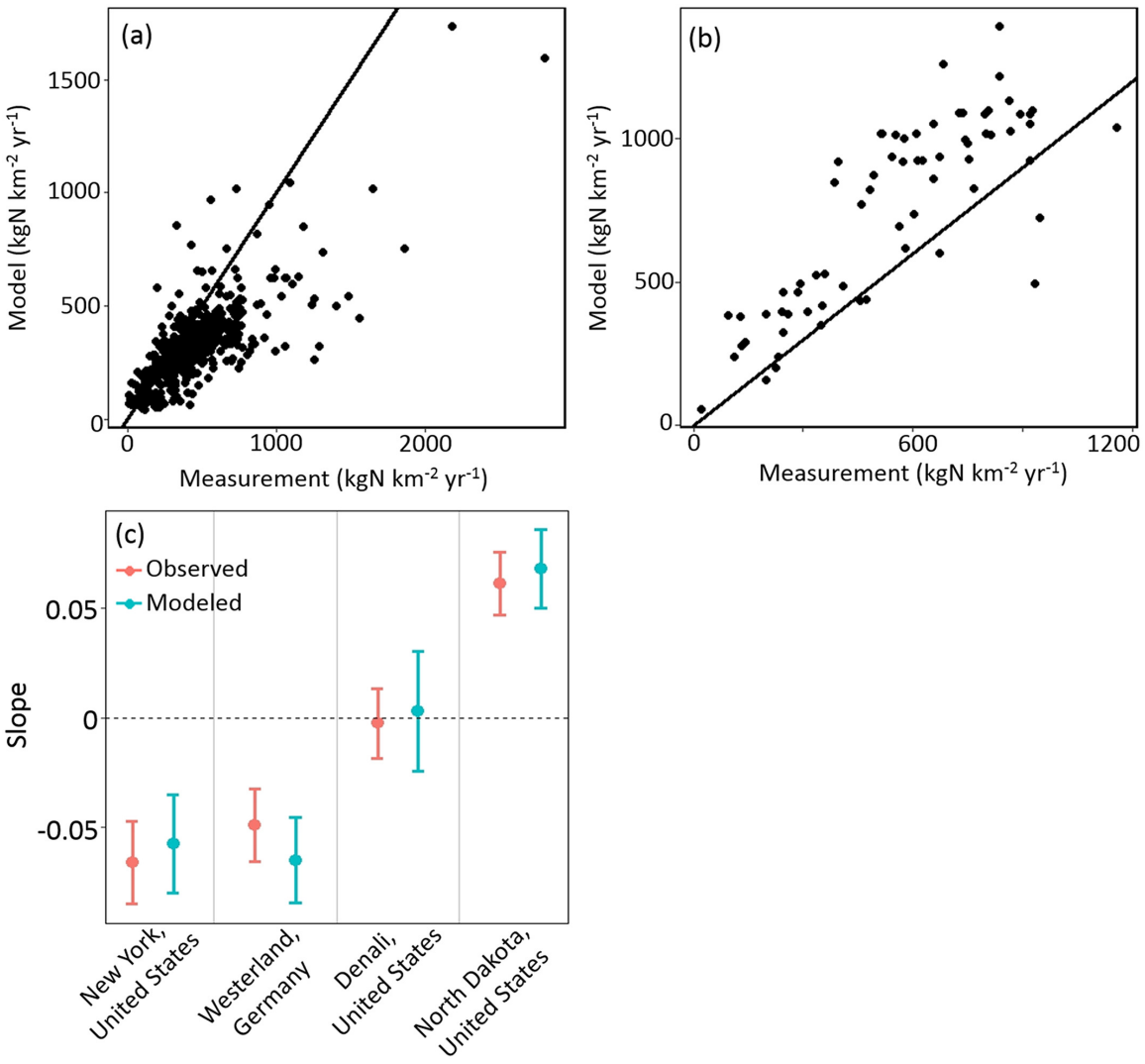

Figure 3.1. Evaluation of simulated spatial and temporal trends in inorganic nitrogen (IN) deposition. For spatial patterns, modeled values of wet IN deposition across the globe (a) show a strong correlation with measured values (r = 0.77, measurements from Vet *et al*., 2014), with a negative bias (95% confidence interval for slope = [0.43, 0.50]) from the one-to-one line. Modeled values of total IN deposition across North America (b) show a strong correlation with measured values (r = 0.83, measurements from Vet *et al*., 2014), with no significant bias (95% confidence interval for slope = [0.76, 1.06]) from the one-to-one line. For temporal trends, (c) slopes of modeled versus observed standardized (Z-scores) IN deposition time series from 1984 to 2016 match in magnitude and direction for four sites across North America and Europe. Error bars represent standard errors of slope estimates.

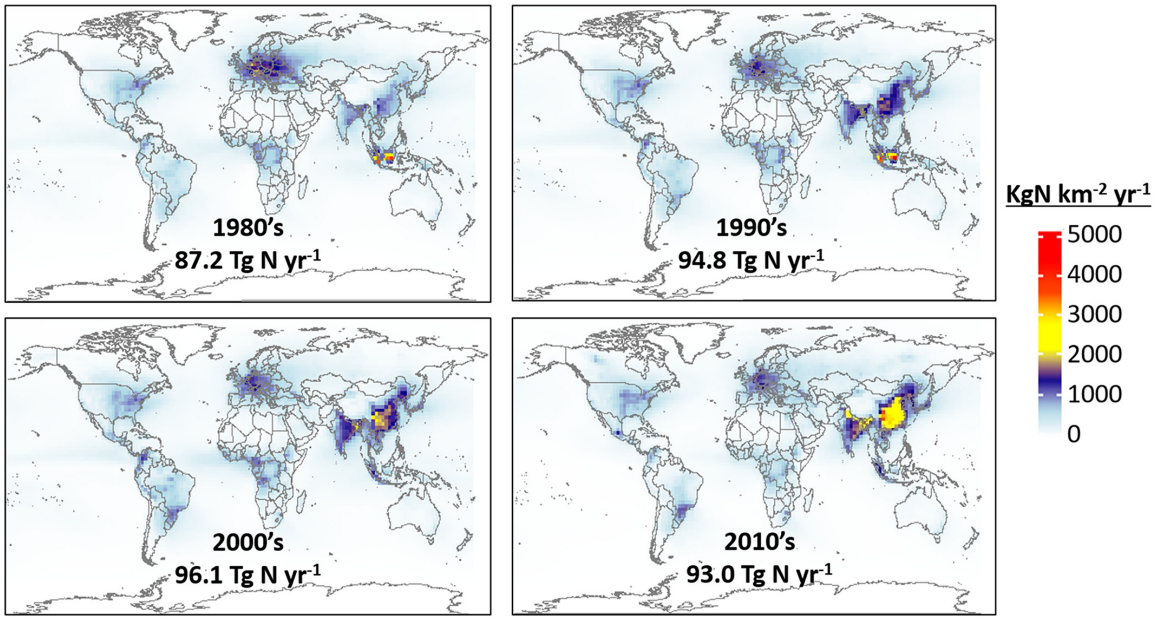

Figure 3.2. Mean annual inorganic nitrogen deposition (wet + dry) as simulated for the past four decades. Total global flux (annual mean) shows inset for each decade.

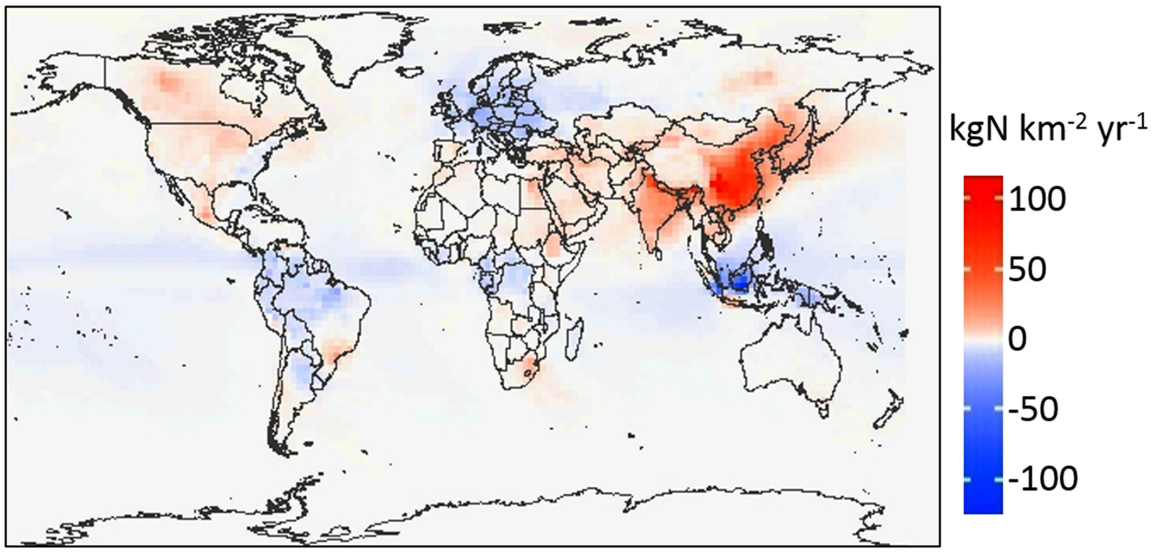

Figure 3.3. Mean annual rate of change in simulated total inorganic nitrogen deposition between 1984 and 2016.

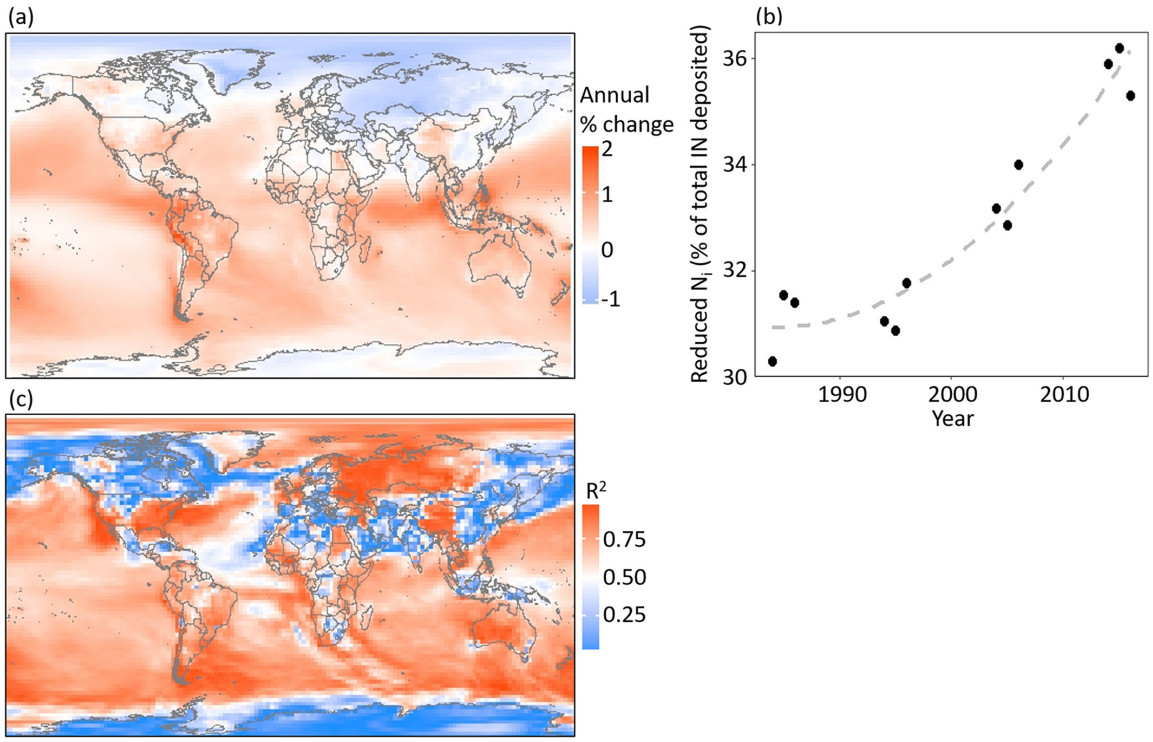

Figure 3.4. Change in percent of inorganic nitrogen deposited as chemically reduced molecules (NH_3 and NH_4) from 1984 to 2016. Direction and magnitude of change (a) varied regionally, but (b) increased on a global scale. The R^2 values associated with the percent change in chemically reduced inorganic nitrogen deposition through time indicate (c) the trend was most coherent in areas such as the United States, eastern Europe, and western China.

Chapter 4

Temperature controls the nitrogen balance of circumarctic watersheds

Summary

Boreal and tundra ecosystem function is impacted by the combined effects of atmospheric nitrogen deposition and warming of extremely cold landscapes. Nitrogen retention, defined here as the balance of atmospheric inputs and streamflow loss, shapes the response of terrestrial, freshwater, and marine ecosystems to rising temperatures. Changes to nitrogen balance are particularly impactful at high latitudes, where terrestrial productivity is often limited by low mineral nitrogen levels, and where soils contain large stocks of organic nitrogen. Here we used linear mixed effects modeling with previously published data to assess the role of temperature and other environmental factors in determining nitrogen retention for watersheds throughout the circumpolar north. We found that mean annual temperature was positively related to the proportion of atmospherically deposited nitrogen retained, but we found no significant effects of other variables including watershed area, annual runoff, and watershed soil properties. Notably, we found a net loss of nitrogen from a subset of watersheds, particularly those with continuous permafrost and relatively mean annual temperatures. Overall, our results suggest that warming could increase the proportion of atmospheric nitrogen inputs retained in high-latitude watersheds. This could favor the growth of plant species with relatively low nitrogen-use efficiencies, due to greater nitrogen availability from gradual permafrost thaw and subsequent soil mineralization. Nitrogen inputs to coastal marine systems may also become more limited with warming. However, we caution that these

potential effects of increased nitrogen retention rates with warming may be counteracted by rapid permafrost thaw, which could mobilize soil nitrogen and export it downstream.

Background

Humans have doubled the amount of reactive nitrogen (N) entering the biosphere (Vitousek *et al.* 1997, Galloway *et al.* 2004). Excess N boosts primary productivity, reduces plant diversity, and can alter competitive balance between species (Stevens *et al.* 2004, Clark and Tilman 2008, Bobbink *et al.* 2010). Effects of anthropogenic N may be particularly pronounced in N-limited ecosystems, which are common across the boreal and tundra biomes (Shaver *et al.* 1992, Elser *et al.* 2007, Holtgrieve *et al.* 2011).

Temperatures are rising rapidly throughout high-latitude systems, with the potential to further influence N fluxes and transformations (Baron *et al.* 2013). Such alterations could promote ecosystem retention of atmospherically-derived N by raising rates of N uptake (by plants, microbes, soils) and removal (through denitrification). For example, warming has been shown to stimulate N mineralization and raise metabolic rates, thereby elevating N uptake by plants and microbes at high latitudes (Schmidt *et al.* 2002). This process could lend a competitive advantage to plant species with low N-use efficiency such as deciduous shrubs in arctic tundra (Chapin and Shaver 1989), accelerating the trend of tundra shrub expansion (Myers-Smith *et al.* 2011, Mekonnen *et al.* 2018). Further, warming and warming-induced changes to plant communities could increase denitrification because of greater microbial activity and labile carbon inputs to terrestrial and aquatic systems, as demonstrated by Myrstener *et al.* (2016).

Alternatively, higher temperatures could promote hydrologic N export from ecosystems, rather than retention, by accelerating leaching from N-rich soils, including those exposed by thawing permafrost (Frey *et al.* 2007, Frey and McClelland 2009, Harms *et al.* 2014, Treat *et al.* 2016, Harms *et al*. 2019). High-latitude soils contain large pools of organic N (Shaver *et al.* 1992) and most inorganic N deposited is converted to organic forms (Yano *et al.* 2010), so leaching losses would likely occur as dissolved organic N. Inorganic N loss, primarily as nitrate, may also occur if soil nitrification and transport are enhanced (Shaver *et al.* 2014, Bowden *et al.* 2014, Kendrick *et al.* 2018). Elevated N export to aquatic systems could fuel algal blooms in N-limited freshwaters (Myrstener *et al.* 2018) and coastal high-latitude oceans (Tank *et al.* 2012). Understanding the net effect of temperature and other watershed characteristics on N retention (Figure 4.1) is vital to predicting the partitioning of N between inland regions and downstream coastal marine systems.

Prior studies of temperature effects on N retention at various spatial scales have yielded mixed results. In a pond warming experiment in Finland, Kankaala *et al.* (2002) found that warming did not influence N retention during the three-year study period. On a regional scale, Schaefer and Alber (2007) found that warmer temperatures positively impacted N retention for watersheds in the eastern United States. Howarth *et al.* (2012) found similar results for watersheds in the United States and western Europe. The net effect of temperature increase on N retention at a circumpolar scale remains uncertain due to a unique confluence in the northern high latitudes of large N pools, low rates of biological activity, and the potential for rapid changes to flow paths as permafrost thaws.

Here, we aimed to clarify the effect of temperature variability on N retention using mixed effects modeling to disentangle the drivers of N retention for watersheds spanning the tundra and boreal forest biomes. Our results will shed light on the fate of anthropogenic N inputs at high latitudes—what proportion is retained versus exported, with implications for altering N-mediated dynamics in inland systems and downstream marine systems? In particular, we test two alternate hypotheses:

(a) Temperature will have a net positive impact on N retention by stimulating processes including organismal N uptake and denitrification.

(b) Temperature will have a net negative impact on N retention by stimulating processes including permafrost thaw and N leaching from soils.

Methods

To test our hypotheses, we created a database of watersheds from the tundra and boreal zones containing previously published information available in the literature about atmospheric N deposition, watershed characteristics, and N export (Table S4.1). We included data from observational monitoring sites or control watersheds in an experimental setting; we excluded experimentally-manipulated watersheds.

We conducted a systematized review (Grant *et al.* 2009) of literature reporting annual export load of total nitrogen (TN) for watersheds of all sizes in boreal and tundra biomes. We searched for such data in both peer-reviewed journals and government monitoring reports. In contrast to a systematic review, our systematized review was not limited to literature returned from a rigid, pre-determined keyword-based search algorithm or set of methods (Grant *et al.* 2009). Given the broad, multi-disciplinary array of research that quantifies TN export, we felt this systematized review method would

capture the widest range of suitable sites for our analysis. In total we obtained annual TN export values for 98 combinations of watershed and year from 66 unique watersheds to include in our analysis (Figure 4.2). Some entries in the dataset (38 of 98) reported TN export as the annual average of a multi-year period; these multi-year average entries were each treated as a single replicate in our mixed modeling analysis (described below). Seven watersheds in the dataset reported annual TN export values for multiple individual years; in these cases, each year within site was treated as its own replicate, and "site" was treated as a random effect in the model.

In cases where specific chemical forms of TN export were reported (49 of 98 cases), loss of dissolved organic nitrogen dominated, accounting for a mean proportion of 0.802 of TN export (standard error = 0.039). This percentage correlated positively with both mean annual temperature (°C; coefficient estimate = 0.018, standard error = 0.006) and atmospheric deposition of inorganic nitrogen (kg N km^{-2} yr^{-1}; coefficient estimate = 0.004, standard error = 0.001).

For the watersheds in our analyses, we also extracted characteristics including temperature, runoff, watershed area, soil organic carbon content, and presence of permafrost in the watershed. These characteristics were selected for their potential to influence N retention, either directly or by proxy. For example, both runoff and permafrost presence could reduce retention via rapid hydrologic removal of soluble N forms. Further, larger watersheds may provide greater total N stocks for mobilization and aquatic export (Perakis and Hedin 2007). Soil organic carbon content is associated with organic N concentration (Murphy 2015, Palmer *et al.* 2017), thus serving as a proxy of the dominant high-latitude soil N pool available for export.

Some of these characteristics were not reported in the studies we analyzed. In such cases, we extracted the values for the corresponding watershed and time period from spatially explicit, publicly available datasets. For example, where mean annual temperature and/or annual precipitation totals were not reported for a given watershed, we obtained these values from Matsuura and Willmott (2015a, 2015b). Where nitrogen deposition levels were not reported, we obtained these values from Ackerman *et al.* (2018). Where permafrost presence and extent were not reported, permafrost data were obtained from Brown *et al.* (2002). Soil organic carbon content data for the top 30 cm of soil were obtained from Wieder *et al.* (2014).

Some watershed characteristics that likely influence N retention could not be incorporated into our analysis due to a lack of suitable circumarctic data; such characteristics include watershed residence time, soil N pool size, N fixation, and denitrification.

Mixed effects modeling

We created two linear mixed effects models with proportional N retention as a response variable. The proportion of nitrogen retained within a watershed (R_p) was calculated as:

$$R_P = 1 - {}^{E}/_{I}$$

where E is the area-normalized stream export of total N (kg N km^{-2} yr^{-1}), and I is the area-normalized atmospherically deposited inorganic N across the watershed (kg N km^{-2} yr^{-1}). We used these proportional (rather than absolute) deposition models to control for variability in atmospheric N deposition among watersheds, thereby isolating some of the key watershed characteristics hypothesized to mediate N retention. This approach is similar to that described by Howarth *et al.* (1996), who calculated N retained as a proportion of net anthropogenic nitrogen inputs (NANI). In their framework, agriculture

and atmospheric deposition are the principal NANI sources, whereas in our study atmospheric deposition alone dominates NANI sources.

The first mixed effects model (hereafter "full proportional retention model") included all relevant predictor variables in our dataset, which were mean annual temperature, watershed area, annual runoff, topsoil organic carbon content, and permafrost presence within the watershed. Next, we created a "parsimonious proportional retention model," which excluded the terms from the full model that were not shown to be significant at the alpha = 0.05 level. In both the full and parsimonious proportional N deposition models, we included site as a random effect.

Complementary to these two proportional deposition models, we created a model (hereafter "absolute retention model") with total N retained per km^2 (R_A) as the response variable, calculated as:

$$R_A = I - E$$

where I and E are area-normalized N atmospheric inputs and stream exports, respectively, as in the prior equation. This absolute retention model was intended to test our assumption that variability in absolute rates of N retention in circumarctic watersheds was strongly related to atmospheric deposition. This model included just temperature and atmospheric N deposition as predictor variables. We included site as a random effect.

Finally, to explore the factors controlling watershed N export, we created a model with area-normalized N export (kg N km^{-2} yr^{-1}) as the response variable. Fixed effects included mean annual temperature, area-normalized atmospheric N deposition, annual runoff, topsoil organic carbon content, and permafrost presence within the watershed. We

included site as a random effect. All mixed effects models were run with the R package *nlme* (Pinheiro *et al.* 2018).

Results

Our full proportional retention model revealed a positive relationship between proportional N retention and mean annual temperature (Table 4.1). N retention increased with temperature, matching expectations of alternate hypothesis (a). Other predictor variables were not significantly related to nitrogen retention at the alpha = 0.05 level, including watershed area, annual runoff, surface soil organic carbon content, and permafrost presence. The marginal R^2 of the full model, which accounts for variability explained by the model's fixed effects, was 0.25 (Nakagawa & Schielzeth 2013). Conditional R^2, which additionally accounts for variability explained by random effects (i.e. site), was 0.38.

Similar to the full model, the parsimonious model showed mean annual temperature was a highly significant predictor of nitrogen retention ($p < 0.001$). However, the marginal R^2 of the parsimonious model was just 0.16, indicating that 84% of the variability in proportional nitrogen retention was not explained by temperature (Figure 4.3). The conditional R^2 of the parsimonious model was 0.42. Comparison of Akaike information criteria (AIC) suggested that the full proportional model (AIC = 452) was preferable to the parsimonious model (AIC = 519).

Our absolute retention model strongly supported our assumption that atmospheric N deposition was a highly significant driver of the total mass of N retained within strongly N-limited high-latitude watersheds ($p < 0.001$, Figure 4.4, Table 4.2). The other fixed effect in the absolute retention model, mean annual temperature, was not significant

at the alpha = 0.05 level. Marginal R^2 was 0.95 and conditional R^2 was 0.97, indicating the dominance of N deposition alone as a driver of total ecosystem N retention. The intercept in this model was estimated to be -79 kg N km^{-2} yr^{-1} (standard error = 21; Table 4.2), due to a range of negative retention values (i.e. net N loss) for watersheds with near-zero rates of atmospheric N deposition.

We found that annual watershed N export was weakly positively related to both annual runoff ($p = 0.03$) and a second-order coefficient for N deposition ($p = 0.04$). No other fixed effects were associated with N export at an alpha = 0.05 level (Table S4.2).

Discussion

Nitrogen retention

Watershed retention of external N inputs is a key ecosystem function that determines terrestrial and aquatic production, and an important indicator of response to human-driven perturbations. In our analyses of N balance of circumpolar watersheds, temperature was the only factor significantly associated with proportion of atmospherically deposited N retained. This positive relationship supports a net positive impact of warming on N retention (hypothesis a), likely by stimulating organismal N uptake and denitrification. This outcome also matches results of Schaefer and Alber (2007) and Howarth *et al.* (2012), who conducted similar analyses in temperate watersheds. Schaefer and Alber (2007) additionally reported a threshold in N retention, whereby watersheds with mean annual temperatures below a breakpoint of 10-12°C retained a smaller proportion of N inputs, likely due to lower denitrification rates below this temperature breakpoint. We did not find a similar temperature breakpoint in our proportional N retention model, because mean annual temperature in all of our

watersheds analyzed was well below 10-12°C. However, we did find differences in proportional N retention among categories of permafrost cover; watersheds with continuous or discontinuous permafrost generally retained a smaller proportion N inputs compared to watersheds with less permafrost cover (Figure S4.2; see also *nitrogen export* section).

As temperatures continue to warm across boreal and tundra biomes, our results suggest that an increasing proportion of atmospherically deposited N will be retained within most high-latitude watersheds, potentially fueling denitrification and/or accelerating a vegetation shift toward low N-use efficiency species like deciduous shrubs (Mekonnen *et al.* 2018). Consequently, proportionally less N may be exported to downstream systems. However, these potential effects of rising temperatures may be weak or variable among watersheds, indicated by the unexplained variability in our proportional N retention model. Schaefer and Alber (2007) found that proportional N retention was inversely related to runoff in temperate regions. Our high-latitude model did not reproduce this finding, perhaps due to the considerable variability in watershed structure in our study, which included multiple stream orders and runoff rates ranging from 124 to 3667 mm yr^{-1}. The presence of permafrost in many of our study watersheds may further complicate a potential relationship between runoff and N retention.

Our model of absolute N retention (rather than proportional N retention) supports our assumption that atmospheric N deposition is the principal determinant of the total mass of N retained within the watershed. Many studies, including our own proportional retention models, control for atmospheric deposition by reporting only proportional N retention and/or export. However, a quantitative understanding of the relationship

between absolute N deposition and retention is useful for constructing N budgets and predicting N export to downstream ecosystems. This task is particularly pressing as N deposition levels change throughout the Arctic. For example, N deposition is declining in Scandinavia but increasing in western Canada (Ackerman *et al.* 2018), while extreme deposition events modify these long-term trends (Hodson *et al.* 2005, Choudhary *et al.* 2016). Along with warming temperatures, these changes in N inputs to high-latitude watersheds will likely impact N-mediated ecosystem processes like productivity or denitrification.

Nitrogen export

We found that annual N export was weakly positively related to annual runoff and to a second-order coefficient of N deposition rate (i.e., the effect size of N deposition on export was greater for higher deposition values). These two relationships are likely explained by hydrologic N mobilization and increasing availability of mobile N forms with higher rates of deposition, respectively. The lack of significant relationship with the other variables in the dataset may be due to limited availability of spring seasonal data. Because the spring freshet is responsible for a disproportionately high level of annual N export (Holmes *et al*. 2012, McClelland *et al*. 2014), poorly resolved spring sampling may result in some error in annual export values.

Notably, our analysis revealed 13 unique watersheds (and a total of 28 unique combinations of year-within-watershed) with significant N export, despite near-zero atmospheric deposition rates. For these watersheds, total N export exceeded atmospheric inputs by between 11 and 653 kg N km^{-2} yr^{-1} (Figure 4.5). Conditions in these watersheds were representative of much of the arctic tundra biome—generally cold and remote from

direct anthropogenic modification. Mean annual temperature did not explain variability in N retention/export among these particular watersheds (Table S4.3), as was the case for our broader circumarctic dataset. We suggest three potential causes of the apparent net loss of nitrogen from these watersheds.

First, atmospheric N deposition could be underestimated if, for example, organic N deposition were disproportionately greater at these colder sites. However, we are not aware of evidence supporting this potential explanation. Organic N deposition comprises less than 5 percent of total N (inorganic plus organic) deposition across most high-latitude regions (Ackerman *et al.* 2018), so organic N deposition is thus highly unlikely to account for the differences of up to 653 kg N km^{-2} yr^{-1} between export and deposition. Our estimates of inorganic N deposition are well-validated across space and time (Ackerman *et al.* 2018; Table S4.4). Overall, error in N deposition estimates are not likely to account for net N losses from the 13 watersheds.

The second potential cause of apparent net N loss for these watersheds could be linked to inputs from biological N fixation. Biological N fixation is generally low at higher latitudes (Wang *et al.* 2009) and suppressed by colder temperatures (Hobara *et al.* 2006, Houlton *et al*. 2008, but see Rousk *et al.* 2018). Still, biological fixation can exceed atmospheric N deposition by an order of magnitude where atmospheric deposition is low (Shaver *et al.* 2014). However, annual N fixation across the colder regions of the high latitudes, which varies between 7 and 380 kg N km^{-2} yr^{-1} (Table S4.4), is likely insufficient to account for the N loss from all 13 watersheds, for which export exceeds deposition by up to 653 kg N km^{-2} yr^{-1}, with an average exceedance of 126 kg N km^{-2} yr^{-1}.

Finally, ongoing warming-induced permafrost thaw and leaching could export N that has long been part of the soil N pool, stored in permafrost or in the active layer. We believe this to be the primary explanation for net N loss from watersheds with near-zero atmospheric deposition, given that all of the watersheds with net N export were in areas of continuous or discontinuous permafrost. Jones *et al.* (2005) and Walter Anthony *et al.* (2014) have also noted a connection between permafrost and N mobilization at high latitudes. N export associated with permafrost thaw is also consistent with a long-term trend of increasing N export at high latitudes (Frey *et al.* 2007, Frey and McClelland 2009, Harms *et al.* 2014, Abbott *et al.* 2015, Treat *et al.* 2016, Kendrick *et al.* 2018).

Permafrost-derived N is dominated by organic N forms and is mobilized predominantly during spring snowmelt (McClelland *et al*. 2014). Given the cold temperatures and low nitrate availability at this time of year, most permafrost-derived N is likely exported to downstream systems with relatively little denitrification. While freshwater productivity at high latitudes is most often phosphorus-limited (Peterson *et al.* 1993, Slavik *et al.* 2004, Kendrick *et al.* 2018), N-limited freshwater hotspots, including stream biofilms in arctic Sweden (Myrstener *et al.* 2018), and coastal zones could be particularly sensitive to elevated N fluxes (Levine and Whalen 2001, Tank *et al.* 2012). In addition to permafrost thaw, meltwater from receding glaciers and ice caps may additionally export N from high-latitude watersheds (Telling *et al*. 2011, Wadham *et al*. 2013, Lawson *et al*. 2014, Wadham *et al*. 2016).

The Arctic Ocean is the ultimate receiving body for a majority of the N exported from watersheds examined in this study. Changes in high-latitude N export caused by increased N deposition or temperature could therefore impact Arctic Ocean primary

productivity, especially in nearshore regions (Tank *et al.* 2012). Our finding of a positive relationship between temperature and the proportion of N retained across high latitude watersheds indicates that future warming could limit riverine N export to the Arctic Ocean, assuming constant N deposition rates. Alternatively, this potential reduction in N export could be outweighed in some watersheds by increased export of N (particularly organic N forms) leached from gradually thawing soils or abrupt thermokarst events (Lepistö *et al.* 2008, Treat *et al.* 2016, Kendrick *et al.* 2018). Future increases in high-latitude precipitation and subsequent runoff could also elevate downstream N delivery, as suggested by our finding of a positive association between annual watershed runoff and N export (Table S4.2). Finally, some high-latitude watersheds, particularly those in northern Europe, may act as N sources following years of elevated N deposition rates (Worral *et al*. 2012). Further research is needed to determine the relative importance of these processes within a given watershed. Understanding connections between continental nutrient inputs and marine productivity is particularly urgent as sea ice coverage declines and light availability for phytoplankton increases (Post *et al.* 2008).

Conclusion

Proportional N retention in high-latitude watersheds remained remarkably constant across a range of environmental variables. Mean annual temperature was the only significant (positive) control on proportional N retention, though accounting for temperature still left significant unexplained variability in retention rates across watersheds. These results suggest that continued warming may on average increase the proportion of atmospherically deposited N retained in watersheds versus exported to downstream systems including the Arctic Ocean, though the strength of this trend will be

difficult to predict for any given watershed and may be counteracted by rapid permafrost thaw. Our study also highlighted the dominant influence of atmospheric N deposition on absolute rates of N retention at high latitudes. This finding implies that future changes in N emissions will have strong impacts on high-latitude nitrogen dynamics, including export rates from inland watersheds to N-limited marine systems. Our study suggests that anthropogenic changes to temperature and N deposition will continue to impact arctic and boreal landscapes. Further research into the controls on N fixation and denitrification in these systems will allow for the development of more accurate process-based models of N dynamics across the circumpolar north.

Acknowledgements

This work was supported by the National Science Foundation Graduate Research Fellowships Program (grant #00039202). We thank Dr. Sarah Hobbie and Dr. Jim Cotner for their thoughtful feedback on drafts of this work. The authors declare no conflicts of interest.

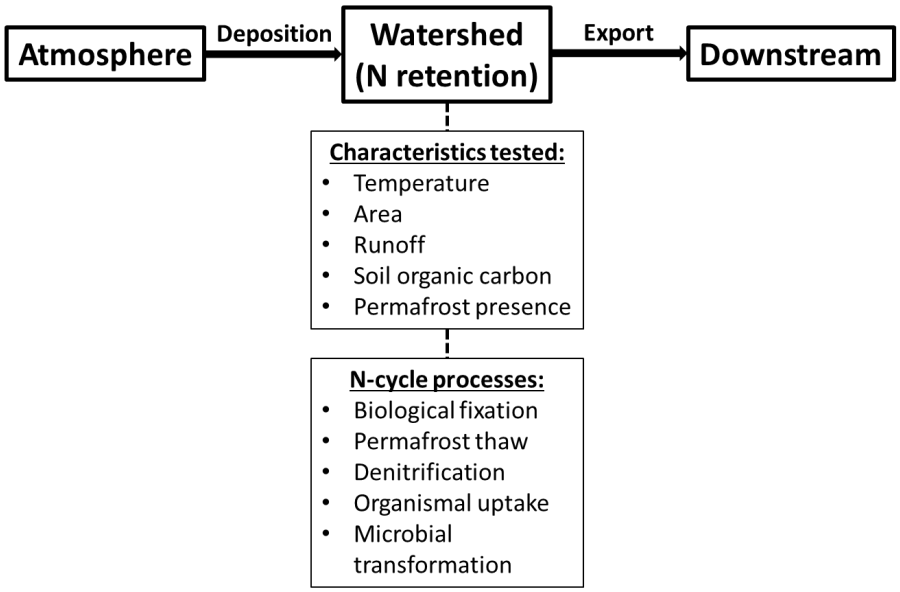

Figure 4.1. Conceptual model of nitrogen transport and watershed retention. The top row of boxes indicates the broad flow of nitrogen from atmosphere to watershed to downstream freshwater and marine ecosystems. For each watershed in our dataset, we tested five hypothesized drivers ("Characteristics tested") for impacts on N retention, which may occur via a range of potential processes ("N-cycle processes").

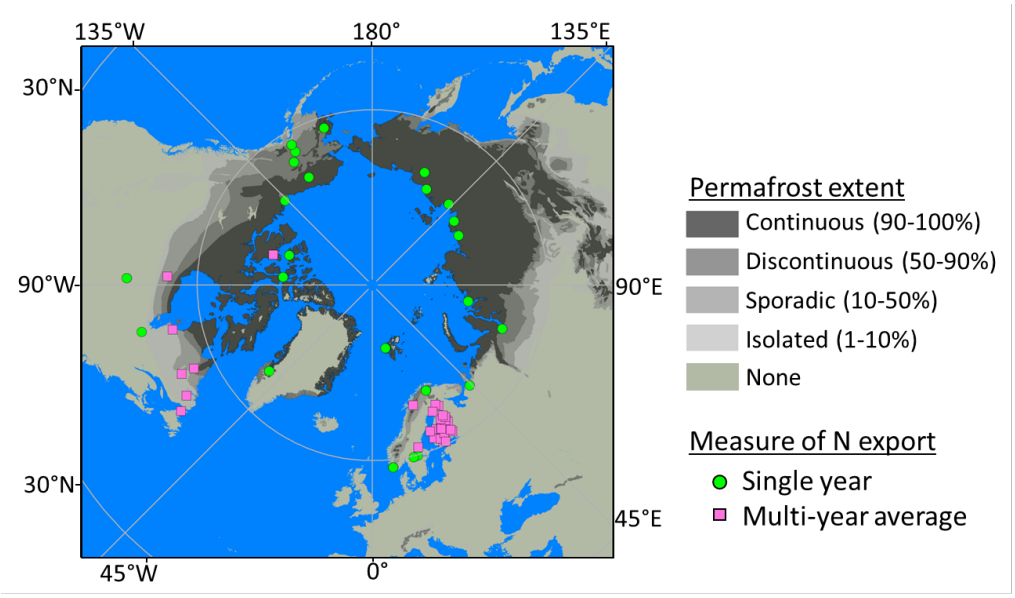

Figure 4.2. Circumpolar stream and river sites with total annual N export measurements used in this analysis. Some sites report export data for individual years (green circles), while other sites report export data as the annual average of multi-year periods (pink squares). Shaded overlay indicates the permafrost extent in a given region (Brown *et al.* 2002).

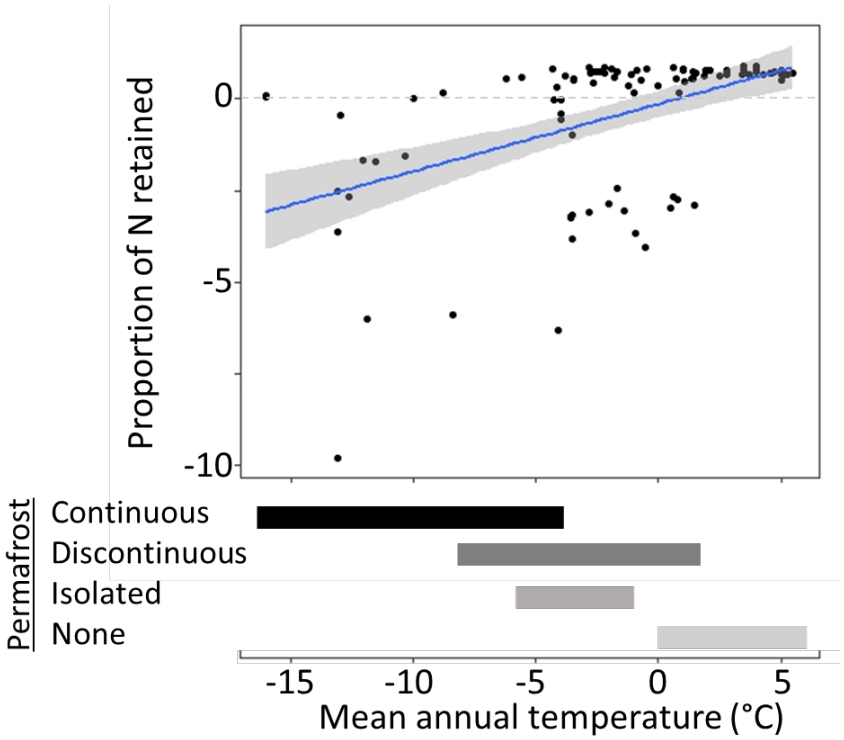

Figure 4.3. Proportional (i.e. area-normalized) N retention was positively related to mean annual temperature for 98 combinations of watersheds and years (from 66 unique watersheds) across the circumpolar north. Gray shaded area represents the standard error of the slope coefficient. Horizontal dashed line indicates a value of 0, where area-normalized retention equals export. Watersheds above this line had positive net N retention, while watersheds below this line had net N loss. Horizontal bars below graph indicate the temperature range of watersheds with various permafrost extents (Brown *et al.* 2002). Only two watersheds had "sporadic" permafrost extent, so this category was combined with "isolated."

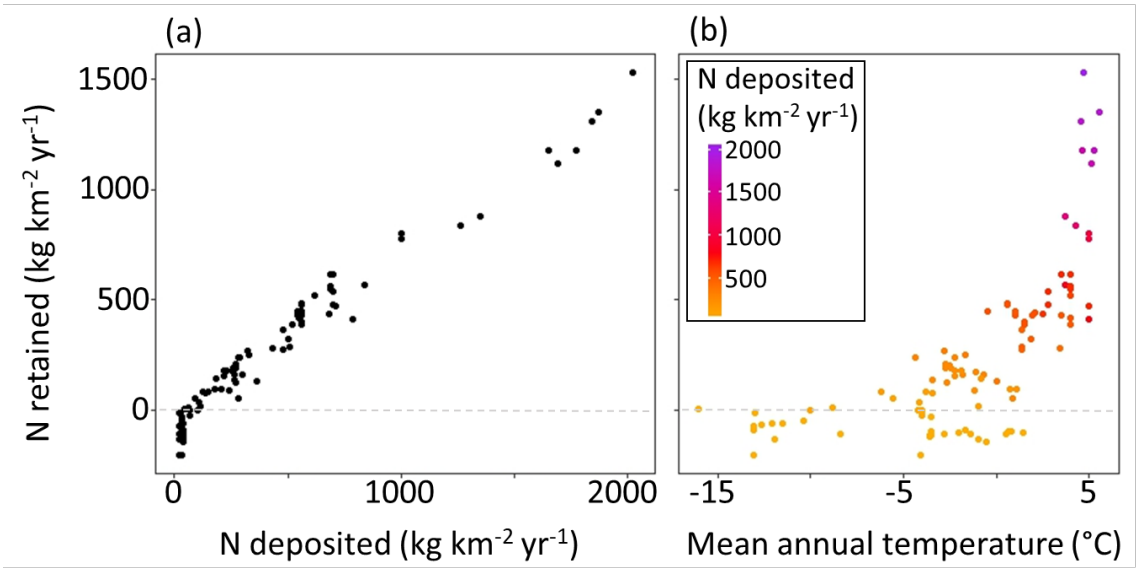

Figure 4.4. Absolute mass of nitrogen retained was positively related to both (a) atmospheric N deposition and (b) mean annual temperature. However, N deposition and mean annual temperature themselves were autocorrelated (r = 0.67), as shown by colors in (b). Mixed effects modeling reveals that N deposition, not temperature, was the primary driver of absolute N retention rates.

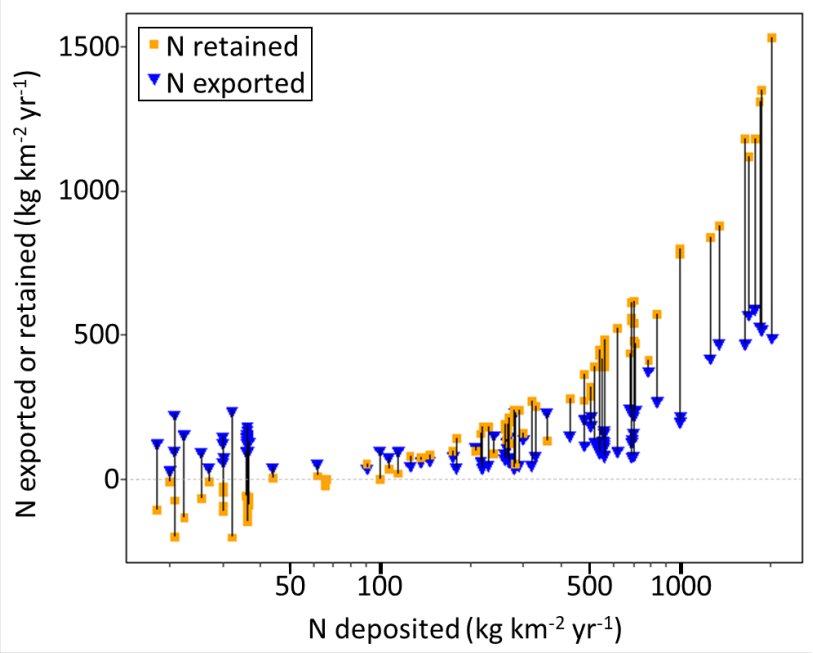

Figure 4.5. Annual nitrogen export via streams and rivers and watershed retention versus atmospheric deposition for 98 high-latitude watersheds. Retention and export values for corresponding watersheds are connected by vertical lines. Export exceeded retention for 28 combinations of watershed and year, in 13 unique watersheds with low deposition levels. Deposition is displayed on a log scale.

Table 4.1. Fixed effects coefficient estimates for the full and parsimonious proportional nitrogen retention models.

	Full model			**Parsimonious model**		
	AIC = 452			AIC = 519		
	$R^2_{conditional}$ = 0.38, $R^2_{marginal}$ = 0.25			$R^2_{conditional}$ = 0.42, $R^2_{marginal}$ = 0.16		
Parameter	Estimate	Standard Error	*p*	Estimate	Standard Error	*p*
Intercept	0.334	0.820	0.686	-0.233	0.391	0.55
Mean annual temperature (°C)	0.282	0.125	**0.041**	0.257	0.065	**<0.001**
Watershed area (km^2)	<0.001	<0.001	0.245		Excluded	
Runoff (mm/yr)	-0.001	0.001	0.294		Excluded	
Soil organic carbon (% weight)	0.017	0.053	0.750		Excluded	
Permafrost presence	-1.447	1.439	0.319		Excluded	

Table 4.2. Fixed effect coefficient estimates for the absolute nitrogen deposition model.

Absolute retention model $R^2_{conditional} = 0.97$, $R^2_{marginal} = 0.95$			
Parameter	Estimate	Standard Error	*p*-value
Intercept	-78.525	21.356	<0.001
N deposition (kgN km^{-2} yr^{-1})	0.828	0.040	**<0.001**
Mean annual temperature (°C)	1.965	2.606	0.456

Bibliography

Abbott, B. W., Jones, J. B., Godsey, S. E., Larouche, J. R., & Bowden, W. B. (2015). Patterns and persistence of hydrologic carbon and nutrient export from collapsing upland permafrost. *Biogeosciences*, *12*(12), 3725-3740.

Ackerman, D. & Breen, A. (2016). Infrastructure Development Accelerates Range Expansion of Trembling Aspen (Populus tremuloides, Salicaceae) into the Arctic. *Arctic*, *69*, 130-136.

Ackerman, D., Griffin, D., Hobbie, S. E., & Finlay, J. C. (2017). Arctic shrub growth trajectories differ across soil moisture levels. Global Change Biology, 23(10), 4294-4302.

Ackerman, D., Millet, D. B., & Chen, X. (2018). Global estimates of inorganic nitrogen deposition across four decades. *Global Biogeochemical Cycles*.

Badding, M. E., Briner, J. P., & Kaufman, D. S. (2013). 10Be ages of late Pleistocene deglaciation and Neoglaciation in the north-central Brooks Range, Arctic Alaska. *Journal of Quaternary Science*, *28*(1), 95-102.

Bär, A, Bräuning, A, & Löffler, J. (2006). Dendroecology of dwarf shrubs in the high mountains of Norway–A methodological approach. *Dendrochronologia*, *24***,** 17-27.

Baron, J. S., Hall, E. K., Nolan, B. T., Finlay, J. C., Bernhardt, E. S., Harrison, J. A., Chan, F. & Boyer, E. W. (2013). The interactive effects of excess reactive nitrogen and climate change on aquatic ecosystems and water resources of the United States. *Biogeochemistry*, *114*(1-3), 71-92.

Berner LT, Alexander HD, Loranty MM, Ganzlin P, Mack MC, Davydov SP, Goetz SJ (2015) Biomass allometry for alder, dwarf birch, and willow in boreal forest and tundra ecosystems of far northeastern Siberia and north-central Alaska. *Forest Ecology and Management*, **337**, 110-118.

Bey, I., D. J. Jacob, R. M. Yantosca, J. A. Logan, B. Field, A. M. Fiore, Q. Li, H. Liu, L. J. Mickley, and M. Schultz. 2001. Global modeling of tropospheric chemistry with assimilated meteorology: Model description and evaluation. *J. Geophys. Res*., 106, 23,073-23,096.

Black, B. A., Von Biela, V. R., Zimmerman, C. E., & Brown, R. J. (2013). Lake trout otolith chronologies as multidecadal indicators of high-latitude freshwater ecosystems. Polar biology, 36(1), 147-153.

Blok, D., Heijmans, M. M. P. D., Schaepman-Strub, G., Kononov, A. V., Maximov, T. C., & Berendse, F. (2010). Shrub expansion may reduce summer permafrost thaw in Siberian tundra. *Global Change Biology*, *16*(4), 1296-1305.

Blok, D., et al. "The cooling capacity of mosses: controls on water and energy fluxes in a Siberian tundra site." *Ecosystems* 14.7 (2011a): 1055-1065.

Blok, D., Sass-Klaassen, U., Schaepman-Strub, G., Heijmans, M. M. P. D., Sauren, P., & Berendse, F. (2011b). What are the main climate drivers for shrub growth in Northeastern Siberian tundra?. *Biogeosciences*, *8*(5), 1169-1179.

Bloom AJ, Chapin FS, Mooney HA (1985) Resource limitation in plants--an economic analogy. *Annual review of Ecology and Systematics*, 363-392.

Bobbink, R., Hicks, K., Galloway, J., Spranger, T., Alkemade, R., Ashmore, M., ... & Emmett, B. (2010). Global assessment of nitrogen deposition effects on terrestrial plant diversity: a synthesis. *Ecological applications*, *20*(1), 30-59.

Bobbink, R., & Hicks, W. K. (2014). Factors affecting nitrogen deposition impacts on biodiversity: An overview. In *Nitrogen Deposition, Critical Loads and Biodiversity* (pp. 127-138). Springer, Dordrecht.

Boelman NT, Gough L, Wingfield J, *et al*. (2015) Greater shrub dominance alters breeding habitat and food resources for migratory songbirds in Alaskan arctic tundra. *Global Change Biology*, **21**, 1508-1520.

Bolund, P., & Hunhammar, S. (1999). Ecosystem services in urban areas. *Ecological economics*, *29*(2), 293-301.

Bowden, W. B., Peterson, B. J., Deegan, L. A., Huryn, A. D., Benstead, J. P., Golden, H., ... & Hobbie, J. E. (2014). Ecology of streams of the Toolik region. *Alaska's changing arctic: Ecological consequences for tundra, streams, and lakes, ed. JE Hobbie, and GW Kling*, 173-258.

Brender, J. D., Weyer, P. J., Romitti, P. A., Mohanty, B. P., Shinde, M. U., Vuong, A. M., ... & Huber Jr, J. C. (2013). Prenatal nitrate intake from drinking water and selected birth defects in offspring of participants in the National Birth Defects Prevention Study. *Environmental health perspectives*, *121*(9), 1083-1089.

Bret-Harte, M. S., Shaver, G. R., Zoerner, J. P., Johnstone, J. F., Wagner, J. L., Chavez, A. S., ... & Laundre, J. A. (2001). Developmental plasticity allows Betula nana to dominate tundra subjected to an altered environment. *Ecology*, *82*(1), 18-32.

Bret-Harte, M. S., Shaver, G. R., & Chapin, F. S. (2002). Primary and secondary stem growth in arctic shrubs: implications for community response to environmental change. Journal of Ecology, 90(2), 251-267.

Briffa K, Jones PD (1990) Basic chronology statistics and assessment. In Methods of Dendrochronology: Applications in the Environmental Sciences (Eds Cook ER, Kairiukstis LA), pp. 137–152, Kluwer Academic Publishers, Dordrecht, Netherlands.

Brown, J., O. Ferrians, J. A. Heginbottom, and E. Melnikov. 2002. *Circum-Arctic Map of Permafrost and Ground-Ice Conditions, Version 2*. Boulder, Colorado USA. NSIDC: National Snow and Ice Data Center. [Accessed 6/1/2017].

Buchwal A, Rachlewicz G, Fonti P, Cherubini P, Gärtner H (2013) Temperature modulates intra-plant growth of *Salix polaris* from a high Arctic site (Svalbard). *Polar Biology*, **36**, 1305-1318.

Carlson, K. M., Curran, L. M., Asner, G. P., Pittman, A. M., Trigg, S. N., & Adeney, J. M. (2013). Carbon emissions from forest conversion by Kalimantan oil palm plantations. *Nature Climate Change*, *3*(3), 283.

Carpenter, S. R., Caraco, N. F., Correll, D. L., Howarth, R. W., Sharpley, A. N., & Smith, V. H. (1998). Nonpoint pollution of surface waters with phosphorus and nitrogen. *Ecological applications*, *8*(3), 559-568.

Carter, L. D. (1981). A Pleistocene sand sea on the Alaskan Arctic coastal plain. *Science*, 211: 381-383.

Chapin, F. S. (1983). Direct and indirect effects of temperature on arctic plants. *Polar Biology*, *2*(1), 47-52.

Chapin, F. S., Fetcher, N., Kielland, K., Everett, K. R., & Linkins, A. E. (1988). Productivity and nutrient cycling of Alaskan tundra: enhancement by flowing soil water. *Ecology*, *69*(3), 693-702.

Chapin, F. S., & Shaver, G. R. (1989). Differences in growth and nutrient use among arctic plant growth forms. *Functional Ecology*, 73-80.

Chapin, F. S., Shaver, G. R., Giblin, A. E., Nadelhoffer, K. J., & Laundre, J. A. (1995). Responses of arctic tundra to experimental and observed changes in climate. *Ecology*, *76*(3), 694-711.

Chapin, F. S., & Shaver, G. R. (1996). Physiological and growth responses of arctic plants to a field experiment simulating climatic change. *Ecology*, *77*(3), 822-840.

Chapin, F. S., et al. "Role of land-surface changes in Arctic summer warming." *Science* 310.5748 (2005): 657-660.

Cherry JE, Dery SJ, Cheng Y, Stieglitz M, Jacobs AS, Pan F (2014). Climate and Hydrometeorology of the Toolik Lake Region and the Kuparuk River Basin. In: Alaska's Changing Arctic (Eds Hobbie JE, Kling GW), pp. 21-60, Oxford University Press, New York, United States.

Choudhary, S., Blaud, A., Osborn, A. M., Press, M. C., & Phoenix, G. K. (2016). Nitrogen accumulation and partitioning in a High Arctic tundra ecosystem from extreme atmospheric N deposition events. *Science of the Total Environment*, *554*, 303-310.

Christie KS, Bryant JP, Gough L, Ravolainen VT, Ruess RW, Tape K (2015) The role of vertebrate herbivores in regulating shrub expansion in the Arctic: a synthesis. *BioScience*, **65**, 1123-1133.

Clark, C. M., & Tilman, D. (2008). Loss of plant species after chronic low-level nitrogen deposition to prairie grasslands. *Nature*, *451*(7179), 712.

Cohen, J. L., Furtado, J. C., Barlow, M. A., Alexeev, V. A., & Cherry, J. E. (2012). Arctic warming, increasing snow cover and widespread boreal winter cooling. *Environmental Research Letters*, *7*(1), 014007.

Conley, D. J., Paerl, H. W., Howarth, R. W., Boesch, D. F., Seitzinger, S. P., Havens, K. E., ... & Likens, G. E. (2009). Controlling eutrophication: nitrogen and phosphorus. *Science*, *323*(5917), 1014-1015.

Cook ER, Kairiukstis, LA (Eds.) (1990) *Methods of dendrochronology: applications in the environmental sciences*. Springer, Netherlands.

Cook ER (1985) A Time Series Approach to Tree-Ring Standardization. Dissertation. University of Arizona, Tucson, Arizona, USA.

Cook ER, Peters K (1981) The smoothing spline: a new approach to standardizing forest interior tree-ring width series for dendroclimatic studies. *Tree-ring bulletin*.

Cook, E. R., Seager, R., Cane, M. A., & Stahle, D. W. (2007). North American drought: Reconstructions, causes, and consequences. *Earth-Science Reviews*, *81*(1-2), 93-134.

Cook, E. R., Anchukaitis, K. J., Buckley, B. M., D'Arrigo, R. D., Jacoby, G. C., & Wright, W. E. (2010). Asian monsoon failure and megadrought during the last millennium. *Science*, *328*(5977), 486-489.

Cook, E. R., & Pederson, N. (2011). Uncertainty, emergence, and statistics in dendrochronology. In *Dendroclimatology* (pp. 77-112). Springer, Dordrecht.

Cook, E. R., Seager, R., Kushnir, Y., Briffa, K. R., Büntgen, U., Frank, D., ... & Baillie, M. (2015). Old World megadroughts and pluvials during the Common Era. *Science advances*, *1*(10), e1500561.

Cowtan, K., & Way, R. G. (2014). Coverage bias in the HadCRUT4 temperature series and its impact on recent temperature trends. Quarterly Journal of the Royal Meteorological Society, 140(683), 1935-1944.

Choudhary, S., Blaud, A., Osborn, A. M., Press, M. C., & Phoenix, G. K. (2016). Nitrogen accumulation and partitioning in a High Arctic tundra ecosystem from extreme atmospheric N deposition events. *Science of the Total Environment*, *554*, 303-310.

Cornelissen, J. HC, et al. "Global change and arctic ecosystems: is lichen decline a function of increases in vascular plant biomass?." *Journal of Ecology* 89.6 (2001): 984-994.

Cornelissen, J. HC, et al. "Global negative vegetation feedback to climate warming responses of leaf litter decomposition rates in cold biomes."*Ecology letters* 10.7 (2007): 619-627.

Cornell, S. E., Jickells, T. D., Cape, J. N., Rowland, A. P., & Duce, R. A. (2003). Organic nitrogen deposition on land and coastal environments: a review of methods and data. *Atmospheric Environment*, *37*(16), 2173-2191.

Crippa, Monica, Greet Janssens-Maenhout, Frank Dentener, Diego Guizzardi, Katerina Sindelarova, Marilena Muntean, Rita Van Dingenen, Claire Granier: Forty years of improvements in European air quality: regional policy-industry interactions with global impacts, Atmos. Chem. Phys., 16, 3825-3841, doi:10.5194/acp-16-3825-2016, 2016.

D'Arrigo R, Wilson R, Liepert B, Cherubini P (2008) On the 'divergence problem'in northern forests: a review of the tree-ring evidence and possible causes. *Global and Planetary Change*, **60**, 289-305.

D'Arrigo R, Jacoby G, Buckley B *et al*. (2009) Tree growth and inferred temperature variability at the North American Arctic treeline. *Global and Planetary Change*, **65**, 71-82.

DeMarco, J., Mack, M. C., Bret-Harte, M. S., Burton, M., & Shaver, G. R. (2014). Long-term experimental warming and nutrient additions increase productivity in tall deciduous shrub tundra. *Ecosphere*, *5*(6), 1-22.

Dentener, F., Drevet, J., Lamarque, J. F., Bey, I., Eickhout, B., Fiore, A. M., ... & Lawrence, M. (2006). Nitrogen and sulfur deposition on regional and global scales: a multimodel evaluation. *Global biogeochemical cycles*, *20*(4).

Dentener, F., Vet, R., Dennis, R. L., Du, E., Kulshrestha, U. C., & Galy-Lacaux, C. (2014). Progress in monitoring and modelling estimates of nitrogen deposition at local, regional and global scales. In *Nitrogen Deposition, Critical Loads and Biodiversity* (pp. 7-22). Springer Netherlands.

Dlugokencky, E.J., P.M. Lang, A.M. Crotwell, J.W. Mund, M.J. Crotwell, and K.W. Thoning (2018), Atmospheric Methane Dry Air Mole Fractions from the NOAA ESRL Carbon Cycle Cooperative Global Air Sampling Network, 1983-2017, Version: 2018-08-01, Path: ftp://aftp.cmdl.noaa.gov/data/trace_gases/ch4/flask/surface/.

Du, E., de Vries, W., Galloway, J. N., Hu, X., & Fang, J. (2014). Changes in wet nitrogen deposition in the United States between 1985 and 2012. *Environmental Research Letters*, *9*(9), 095004.

Ehrich D, Henden JA, Ims RA *et al*. (2012b) The importance of willow thickets for ptarmigan and hares in shrub tundra: the more the better?, *Oecologia*, **168**, 141-151.

Elmendorf, S. C., Henry, G. H., Hollister, R. D., Björk, R. G., Bjorkman, A. D., Callaghan, T. V., ... & Fosaa, A. M. (2012). Global assessment of experimental climate warming on tundra vegetation: heterogeneity over space and time. *Ecology letters*, *15*(2), 164-175.

Elmendorf SC, Henry GH, Hollister RD *et al*. (2012b) Plot-scale evidence of tundra vegetation change and links to recent summer warming. *Nature Climate Change*, **2**, 453-457.

Elser, J. J., Marzolf, E. R., & Goldman, C. R. (1990). Phosphorus and nitrogen limitation of phytoplankton growth in the freshwaters of North America: a review and critique of experimental enrichments. *Canadian Journal of fisheries and aquatic sciences*, *47*(7), 1468-1477.

Elser, J. J., Bracken, M. E., Cleland, E. E., Gruner, D. S., Harpole, W. S., Hillebrand, H., ... & Smith, J. E. (2007). Global analysis of nitrogen and phosphorus limitation of primary producers in freshwater, marine and terrestrial ecosystems. *Ecology letters*, *10*(12), 1135-1142.

Environmental Data Center Team. 2016. Meteorological monitoring program at Toolik, Alaska. Toolik Field Station, Institute of Arctic Biology, University of Alaska Fairbanks, Fairbanks, AK 99775. http://toolik.alaska.edu/edc/abiotic_monitoring/data_query.php

Environmental Data Center Team (2017). Meteorological monitoring program at Toolik, Alaska. Toolik Field Station, Institute of Arctic Biology, University of Alaska Fairbanks, Fairbanks, AK. http://toolik.alaska.edu/edc/abiotic_monitoring/data_query.php

Fairlie, T.D., D.J. Jacob, and R.J. Park, *The impact of transpacific transport of mineral dust in the United States*, Atmos. Environ., 1251-1266, 2007.

Fan, Y., & van den Dool, H. (2004). Climate Prediction Center global monthly soil moisture data set at 0.5 resolution for 1948 to present. *Journal of Geophysical Research: Atmospheres*, *109*(D10).

Field, R. D., Van Der Werf, G. R., & Shen, S. S. (2009). Human amplification of drought-induced biomass burning in Indonesia since 1960. *Nature Geoscience*, *2*(3), 185.

Finlay, J. C., Small, G. E., & Sterner, R. W. (2013). Human influences on nitrogen removal in lakes. *Science*, *342*(6155), 247-250.

Fisher, J.A., D.J. Jacob, Q. Wang, R. Bahreini, C.C. Carouge, M.J. Cubison, J.E. Dibb, T. Diehl, J.L. Jimenez, E.M. Leibensperger, M.B.J. Meinders, H.O.T. Pye, P.K. Quinn, S. Sharma, A. van Donkelaar, & R.M. Yantosca, Sources, distribution, and acidity of sulfate-ammonium aerosol in the Arctic in winter-spring, Atmos. Environ., 45, 7301-7318, 2011.

Fonti P, Solomonoff N, García-González I (2007) Earlywood vessels of Castanea sativa record temperature before their formation. *New Phytologist*, **173**, 562-570.

Forbes BC, Macias-Fauria M, Zetterberg P (2010) Russian Arctic warming and 'greening' are closely tracked by tundra shrub willows. *Global Change Biology*, **16**, 1542-1554.

Frey, K. E., McClelland, J. W., Holmes, R. M., & Smith, L. C. (2007). Impacts of climate warming and permafrost thaw on the riverine transport of nitrogen and phosphorus to the Kara Sea. *Journal of Geophysical Research: Biogeosciences*, *112*(G4).

Frey, K. E., & McClelland, J. W. (2009). Impacts of permafrost degradation on arctic river biogeochemistry. *Hydrological Processes: An International Journal*, *23*(1), 169-182.

Fountoukis, C., and A. Nenes, ISORROPIA II: A computationally efficient thermodynamic equilibrium model for K+-Ca2+-Mg2+-NH4+-Na+-SO42-NO3--Cl-H2O aerosols, Atmos. Chem. Phys., 7(17), 4639-4659, 2007.

Fowler, D., Smith, R., Muller, J., Cape, J. N., Sutton, M., Erisman, J. W., & Fagerli, H. (2007). Long term trends in sulphur and nitrogen deposition in Europe and the cause of non-linearities. *Water, Air, & Soil Pollution: Focus*, *7*(1-3), 41-47.

Fowler, D., Coyle, M., Skiba, U., Sutton, M. A., Cape, J. N., Reis, S., ... & Vitousek, P. (2013). The global nitrogen cycle in the twenty-first century. Phil. Trans. R. Soc. B, 368(1621), 20130164.

Fritts HC (1976) Tree Rings and Climate, Academic Press, New York, New York.

Galloway, J. N., Dentener, F. J., Capone, D. G., Boyer, E. W., Howarth, R. W., Seitzinger, S. P., ... & Karl, D. M. (2004). Nitrogen cycles: past, present, and future. *Biogeochemistry*, *70*(2), 153-226.

Galloway, J. N., Townsend, A. R., Erisman, J. W., Bekunda, M., Cai, Z., Freney, J. R., ... & Sutton, M. A. (2008). Transformation of the nitrogen cycle: recent trends, questions, and potential solutions. *Science*, *320*(5878), 889-892.

Galván, J. D., Camarero, J. J., & Gutiérrez, E. (2014). Seeing the trees for the forest: drivers of individual growth responses to climate in Pinus uncinata mountain forests. *Journal of Ecology*, *102*(5), 1244-1257.

Gamm, C. M., Sullivan, P. F., Buchwal, A., Dial, R. J., Young, A. B., Watts, D. A., ... & Post, E. Declining growth of deciduous shrubs in the warming climate of continental western Greenland. Journal of Ecology.

Gärtner H, Cherubini P, Fonti P *et al*. (2015) A Technical Perspective in Modern Tree-ring Research-How to Overcome Dendroecological and Wood Anatomical Challenges. *Journal of visualized experiments*, **97**.

Gelaro, R., McCarty, W., Suárez, M. J., Todling, R., Molod, A., Takacs, L., ... & Wargan, K. (2017). The modern-era retrospective analysis for research and applications, version 2 (MERRA-2). *Journal of Climate*, *30*(14), 5419-5454.

GEOS-Chem. <GEOS-Chem.org>. Retrieved April 6, 2018.

Gleeson SK, Tilman D (1992) Plant allocation and the multiple limitation hypothesis. *American Naturalist*, 1322-1343.

Grennfelt, P., & Hultberg, H. (1986). Effects of nitrogen deposition on the acidification of terrestrial and aquatic ecosystems. Water, Air, and Soil Pollution, 30(3-4), 945-963.

Gough L, Shaver GR, Carroll J, Royer DL, Laundre JA (2000) Vascular plant species richness in Alaskan arctic tundra: the importance of soil pH. *Journal of Ecology*, **88**, 54-66.

Gough L, Bettez ND, Slavik KA *et al*. (2016) Effects of long-term nutrient additions on Arctic tundra, stream, and lake ecosystems: beyond NPP. *Oecologia*, **182**, 653-665.

Hamilton, T. D. (2003). Glacial geology of the Toolik Lake and upper Kuparuk River regions. University of Alaska. Institute of Arctic Biology.

Harms, T. K., Abbott, B. W., & Jones, J. B. (2014). Thermo-erosion gullies increase nitrogen available for hydrologic export. *Biogeochemistry*, *117*(2-3), 299-311.

Harms, T. K., Cook, C. L., Wlostowski, A. N., Gooseff, M. N., & Godsey, S. E. Spiraling Down Hillslopes: Nutrient Uptake from Water Tracks in a Warming Arctic. *Ecosystems*, 1-15.

Hayhoe, K., D.J. Wuebbles, D.R. Easterling, D.W. Fahey, S. Doherty, J. Kossin, W. Sweet, R. Vose, and M. Wehner, 2018: Our Changing Climate. In *Impacts, Risks, and Adaptation in the United States: Fourth National Climate Assessment, Volume II* [Reidmiller, D.R., C.W. Avery, D.R. Easterling, K.E. Kunkel, K.L.M. Lewis, T.K. Maycock, and B.C. Stewart (eds.)]. U.S. Global Change Research Program, Washington, DC, USA, pp. 72–144. doi: 10.7930/NCA4.2018.CH2

Hobara, S., McCalley, C., Koba, K., Giblin, A. E., Weiss, M. S., Gettel, G. M., & Shaver, G. R. (2006). Nitrogen fixation in surface soils and vegetation in an Arctic tundra watershed: a key source of atmospheric nitrogen. *Arctic, Antarctic, and Alpine Research*, *38*(3), 363-372.

Hobbie SE (1996) Temperature and plant species control over litter decomposition in Alaskan tundra. *Ecological Monographs*, **66**, 503-522.

Hobbie SE, Chapin III FS (1998) The response of tundra plant biomass, aboveground production, nitrogen, and CO2 flux to experimental warming. *Ecology*, **79**, 1526-1544.

Hobbie, S. E., & Gough, L. (2002). Foliar and soil nutrients in tundra on glacial landscapes of contrasting ages in northern Alaska. Oecologia, 131(3), 453-462.

Hobbie, S. E., Miley, T. A., & Weiss, M. S. (2002). Carbon and nitrogen cycling in soils from acidic and nonacidic tundra with different glacial histories in Northern Alaska. Ecosystems, 5(8), 0761-0774.

Hobbie, S. E., Gough, L., & Shaver, G. R. (2005). Species compositional differences on different-aged glacial landscapes drive contrasting responses of tundra to nutrient addition. *Journal of Ecology*, *93*(4), 770-782.

Hobbie JE, Kling GW (2014) Ecological Consequences of Present and Future Changes in Arctic Alaska. In: Alaska's Changing Arctic (Eds Hobbie JE, Kling GW), pp. 303-324, Oxford University Press, New York, United States.

Hodson, A. J., Mumford, P. N., Kohler, J., & Wynn, P. M. (2005). The High Arctic glacial ecosystem: new insights from nutrient budgets. *Biogeochemistry*, *72*(2), 233-256.

Hollesen J, Buchwal A, Rachlewicz G, Hansen BU, Hansen MO, Stecher O, Elberling B (2015) Winter warming as an important co-driver for Betula nana growth in western Greenland during the past century. *Global Change Biology*, **21**, 2410-2423.

Holmes, R. M., McClelland, J. W., Peterson, B. J., Tank, S. E., Bulygina, E., Eglinton, T. I., ... & Staples, R. (2012). Seasonal and annual fluxes of nutrients and organic matter

from large rivers to the Arctic Ocean and surrounding seas. *Estuaries and Coasts*, *35*(2), 369-382.

Holmes, C. D., Prather, M. J., and Vinken, G. C. M. (2014). The climate impact of ship NOx emissions: an improved estimate accounting for plume chemistry, *Atmos. Chem. Phys.*, 14, 6801-6812, doi:10.5194/acp-14-6801-2014.

Holtgrieve, G. W., Schindler, D. E., Hobbs, W. O., Leavitt, P. R., Ward, E. J., Bunting, L., ... & Lisac, M. J. (2011). A coherent signature of anthropogenic nitrogen deposition to remote watersheds of the northern hemisphere. *Science*, *334*(6062), 1545-1548.

Houlton, B. Z., Wang, Y. P., Vitousek, P. M., & Field, C. B. (2008). A unifying framework for dinitrogen fixation in the terrestrial biosphere. *Nature*, *454*(7202), 327.

Howarth, R. W., Billen, G., Swaney, D., Townsend, A., Jaworski, N., Lajtha, K., ... & Berendse, F. (1996). Regional nitrogen budgets and riverine N & P fluxes for the drainages to the North Atlantic Ocean: Natural and human influences. In *Nitrogen cycling in the North Atlantic Ocean and its watersheds* (pp. 75-139). Springer, Dordrecht.

Howarth, R. W., & Marino, R. (2006). Nitrogen as the limiting nutrient for eutrophication in coastal marine ecosystems: evolving views over three decades. *Limnology and Oceanography*, *51*(1part2), 364-376.

Howarth, R., Swaney, D., Billen, G., Garnier, J., Hong, B., Humborg, C., ... & Marino, R. (2012). Nitrogen fluxes from the landscape are controlled by net anthropogenic nitrogen inputs and by climate. *Frontiers in Ecology and the Environment,* 10(1), 37-43.

Hudman, R.C., N.E. Moore, R.V. Martin, A.R. Russell, A.K. Mebust, L.C. Valin, and R.C. Cohen. (2012). *A mechanistic model of global soil nitric oxide emissions: implementation and space based-constraints*. *Atm. Chem. Phys.*, **12**, 7779-7795, doi:10.5194/acp-12-7779-2012,

Hugelius, G., Strauss, J., Zubrzycki, S., Harden, J. W., Schuur, E., Ping, C. L., ... & O'Donnell, J. A. (2014). Estimated stocks of circumpolar permafrost carbon with quantified uncertainty ranges and identified data gaps. Biogeosciences, 11(23), 6573-6593.

IPCC (2013) Annex I: Atlas of Global and Regional Climate Projections (eds van Oldenborgh GJ, Collins M, Arblaster JH, *et al*.). In: Climate Change 2013: The Physical Science Basis. Contribution of Working Group I to the Fifth Assessment Report of the Intergovernmental Panel on Climate Change (eds Stocker TF, Qin D, Plattner GK, *et al.*). Cambridge University Press, Cambridge, United Kingdom and New York, NY, USA.

Jaeglé, L., P.K. Quinn, T. Bates, B. Alexander, and J.-T. Lin, Global distribution of sea salt aerosols: New constraints from in situ and remote sensing observations, Atmos. Chem. Phys., 11, 3137-3157, doi:10.5194/acp-11-3137-2011, 2011.

Jia, Y., Yu, G., He, N., Zhan, X., Fang, H., Sheng, W., ... & Wang, Q. (2014). Spatial and decadal variations in inorganic nitrogen wet deposition in China induced by human activity. *Scientific Reports*, 4, 3763.

Jørgensen RH, Hallinger M, Ahlgrimm S, Friemel J, Kollmann J, Meilby H (2015) Growth response to climatic change over 120 years for *Alnus viridis* and *Salix glauca* in West Greenland. *Journal of Vegetation Science*, **26**, 155-165.

Kahmen, A., Renker, C., Unsicker, S. B., & Buchmann, N. (2006). Niche complementarity for nitrogen: an explanation for the biodiversity and ecosystem functioning relationship?. *Ecology*, *87*(5), 1244-1255.

Kanakidou, M., Stelios Myriokefalitakis, Nikos Daskalakis, G. Fanourgakis, Athanasios Nenes, A. R. Baker, K. Tsigaridis, and N. Mihalopoulos. (2016). Past, present, and future atmospheric nitrogen deposition. *Journal of the Atmospheric Sciences,* 73(5), 2039-2047.

Kanakidou, M., Myriokefalitakis, S., & Tsigaridis, K. (2018). Aerosols in atmospheric chemistry and biogeochemical cycles of nutrients. Environmental Research Letters, 13(6), 063004.

Kankaala, P., Ojala, A., Tulonen, T., & Arvola, L. (2002). Changes in nutrient retention capacity of boreal aquatic ecosystems under climate warming: a simulation study. *Hydrobiologia*, *469*(1-3), 67-76.

Keiser, D., Lade, G., & Rudik, I. (2018). Air pollution and visitation at US national parks. *Science advances*, *4*(7), eaat1613.

Kendrick, M. R., Huryn, A. D., Bowden, W. B., Deegan, L. A., Findlay, R. H., Hershey, A. E., ... & Schuett, E. B. (2018). Linking permafrost thaw to shifting biogeochemistry and food web resources in an arctic river. *Global change biology*.

Knorr, M., Frey, S. D., & Curtis, P. S. (2005). Nitrogen additions and litter decomposition: A meta-analysis. *Ecology*, *86*(12), 3252-3257.

Lamarque, J. F., Dentener, F., McConnell, J., Ro, C. U., Shaw, M., Vet, R., ... & Faluvegi, G. (2013). Multi-model mean nitrogen and sulfur deposition from the Atmospheric Chemistry and Climate Model Intercomparison Project (ACCMIP): evaluation of historical and projected future. Atmospheric Chemistry and Physics, 13(LLNL-JRNL-644459).

Larsson L (2013) CooRecorder and Cdendro programs of the CooRecorder/Cdendro package version 7.6.

Lawrence, D. M., & Swenson, S. C. (2011). Permafrost response to increasing Arctic shrub abundance depends on the relative influence of shrubs on local soil cooling versus large-scale climate warming. *Environmental Research Letters*, *6*(4), 045504.

Lawson, E. C., Bhatia, M. P., Wadham, J. L., & Kujawinski, E. B. (2014). Continuous summer export of nitrogen-rich organic matter from the Greenland Ice Sheet inferred by ultrahigh resolution mass spectrometry. *Environmental science & technology*, 48(24), 14248-14257.

LeBauer, D. S., & Treseder, K. K. (2008). Nitrogen limitation of net primary productivity in terrestrial ecosystems is globally distributed. *Ecology*, *89*(2), 371-379.

Lepistö, A., Kortelainen, P., & Mattsson, T. (2008). Increased organic C and N leaching in a northern boreal river basin in Finland. *Global Biogeochemical Cycles*, *22*(3).

Levine, M. A., & Whalen, S. C. (2001). Nutrient limitation of phytoplankton production in Alaskan Arctic foothill lakes. *Hydrobiologia*, *455*(1-3), 189-201.

Li, Y., Schichtel, B. A., Walker, J. T., Schwede, D. B., Chen, X., Lehmann, C. M., ... & Collett, J. L. (2016). Increasing importance of deposition of reduced nitrogen in the United States. Proceedings of the National Academy of Sciences, 113(21), 5874-5879.

Lin, S.-J., and R.B. Rood, 1996: Multidimensional flux form semi-Lagrangian transport schemes, Mon. Wea. Rev., 124, 2046-2070

Lin, J.-T., and M. McElroy, Impacts of boundary layer mixing on pollutant vertical profiles in the lower troposphere: Implications to satellite remote sensing, Atmospheric Environment, 44(14), 1726-1739, doi:10.1016/j.atmosenv.2010.02.009, 2010.

Liu, H., D.J. Jacob, I. Bey, and R.M. Yantosca, Constraints from 210Pb and 7Be on wet deposition and transporting a global threee-dimensional chemical tracer model driven by asimilated meteorological fields, J. Geophys. Res., 106, 12,109-12,128, 2001.

Liu, X., Zhang, Y., Han, W., Tang, A., Shen, J., Cui, Z., ... & Fangmeier, A. (2013). Enhanced nitrogen deposition over China. *Nature*, *494*(7438), 459.

Liu, X. Y., Koba, K., Koyama, L. A., Hobbie, S. E., Weiss, M. S., Inagaki, Y., ... & Sommerkorn, M. (2018). Nitrate is an important nitrogen source for Arctic tundra plants. *Proceedings of the National Academy of Sciences*, *115*(13), 3398-3403.

Mao, J., F. Paulot, D.J. Jacob, R.C. Cohen, J.D. Crounse, P.O. Wennberg, C.A. Keller, R.C. Hudman, M.P. Barkley, and L.W. Horowitz, *Ozone and organic nitrates over the eastern United States: sensitivity to isoprene chemistry, J. Geophys. Res., 118,* 11,256–11,268, 2013a.

Martin, A. C., Jeffers, E., Petrokofsky, G., Myers-Smith, I., & Macias-Fauria, M. (2017). Shrub growth and expansion in the Arctic tundra: an assessment of controlling factors using an evidence-based approach. Environmental Research Letters.

Matsuura, K., and C. J. Willmott. 2015a. Terrestrial Air Temperature: 1900-2014 Gridded Monthly Time Series. http://climate.geog.udel.edu/~climate/html_pages/Global2014/README.GlobalTsT2014.html. Accessed 10 January 2018.

Matsuura, K., and C. J. Wilmott. 2015b. Terrestrial Precipitation: 1900-2014 Gridded Monthly Time Series. http://climate.geog.udel.edu/~climate/html_pages/Global2014/README.GlobalTsP2014.html Accesses 10 January 2018.

McClelland, J. W., Townsend-Small, A., Holmes, R. M., Pan, F., Stieglitz, M., Khosh, M., & Peterson, B. J. (2014). River export of nutrients and organic matter from the North Slope of Alaska to the Beaufort Sea. *Water Resources Research*, *50*(2), 1823-1839.

Meko D, Graybill DA (1995) Tree-ring reconstruction of Upper Gila River discharge. *Journal of the American Water Resources Association*, **31**, 605-616.

Mekonnen, Z. A., Riley, W. J., & Grant, R. F. (2018). Accelerated nutrient cycling and increased light competition will lead to 21st century shrub expansion in North American Arctic tundra. *Journal of Geophysical Research: Biogeosciences*, 123(5), 1683-1701.

Miller, G. H., Alley, R. B., Brigham-Grette, J., Fitzpatrick, J. J., Polyak, L., Serreze, M. C., & White, J. W. (2010). Arctic amplification: can the past constrain the future?. *Quaternary Science Reviews*, *29*(15-16), 1779-1790.

Millet, D.B., M. Baasandorj, D.K. Farmer, J.A. Thornton, K. Baumann, P. Brophy, S. Chaliyakunnel, J.A. de Gouw, M. Graus, L. Hu, A. Koss, B.H. Lee, F.D. Lopez-Hilfiker, J.A. Neuman, F. Paulot, J. Peischl, I.B. Pollack, T.B. Ryerson, C. Warneke, B.J. Williams, and J. Xu (2015), A large and ubiquitous source of atmospheric formic acid, *Atmos. Chem. Phys.*, 15, 6283-6304, doi:10.5194/acp-15-6283-2015.

Murphy, B. W. (2015). Impact of soil organic matter on soil properties—a review with emphasis on Australian soils. *Soil Research*, *53*(6), 605-635.

Murray, L.T., D.J. Jacob, J.A. Logan, R.C. Hudman, and W.J. Koshak. (2012). *Optimized regional and interannual variability of lightning in a global chemical transport model constrained by LIS/OTD satellite data*, , J. Geophus. Res., 117, D20307.

Myers-Smith, I. H., Forbes, B. C., Wilmking, M., Hallinger, M., Lantz, T., Blok, D., ... & Boudreau, S. (2011). Shrub expansion in tundra ecosystems: dynamics, impacts and research priorities. *Environmental Research Letters*, *6*(4), 045509.

Myers-Smith, I. H., Elmendorf, S. C., Beck, P. S., Wilmking, M., Hallinger, M., Blok, D., ... & Speed, J. D. (2015a). Climate sensitivity of shrub growth across the tundra biome. *Nature Climate Change*, *5*(9), 887.

Myers-Smith IH, Hallinger M, Blok D *et al*. (2015b) Methods for measuring arctic and alpine shrub growth: a review. *Earth-Science Reviews*, **140**, 1-13.

Myrstener, M., Jonsson, A., & Bergström, A. K. (2016). The effects of temperature and resource availability on denitrification and relative N2O production in boreal lake sediments. *Journal of Environmental Sciences*, *47*, 82-90.

Myrstener, M., Rocher-Ros, G., Burrows, R. M., Bergström, A. K., Giesler, R., & Sponseller, R. A. (2018). Persistent nitrogen limitation of stream biofilm communities along climate gradients in the Arctic. *Global change biology*.

Nakagawa, S., & Schielzeth, H. (2013). A general and simple method for obtaining R2 from generalized linear mixed-effects models. *Methods in Ecology and Evolution*, *4*(2), 133-142.

National Atmospheric Deposition Program (NADP). (2018). NADP Program Office, Wisconsin State Laboratory of Hygiene, 465 Henry Mall, Madison, WI 53706. < http://nadp.slh.wisc.edu/data/NTN/>. Retrieved April 6, 2018.

Nauta AL, Heijmans MM, Blok D *et al*. (2015) Permafrost collapse after shrub removal shifts tundra ecosystem to a methane source. *Nature Climate Change*, **5**, 67-70.

NOAA Gridded Climate Divisional Dataset (CLIMDIV), North Slope, Alaska. NOAA National Climatic Data Center. Retrieved from https://www.ncdc.noaa.gov/cag/ (Accessed September 1, 2016).

Olofsson J, Oksanen L, Callaghan T, Hulme PE, Oksanen T, Suominen O (2009) Herbivores inhibit climate-driven shrub expansion on the tundra. *Global Change Biology*, **15**, 2681-2693.

Oswald, W. W., Brubaker, L. B., Hu, F. S., & Kling, G. W. (2014). Late-Quaternary environmental and ecological history of the Arctic Foothills, northern Alaska. Alaska's Changing Arctic, Oxford University Press, New York, NY, 81-89.

Overland, J. E., Spillane, M. C., Percival, D. B., Wang, M., & Mofjeld, H. O. (2004). Seasonal and regional variation of pan-Arctic surface air temperature over the instrumental record. Journal of Climate, 17(17), 3263-3282.

Palmer, J., Thorburn, P. J., Biggs, J. S., Dominati, E. J., Probert, M. E., Meier, E. A., ... & Parton, W. J. (2017). Nitrogen cycling from increased soil organic carbon contributes both positively and negatively to ecosystem services in wheat agro-ecosystems. *Frontiers in plant science*, *8*, 731.

Parrella, J.P., D.J. Jacob, Q. Liang, Y. Zhang, L.J. Mickley, B. Miller, M.J. Evans, X. Yang, J.A. Pyle, N. Theys, and M. Van Roozendael, *Tropospheric bromine chemistry: implications for present and pre-industrial ozone and mercury*, Atmos. Chem. Phys., **12**, 6,723-6,740, 2012.

Paul, M. J., & Meyer, J. L. (2001). Streams in the urban landscape. *Annual review of Ecology and Systematics*, *32*(1), 333-365.

Perakis, S. S., & Hedin, L. O. (2007). State factor relationships of dissolved organic carbon and nitrogen losses from unpolluted temperate forest watersheds. *Journal of Geophysical Research: Biogeosciences*, *112*(G2).

Peterson, B. J., Deegan, L., Helfrich, J., Hobbie, J. E., Hullar, M., Moller, B., ... & Lock, M. A. (1993). Biological responses of a tundra river to fertilization. *Ecology*, *74*(3), 653-672.

Petrenko, V. V., Smith, A. M., Schaefer, H., Riedel, K., Brook, E., Baggenstos, D., ... & Fain, X. (2017). Minimal geological methane emissions during the Younger Dryas–Preboreal abrupt warming event. *Nature*, *548*(7668), 443.

Phoenix, G. K., Hicks, W. K., Cinderby, S., Kuylenstierna, J. C., Stock, W. D., Dentener, F. J., ... & Ashmore, M. R. (2006). Atmospheric nitrogen deposition in world biodiversity hotspots: the need for a greater global perspective in assessing N deposition impacts. *Global Change Biology*, *12*(3), 470-476.

Pye, H.O.T., H. Liao, S. Wu, L.J. Mickley, D.J. Jacob, D.K. Henze, and J.H. Seinfeld, Effect of changes in climate and emissions on future sulfate-nitrate-ammonium aerosol levels in the United States, J. Geophys. Res., 114, D01205, 2009.

Pinheiro J, Bates D, DebRoy S, Sarkar D (2014) R Core Team. nlme: linear and nonlinear mixed effects models. R package version 3.1-117. Available at h ttp://CRAN. R-project. org/package= nlme.

Pinheiro J, Bates D, DebRoy S, Sarkar D and R Core Team (2018). nlme: Linear and Nonlinear Mixed Effects Models. **R** package version 3.1-137

Post, E., *et al.* (2013). Ecological consequences of sea-ice decline. *Science*, *341*(6145), 519-524.

Radville, L., Post, E., & Eissenstat, D. M. (2016). Root phenology in an Arctic shrub-graminoid community: the effects of long-term warming and herbivore exclusion. Climate Change Responses, 3(1), 4.

Rayback SA, Henry GH (2005) Dendrochronological potential of the Arctic dwarf-shrub Cassiope tetragona. *Tree-Ring Research*, **61**, 43-53.

Raynolds, M. K., & Walker, D. A. (2009). Effects of deglaciation on circumpolar distribution of arctic vegetation. *Canadian Journal of Remote Sensing*, *35*(2), 118-129.
Reis, S., Pinder, R. W., Zhang, M., Lijie, G., & Sutton, M. A. (2009). Reactive nitrogen in atmospheric emission inventories. *Atmospheric Chemistry and Physics*, *9*(19), 7657-7677.
Riahi, K., Rao, S., Krey, V., Cho, C. H., Chirkov, V., Fischer, G., Kindermann, G., Nakicenovic, N., & Rafaj, P. (2011). RCP 8.5-A scenario of comparatively high greenhouse gas emissions. *Clim. Change*, *109(1−2)*, 33−57.
Ropars P, Levesque E, Boudreau S (2015) How do climate and topography influence the greening of the forest-tundra ecotone in northern Québec? A dendrochronological analysis of *Betula glandulosa*. *Journal of Ecology*, **103**, 679-690.
Ropars, P., Angers-Blondin, S., Gagnon, M., Myers-Smith, I. H., Lévesque, E., & Boudreau, S. (2017). Different parts, different stories: climate sensitivity of growth is stronger in root collars vs. stems in tundra shrubs. Global change biology.
Rousk, K., Sorensen, P. L., & Michelsen, A. (2018). What drives biological nitrogen fixation in high arctic tundra: Moisture or temperature?. *Ecosphere*, *9*(2).
Running, S. W., Nemani, R. R., Heinsch, F. A., Zhao, M., Reeves, M., & Hashimoto, H. (2004). A continuous satellite-derived measure of global terrestrial primary production. *BioScience*, *54*(6), 547-560.
Schaefer, S. C., & Alber, M. (2007). Temperature controls a latitudinal gradient in the proportion of watershed nitrogen exported to coastal ecosystems. Biogeochemistry, 85(3), 333-346.
Schimel, J. P., & Chapin, F. S. (1996). Tundra plant uptake of amino acid and NH4+ nitrogen in situ: plants complete well for amino acid N. *Ecology*, *77*(7), 2142-2147.
Schimel, J. P., & Bennett, J. (2004). Nitrogen mineralization: challenges of a changing paradigm. *Ecology*, *85*(3), 591-602.
Schimel JP, Bilbrough C, Welker JM (2004) Increased snow depth affects microbial activity and nitrogen mineralization in two Arctic tundra communities. *Soil Biology and Biochemistry*, **36**, 217-227.
Schmidt, I. K., Jonasson, S., Shaver, G. R., Michelsen, A., & Nordin, A. (2002). Mineralization and distribution of nutrients in plants and microbes in four arctic ecosystems: responses to warming. *Plant and Soil*, *242*(1), 93-106.
Schuur EA, Crummer KG, Vogel JG, Mack MC (2007) Plant species composition and productivity following permafrost thaw and thermokarst in Alaskan tundra. *Ecosystems*, **10**, 280-292.
Schuur, E. A., McGuire, A. D., Schädel, C., Grosse, G., Harden, J. W., Hayes, D. J., ... & Natali, S. M. (2015). Climate change and the permafrost carbon feedback. *Nature*, *520*(7546), 171.
Schaefer, S. C., & Alber, M. (2007). Temperature controls a latitudinal gradient in the proportion of watershed nitrogen exported to coastal ecosystems. *Biogeochemistry*, 85(3), 333-346.
Serreze, M. C., & Barry, R. G. (2011). Processes and impacts of Arctic amplification: A research synthesis. *Global and planetary change*, *77*(1-2), 85-96.

Seto, K. C., Güneralp, B., & Hutyra, L. R. (2012). Global forecasts of urban expansion to 2030 and direct impacts on biodiversity and carbon pools. *Proceedings of the National Academy of Sciences*, *109*(40), 16083-16088.

Shaver, G. R. (1986). Woody stem production in Alaskan tundra shrubs. Ecology, 67(3), 660-669.

Shaver, G. R., Billings, W. D., Chapin III, F. S., Giblin, A. E., Nadelhoffer, K. J., Oechel, W. C., & Rastetter, E. B. (1992). Global change and the carbon balance of arctic ecosystems: Carbon/nutrient interactions should act as major constraints on changes in global terrestrial carbon cycling. *Bioscience*, *42*(6), 433-441.

Shaver, G. R., & Jonasson, S. (1999). Response of Arctic ecosystems to climate change: results of long-term field experiments in Sweden and Alaska. *Polar Research*, *18*(2), 245-252.er, G. R. (1986). Woody stem production in Alaskan tundra shrubs.*Ecology*, 660-669.

Shaver, G. R., Laundre, J. A., Bret-Harte, M. S., Chapin, F. S., Mercado-Dıaz, J. A., Giblin, A. E., ... & Gould, W. A. (2014). Terrestrial ecosystems at toolik Lake, Alaska. *Alaska's changing Arctic: Ecological consequences for tundra, streams, and lakes, ed. JE Hobbie, and GW Kling*, 90-142.

Simmons, A. J., & Poli, P. (2015). Arctic warming in ERA-Interim and other analyses. Quarterly Journal of the Royal Meteorological Society, 141(689), 1147-1162.

Simmons, A. J., Berrisford, P., Dee, D. P., Hersbach, H., Hirahara, S., & Thépaut, J. N. (2017). A reassessment of temperature variations and trends from global reanalyses and monthly surface climatological datasets. Quarterly Journal of the Royal Meteorological Society, 143(702), 101-119.

Sitch S, Smith B, Prentice *et al*. (2003) Evaluation of ecosystem dynamics, plant geography and terrestrial carbon cycling in the LPJ dynamic global vegetation model. *Global Change Biology*, **9**, 161-185.

Slavik K, Peterson BJ, Deegan LA, Bowden WB, Hershey AE, Hobbie JE (2004) Long-term responses of the Kuparuk River ecosystem to phosphorus fertilization. *Ecology*, **85**, 939-954.

Spalding, R. F., & Exner, M. E. (1993). Occurrence of nitrate in groundwater—a review. *Journal of environmental quality*, *22*(3), 392-402.

Stettler, M.E.J., S. Eastham, S.R.H. Barrett, Air quality and public health impacts of UK airports. Part I: Emissions, Atmos. Environ., 45, 5415-5424, 2011.

Stevens, C. J., Dise, N. B., Mountford, J. O., & Gowing, D. J. (2004). Impact of nitrogen deposition on the species richness of grasslands. *Science*, *303*(5665), 1876-1879.

Stokes MA, Smiley TL (1968) Tree-ring dating. University of Chicago Press, Chicago, Illinois.

Sturm, Matthew, et al. "Snow-shrub interactions in Arctic tundra: a hypothesis with climatic implications." *Journal of Climate* 14.3 (2001): 336-344.

Sweet SK, Gough L, Griffin KL, Boelman NT (2014) Tall deciduous shrubs offset delayed start of growing season through rapid leaf development in the Alaskan arctic tundra. *Arctic, Antarctic, and Alpine Research*, **46**, 682-697.

Sweet, SK., et al. "Greater deciduous shrub abundance extends tundra peak season and increases modeled net CO2 uptake." *Global change biology* 21.6 (2015): 2394-2409.

Tamm, C. O. (1991). Introduction: geochemical occurrence of nitrogen. Natural nitrogen cycling and anthropogenic nitrogen emissions. In *Nitrogen in Terrestrial Ecosystems* (pp. 1-6). Springer, Berlin, Heidelberg.

Tank, S. E., Manizza, M., Holmes, R. M., McClelland, J. W., & Peterson, B. J. (2012). The processing and impact of dissolved riverine nitrogen in the Arctic Ocean. *Estuaries and Coasts*, *35*(2), 401-415.

Tape, K. E. N., Sturm, M., & Racine, C. (2006). The evidence for shrub expansion in Northern Alaska and the Pan-Arctic. *Global Change Biology*, *12*(4), 686-702.

Tape, K. D., Lord, R., Marshall, H. P., & Ruess, R. W. (2010). Snow-mediated ptarmigan browsing and shrub expansion in arctic Alaska.

Tape, K. D., Hallinger, M., Welker, J. M., & Ruess, R. W. (2012). Landscape heterogeneity of shrub expansion in Arctic Alaska. *Ecosystems*, *15*(5), 711-724.

Tape KD, Gustine DD, Ruess RW, Adams LG, Clark JA (2016) Range Expansion of Moose in Arctic Alaska Linked to Warming and Increased Shrub Habitat. *PloS one*, **11**, e0152636.

Tarnocai, C., Canadell, J. G., Schuur, E. A. G., Kuhry, P., Mazhitova, G., & Zimov, S. (2009). Soil organic carbon pools in the northern circumpolar permafrost region. *Global biogeochemical cycles*, *23*(2).

Telling, J., Anesio, A. M., Tranter, M., Irvine-Fynn, T., Hodson, A., Butler, C., & Wadham, J. (2011). Nitrogen fixation on Arctic glaciers, Svalbard. *Journal of Geophysical Research: Biogeosciences*, 116(G3).

Throop, H. L., & Lerdau, M. T. (2004). Effects of nitrogen deposition on insect herbivory: implications for community and ecosystem processes. *Ecosystems*, *7*(2), 109-133.

Tørseth, K., Aas, W., Breivik, K., Fjæraa, A. M., Fiebig, M., Hjellbrekke, A. G., ... & Yttri, K. E. (2012). Introduction to the European Monitoring and Evaluation Programme (EMEP) and observed atmospheric composition change during 1972–2009. Atmospheric Chemistry and Physics, 12(12), 5447-5481.

Torvinen, E. S. (2017). Lake Trout (Salvelinus Namaycush) Otoliths as Indicators of Past Climate Patterns and Growth in Arctic Lakes (Doctoral dissertation, University of Alaska Fairbanks).

Treat, C. C., Wollheim, W. M., Varner, R. K., & Bowden, W. B. (2016). Longer thaw seasons increase nitrogen availability for leaching during fall in tundra soils. *Environmental Research Letters*, *11*(6), 064013.

van der Werf, G. R., Randerson, J. T., Giglio, L., Van Leeuwen, T. T., Chen, Y., Rogers, B. M., ... & Yokelson, R. J. (2017). Global fire emissions estimates during 1997–2016. *Earth System Science Data*, *9*(2), 697.

Van Wijk, M. T., Clemmensen, K. E., Shaver, G. R., Williams, M., Callaghan, T. V., Chapin III, F. S., ... & Lee, J. A. (2004). Long-term ecosystem level experiments at Toolik Lake, Alaska, and at Abisko, Northern Sweden: generalizations and differences in ecosystem and plant type responses to global change. *Global Change Biology*, *10*(1), 105-123.

Vet, R., Artz, R. S., Carou, S., Shaw, M., Ro, C. U., Aas, W., ... & Hou, A. (2014). A global assessment of precipitation chemistry and deposition of sulfur, nitrogen, sea

salt, base cations, organic acids, acidity and pH, and phosphorus. Atmospheric Environment,93, 3-100.

Vet, R., R.S. Artz, S. Carou, M. Shaw, C.-U. Ro, W. Aas, A. Baker, V.C. Bowersox, F. Dentener, C. Galy-Lacaux, A. Hou, J.J. Pienaar, R. Gillett, M.C. Forti, S. Gromov, H. Hara, T. Khodzher, N.M. Mahowald, S. Nickovic, P.S.P. Rao, N.W. Reid. 2018. Data associated with the following publication: Vet et al. (2014). A global assessment of precipitation chemistry and deposition of sulfur, nitrogen, sea salt, base cations, organic acids, acidity and pH, and phosphorus. Atmospheric Environment, 93, 3-100, August 2014, doi.org/10.1016/j.atmosenv.2013.10.060. [Data files: Global Wet Concentration and Deposition Observations: 2005-2007; North American Dry Deposition Observations: 2005-2007] accessed from the World Data Centre for Precipitation Chemistry (http://wdcpc.org/assessment).

Vitousek, P. M., Aber, J. D., Howarth, R. W., Likens, G. E., Matson, P. A., Schindler, D. W., Schlesinger, W. H., & Tilman, D. G. (1997). Human alteration of the global nitrogen cycle: sources and consequences. *Ecological applications*, *7*(3), 737-750.

Vose, R. S., Applequist, S., Squires, M., Durre, I., Menne, M. J., Williams Jr, C. N., ... & Arndt, D. (2014). Improved historical temperature and precipitation time series for US climate divisions. Journal of Applied Meteorology and Climatology, 53(5), 1232-1251.

Wadham, J. L., Hawkings, J., Telling, J., Chandler, D., Alcock, J., Lawson, E., ... & Nienow, P. (2016). Sources, cycling and export of nitrogen on the Greenland Ice Sheet. *Biogeosciences Discussions*.

Wadham, J. L., De'Ath, R., Monteiro, F. M., Tranter, M., Ridgwell, A., Raiswell, R., & Tulaczyk, S. (2013). The potential role of the Antarctic Ice Sheet in global biogeochemical cycles. Earth and Environmental Science Transactions of the Royal Society of Edinburgh, 104(1), 55-67.

Walker DA, Raynolds MK, Daniëls FJ *et al*. (2005) The circumpolar Arctic vegetation map. *Journal of Vegetation Science*, **16**, 267-282.

Walker, D. A., Hamilton, T. D., Maier, H. A., Munger, C. A., & Raynolds, M. K. (2014). Glacial history and long-term ecology in the Toolik Lake region. Alaska's changing Arctic: Ecological consequences for tundra, streams, and lakes. Oxford, New York, 61-80.

Walter Anthony, K., *et al.* (2014). A shift of thermokarst lakes from carbon sources to sinks during the Holocene epoch. *Nature*, *511*(7510), 452.

Wang, Y., D.J. Jacob, and J.A. Logan, *Global simulation of tropospheric O3-NOx-hydrocarbon chemistry, 1. Model formulation*, J. Geophys. Res., **103**/D9, 10,713-10,726, 1998

Wang, Y. P., & Houlton, B. Z. (2009). Nitrogen constraints on terrestrial carbon uptake: Implications for the global carbon-climate feedback. *Geophysical Research Letters*, *36*(24).

Wang, Q., D.J. Jacob, J.A. Fisher, J. Mao, E.M. Leibensperger, C.C. Carouge, P. Le Sager, Y. Kondo, J.L. Jimenez, M.J. Cubison, and S.J. Doherty, Sources of carbonaceous aerosols and deposited black carbon in the Arctic in winter-spring: implications for radiative forcing, Atmos. Chem. Phys., 11, 12,453-12,473, 2011.

Wang, Q., D.J. Jacob,J.R Spackman, A.E. Perring, J.P. Schwarz, N. Moteki, E.A. Marais, C. Ge, J. Wang, and S.R.H. Barrett, Global budget and radiative forcing of black carbon aerosol: constraints from pole-to-pole (HIPPO) observations across the Pacific, J. Geophys. Res., 119, 195-206, 2014.

Weijers, S., Broekman, R., & Rozema, J. (2010). Dendrochronology in the High Arctic: July air temperatures reconstructed from annual shoot length growth of the circumarctic dwarf shrub Cassiope tetragona. *Quaternary Science Reviews*, *29*(27-28), 3831-3842.

Weyer, P. J., Kantamneni, J. R., Lu, X., Ward, M. H., & Cerhan, J. R. (2008). Nitrate Ingestion from drinking water and diet and cancer risk. *Epidemiology*, *19*(6), S55.

Whittinghill, K. A., & Hobbie, S. E. (2011). Effects of Landscape Age on Soil Organic Matter Processing in Northern Alaska. Soil Science Society of America Journal, 75(3), 907-917.

Wieder, W.R., J. Boehnert, G.B. Bonan, and M. Langseth. (2014). Regridded Harmonized World Soil Database v1.2. Data set. Available on-line [http://daac.ornl.gov] from Oak Ridge National Laboratory Distributed Active Archive Center, Oak Ridge, Tennessee, USA.http://dx.doi.org/10.3334/ORNLDAAC/1247 .

Williams, N. S., Schwartz, M. W., Vesk, P. A., McCarthy, M. A., Hahs, A. K., Clemants, S. E., ... & McDonnell, M. J. (2009). A conceptual framework for predicting the effects of urban environments on floras. *Journal of ecology*, *97*(1), 4-9.

Wilmking M, D'arrigo R, Jacoby GC, Juday GP (2005) Increased temperature sensitivity and divergent growth trends in circumpolar boreal forests. *Geophysical Research Letters*, **32**.

Wookey, P. A., Welker, J. M., Parsons, A. N., Press, M. C., Callaghan, T. V., & Lee, J. A. (1994). Differential growth, allocation and photosynthetic responses of Polygonum viviparum to simulated environmental change at a high arctic polar semi-desert. *Oikos*, 131-139.

Worrall, F., Clay, G. D., Burt, T. P., & Rose, R. (2012). The multi-annual nitrogen budget of a peat-covered catchment—Changing from sink to source?. *Science of the total environment*, *433*, 178-188.

Wu, S, L.J. Mickley, D.J. Jacob, J.A. Logan, and R.M. Yantosca, Why are there large differences between models in global budgets of tropospheric ozone?, J. Geophys. Res, 112, D05302, doi:10.1029/2006JD007801, 2007

Yano, Y., Shaver, G. R., Giblin, A. E., Rastetter, E. B., & Nadelhoffer, K. J. (2010). Nitrogen dynamics in a small arctic watershed: retention and downhill movement of 15N. *Ecological Monographs*, *80*(2), 331-351.

Young, A. B., Watts, D. A., Taylor, A. H., & Post, E. (2016). Species and site differences influence climate-shrub growth responses in West Greenland. *Dendrochronologia*, *37*, 69-78.

Zamin TJ, Grogan P (2012) Birch shrub growth in the low Arctic: the relative importance of experimental warming, enhanced nutrient availability, snow depth and caribou exclusion. *Environmental Research Letters*, **7**, 034027.

Zang C, Biondi F (2015) treeclim: an R package for the numerical calibration of proxy-climate relationships. *Ecography*, **38**, 431-436.

Zhang, L.M., S.L. Gong, J. Padro, and L. Barrie, A size-segregated particle dry deposition scheme for an atmospheric aerosol module, Atmos. Environ., 35(3), 549-560, doi:10.1016/s1352-2310(00)00326-5, 2001.

Zhang, Y., Mathur, R., Bash, J. O., Hogrefe, C., Xing, J., & Roselle, S. J. (2018). Long-term trends in total inorganic nitrogen and sulfur deposition in the US from 1990 to 2010. Atmospheric Chemistry and Physics, 18, 9091-9106.

Appendix 1

Chapter 1 Supplemental Material

Table S1.1 Monthly climate correlation analysis for upland chronology detrended with cubic smoothing spline. Output is from *treeclim* (Zang & Biondi, 2015). CL = confidence limit.

Month	Variable	Coefficient estimate	p < 0.05	Lower 95% CI	Upper 95% CI
Previous October	Precipitation	0.194	FALSE	-0.025	0.311
Previous November	Precipitation	-0.131	FALSE	-0.35	0.049
Previous December	Precipitation	-0.106	FALSE	-0.284	0.18
Current January	Precipitation	0.069	FALSE	-0.132	0.239
Current February	Precipitation	-0.241	FALSE	-0.48	0.068
Current March	Precipitation	0.136	FALSE	-0.037	0.317
Current April	Precipitation	0.029	FALSE	-0.291	0.19
Current May	Precipitation	-0.023	FALSE	-0.229	0.2
Current June	Precipitation	-0.12	FALSE	-0.258	0.126
Current July	Precipitation	-0.216	TRUE	-0.4	-0.018
Current August	Precipitation	0.058	FALSE	-0.109	0.331
Previous October	Temperature	-0.012	FALSE	-0.213	0.333
Previous November	Temperature	-0.066	FALSE	-0.259	0.225
Previous December	Temperature	0.079	FALSE	-0.192	0.231
Current January	Temperature	-0.001	FALSE	-0.148	0.173
Current February	Temperature	-0.138	FALSE	-0.33	0.19
Current March	Temperature	0.198	FALSE	-0.009	0.398
Current April	Temperature	0.078	FALSE	-0.153	0.285
Current May	Temperature	-0.212	FALSE	-0.395	0.023
Current June	Temperature	0.489	TRUE	0.097	0.727
Current July	Temperature	-0.025	FALSE	-0.257	0.18
Current August	Temperature	0.032	FALSE	-0.182	0.33

Table S1.2 Monthly climate correlation analysis for upland chronology detrended with negative exponential function. Output is from *treeclim* (Zang & Biondi, 2015). CL = confidence limit.

Month	Variable	Coefficient estimate	p < 0.05	Lower 95% CL	Upper 95% CL
Previous October	Precipitation	0.131	FALSE	-0.055	0.279
Previous November	Precipitation	-0.199	FALSE	-0.437	0.062
Previous December	Precipitation	0.024	FALSE	-0.271	0.43
Current January	Precipitation	-21	FALSE	-0.229	0.169

Current February	Precipitation	-0.28	FALSE	-0.599	0.075
Current March	Precipitation	0.057	FALSE	-0.117	0.227
Current April	Precipitation	-0.022	FALSE	-0.28	0.18
Current May	Precipitation	-0.013	FALSE	-0.235	0.248
Current June	Precipitation	-0.13	FALSE	-0.374	0.17
Current July	Precipitation	-0.093	FALSE	-0.303	0.107
Current August	Precipitation	0.142	FALSE	-0.112	0.443
Previous October	Temperature	-0.099	FALSE	-0.333	0.234
Previous November	Temperature	0.056	FALSE	-0.214	0.307
Previous December	Temperature	0.067	FALSE	-0.156	0.32
Current January	Temperature	0.032	FALSE	-0.235	0.209
Current February	Temperature	0.009	FALSE	-0.311	0.258
Current March	Temperature	0.143	FALSE	-0.176	0.394
Current April	Temperature	-0.005	FALSE	-0.261	0.251
Current May	Temperature	-0.119	FALSE	-0.401	0.146
Current June	Temperature	0.388	TRUE	0.063	0.663
Current July	Temperature	-0.095	FALSE	-0.437	0.163
Current August	Temperature	0.029	FALSE	-0.246	0.272

Table S1.3 Monthly climate correlation analysis for riparian chronology detrended with cubic smoothing spline. Output is from *treeclim* (Zang & Biondi, 2015). CL = confidence limit.

Month	Variable	Coefficient estimate	p < 0.05	Lower 95% CL	Upper 95% CL
Previous October	Precipitation	0.03	FALSE	-0.151	0.185
Previous November	Precipitation	-0.2	FALSE	-0.458	0.032
Previous December	Precipitation	0.051	FALSE	-0.213	0.325
Current January	Precipitation	-0.046	FALSE	-0.228	0.107
Current February	Precipitation	-0.077	FALSE	-0.284	0.109
Current March	Precipitation	-0.046	FALSE	-0.181	0.125
Current April	Precipitation	-0.179	FALSE	-0.439	0.007
Current May	Precipitation	0.051	FALSE	-0.234	0.284
Current June	Precipitation	-0.058	FALSE	-0.296	0.115
Current July	Precipitation	0.106	FALSE	-0.084	0.295
Current August	Precipitation	-0.101	FALSE	-0.359	0.208
Previous October	Temperature	0.121	FALSE	-0.123	0.358
Previous November	Temperature	-0.021	FALSE	-0.249	0.202
Previous December	Temperature	-0.17	FALSE	-0.434	0.023
Current January	Temperature	-0.066	FALSE	-0.297	0.172
Current February	Temperature	-0.195	FALSE	-0.476	0.096
Current March	Temperature	-0.086	FALSE	-0.322	0.161
Current April	Temperature	-0.048	FALSE	-0.32	0.173
Current May	Temperature	-0.058	FALSE	-0.271	0.192
Current June	Temperature	0.283	TRUE	0.021	0.53
Current July	Temperature	0.118	FALSE	-0.134	0.361
Current August	Temperature	-0.001	FALSE	-0.234	0.207

Table S1.4 Monthly climate correlation analysis for riparian chronology detrended with negative exponential function. Output is from *treeclim* (Zang & Biondi, 2015). CL = confidence limit.

Month	Variable	Coefficient estimate	p < 0.05	Lower 95% CL	Upper 95% CL
Previous October	Precipitation	-0.014	FALSE	-0.248	0.133
Previous November	Precipitation	-0.164	FALSE	-0.432	0.065
Previous December	Precipitation	0.044	FALSE	-0.293	0.317
Current January	Precipitation	-0.023	FALSE	-0.263	0.193
Current February	Precipitation	0.003	FALSE	-0.221	0.257
Current March	Precipitation	-0.025	FALSE	-0.23	0.162
Current April	Precipitation	-0.13	FALSE	-0.412	0.083
Current May	Precipitation	0.022	FALSE	-0.274	0.294
Current June	Precipitation	0.004	FALSE	-0.265	0.21
Current July	Precipitation	0.142	FALSE	-0.05	0.35
Current August	Precipitation	-0.079	FALSE	-0.323	0.254
Previous October	Temperature	0.09	FALSE	-0.182	0.359
Previous November	Temperature	0.02	FALSE	-0.322	0.264
Previous December	Temperature	-0.258	FALSE	-0.556	0.006
Current January	Temperature	-0.067	FALSE	-0.32	0.201
Current February	Temperature	-0.175	FALSE	-0.507	0.198
Current March	Temperature	-0.134	FALSE	-0.425	0.192
Current April	Temperature	-0.142	FALSE	-0.487	0.156
Current May	Temperature	-0.068	FALSE	-0.292	0.248
Current June	Temperature	0.302	FALSE	-0.021	0.636
Current July	Temperature	0.072	FALSE	-0.227	0.338
Current August	Temperature	0.024	FALSE	-0.287	0.281

Table S1.5 Fixed effects output of individual-based hierarchical mixed effects model, using detrended (20-year cubic smoothing spline) upland ring width index as a response variable. Mean June temperature ("temp") was a fixed effect, as was a second-order temperature term. Year and individual were random effects. Output is from R package *nlme* (Pinheiro *et al*., 2014).

Term	Value	Std. error	df	t	p
Intercept	-1.922	0.953	442	-2.06	0.044
temp	0.581	0.214	23	2.71	0.013
I(temp^2)	-0.028	0.012	3	-2.33	0.029

Table S1.6 Fixed effects output of individual-based hierarchical mixed effects model, using raw upland ring width (mm) as a response variable. Mean June temperature ("temp") was a fixed effect, as was a second-order temperature term. Year and individual were random effects. Output is from R package *nlme* (Pinheiro *et al*., 2014). Raw data are available at the International Tree-Ring Data Bank (https://data.noaa.gov/dataset/international-tree-ring-data-bank-itrdb).

Term	Value	Std. error	df	t	p
Intercept	-0.393	0.348	442	-1.13	0.259
temp	0.125	0.078	23	1.61	0.122
I(temp^2)	-0.007	0.004	23	-1.516	0.143

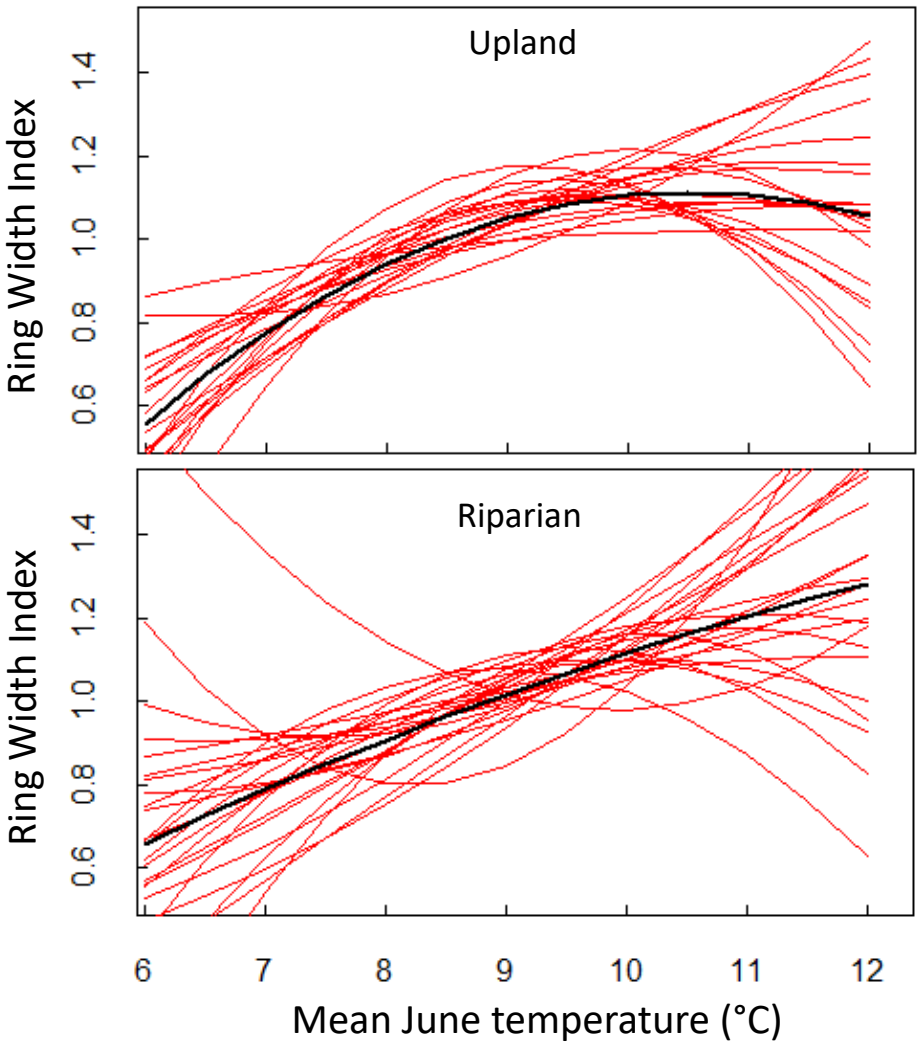

Fig S1.1 Individual curve fits (red) for second order relationship between ring width index and June temperature for upland (top) and riparian (bottom) shrubs. Site mean relationships are shown in black. All but one individual from the upland site show a decelerating relationship between ring width index and temperature, whereas the climate-growth relationship varies for individuals at the riparian site, with riparian site mean showing minimal deceleration.

Appendix 2

Chapter 3 Supplemental Material

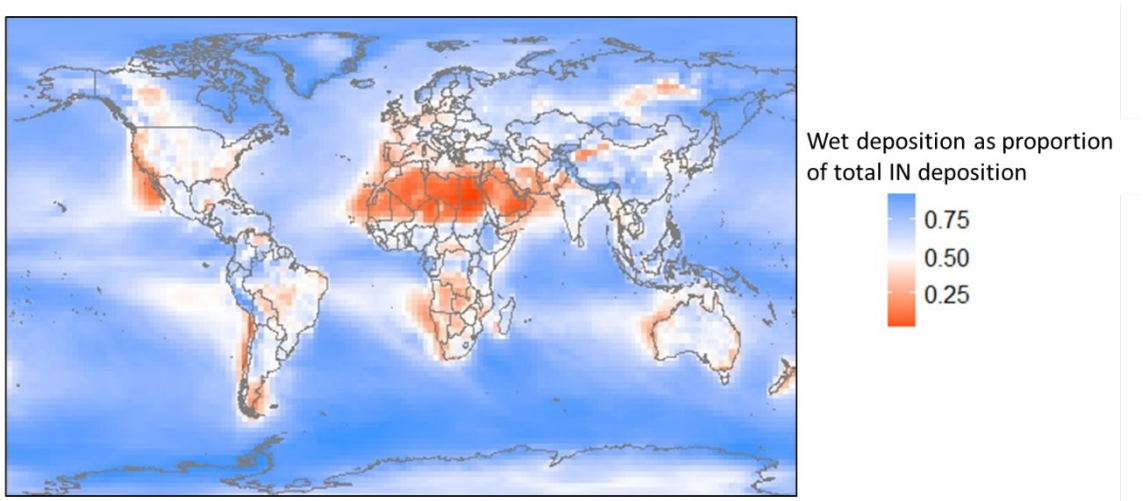

Figure S3.1. Wet IN deposition as a fraction of total (wet + dry) IN deposition as simulated for 2016.

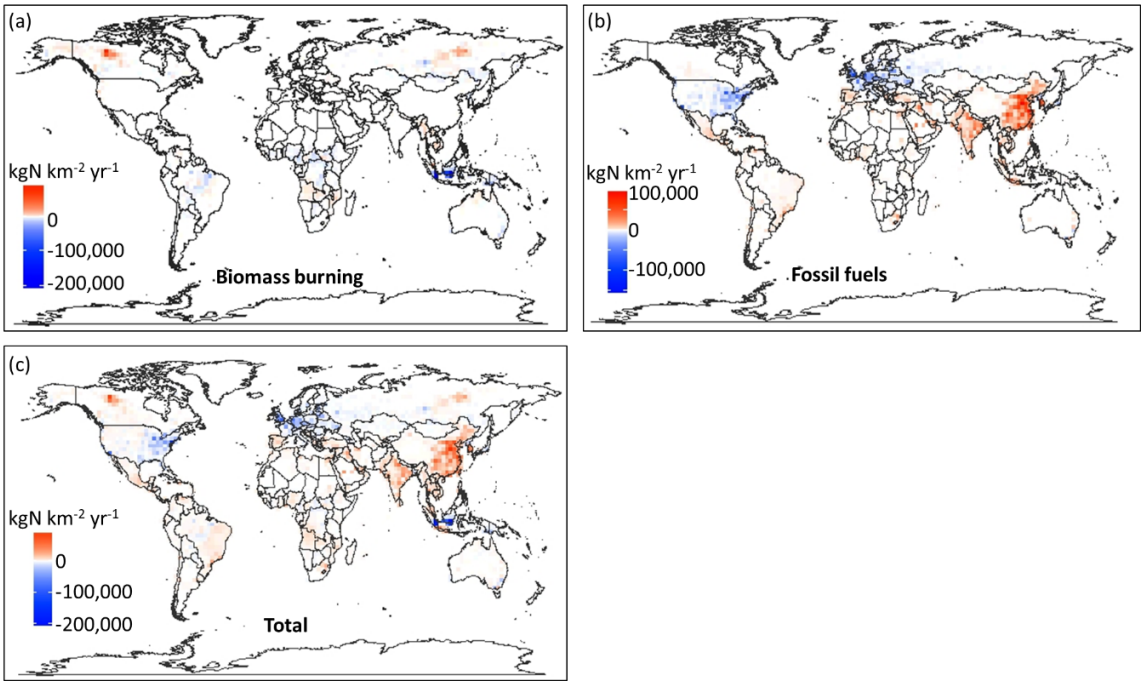

Figure S3.2. Mean annual change in nitrogen emissions from 1984 to 2016. Nitrogen emissions due to biomass burning, including agricultural fires (a) and emissions from fossil fuel combustion (b) show variable rates of change across the globe. Total nitrogen emissions (c) constitute the

sum of emissions from biomass burning, fossil fuel combustion, agriculture, and natural sources (including soils, lightning, and biogenic compounds).

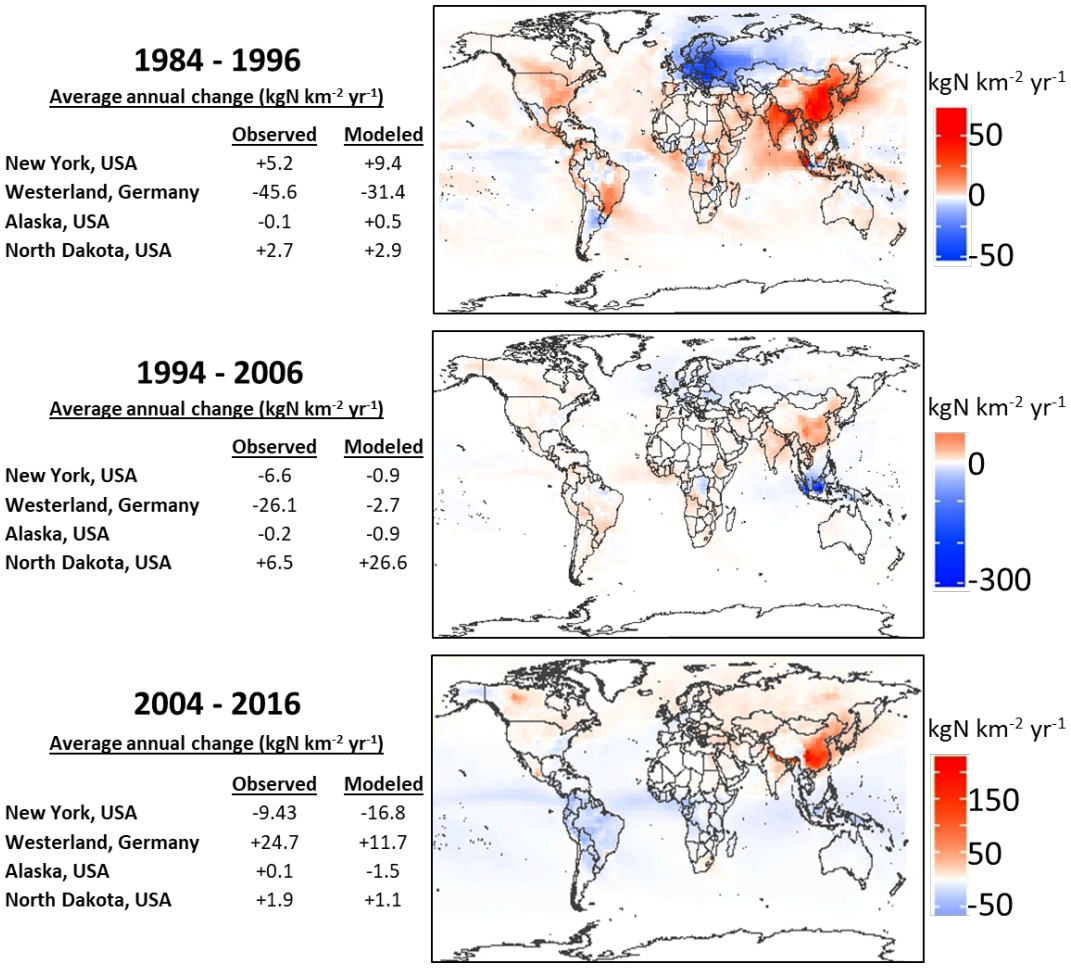

Figure S3.3. Modeled interdecadal trends in IN deposition. Table to the left of each interdecadal period compares the modeled change with observed change in IN deposition over the same time period for four long-term monitoring sites (NADP 2018).

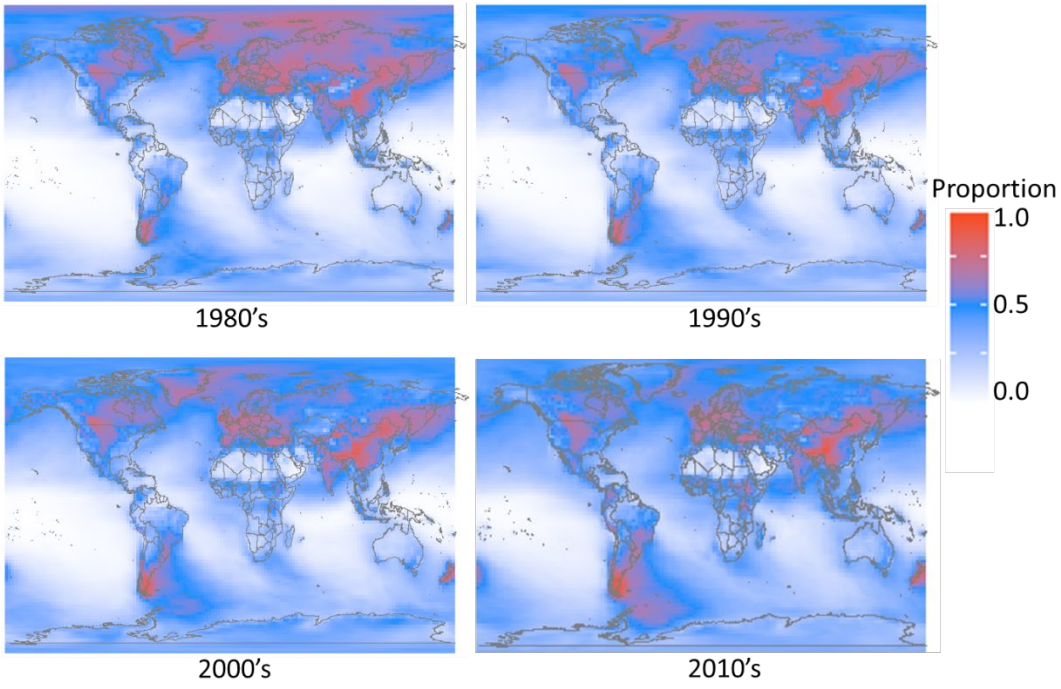

Figure S3.4. Proportion of IN deposited as reduced molecules (NH_3 and NH_4) as simulated for each decade.

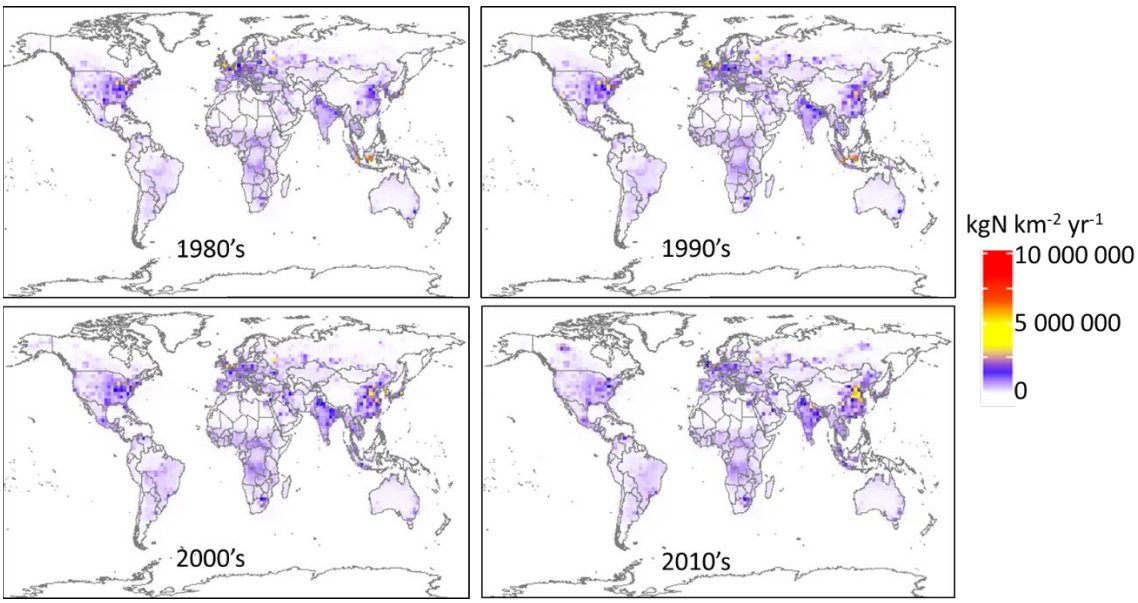

Figure S3.5. Mean annual total nitrogen emissions as simulated for each decade.

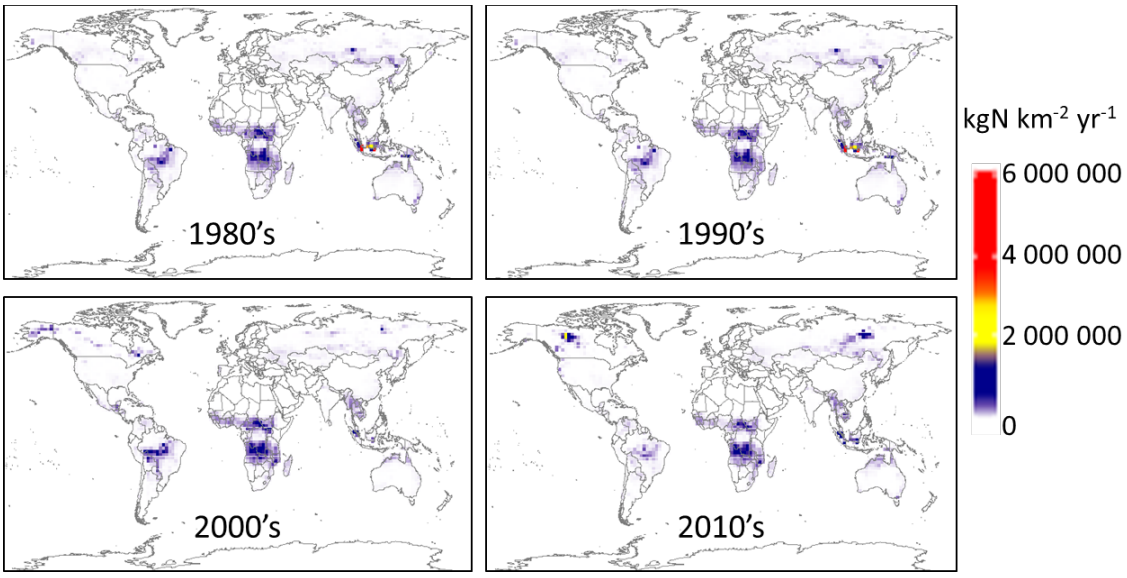

Figure S3.6. Mean annual nitrogen emissions due to biomass burning as simulated for each decade.

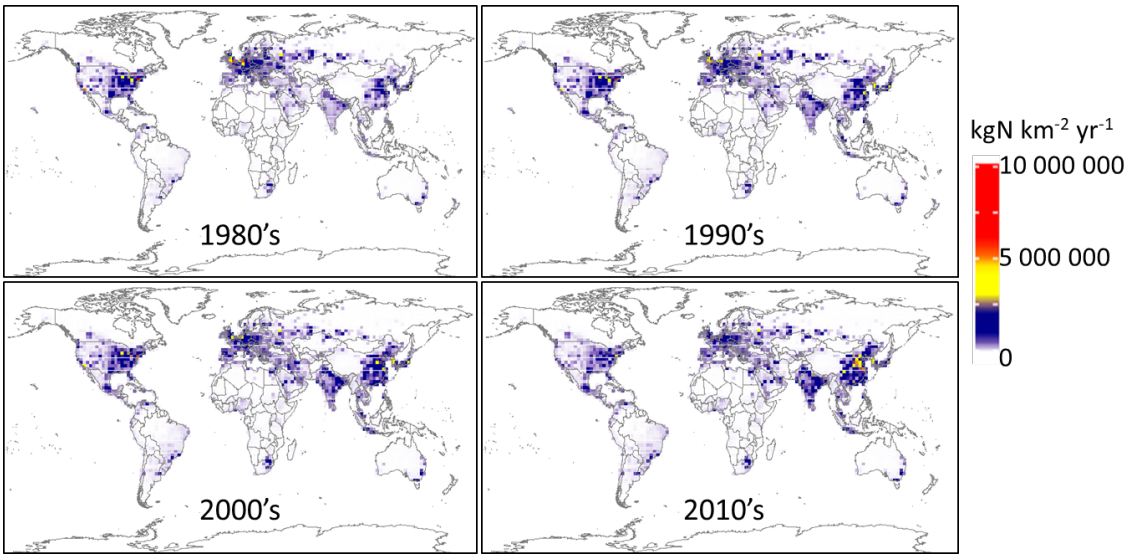

Figure S3.7. Mean annual nitrogen emissions from fossil fuel combustion as simulated for each decade.

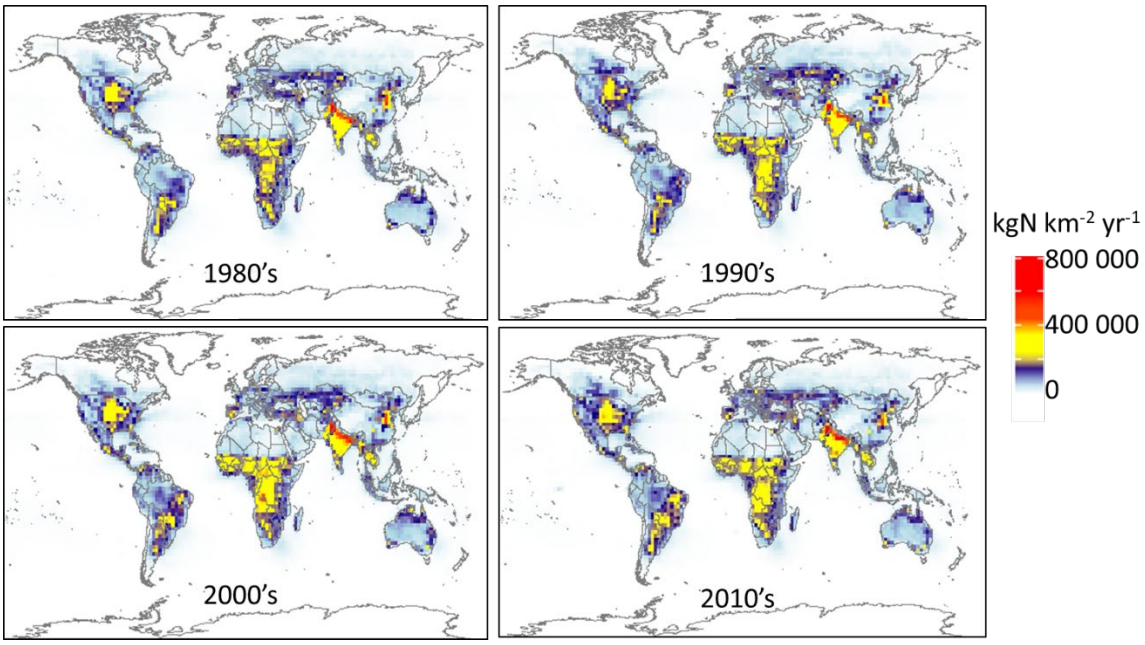

Figure S3.8. Mean annual nitrogen emissions from soils (natural and agricultural) simulated for each decade.

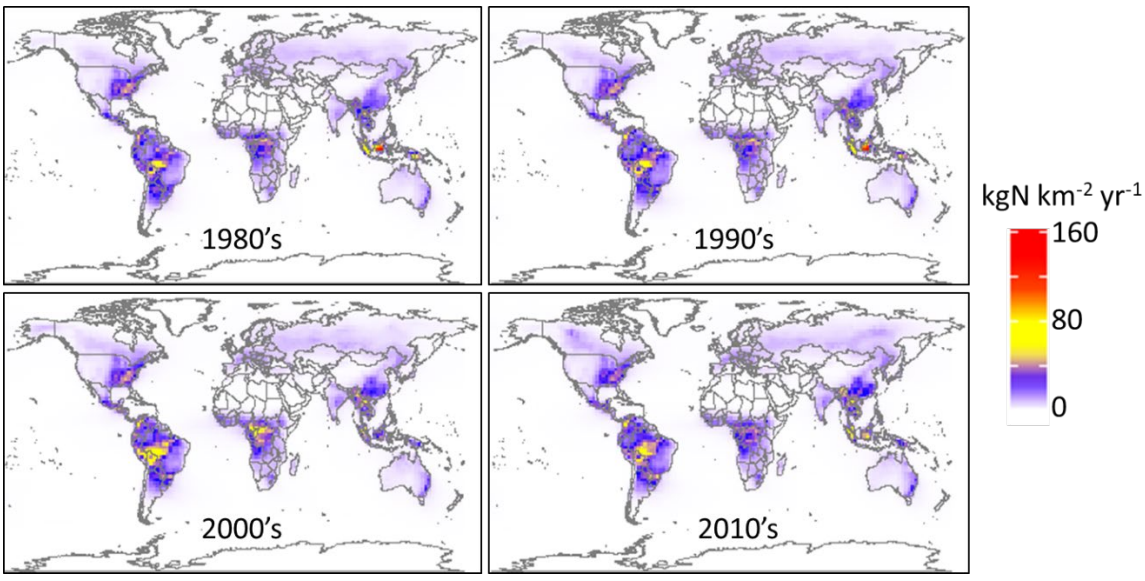

Figure S3.9. Mean annual deposition of nitrogen in organic compounds, as simulated for each decade. Compounds included in the simulation are propanone nitrate, isoprene hydroxynitrate,

methyl vinyl ketone + methacrolein nitrates, ≥C4 alkylnitrates, methyl peroxy nitrate, peroxyacetylnitrate, peroxypropionylnitrate, and peroxymethacryloyl nitrate.

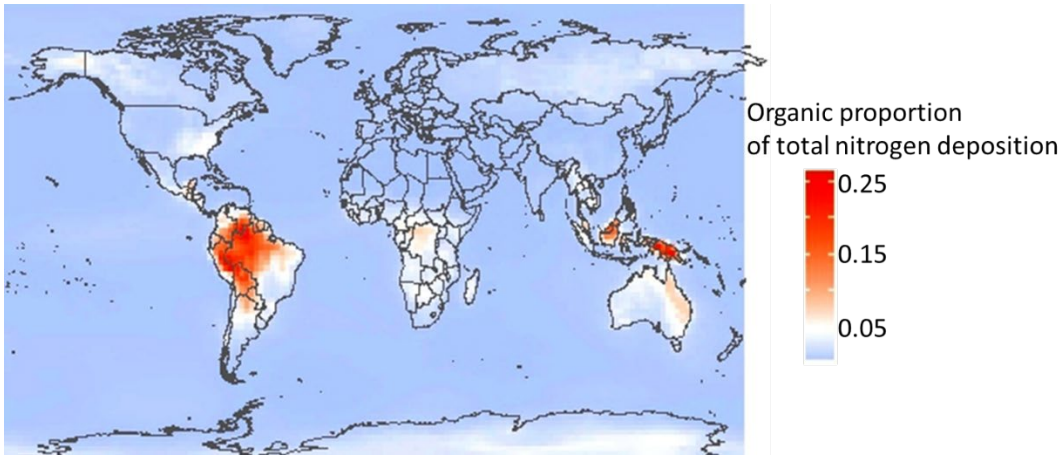

Figure S3.10. Organic nitrogen deposition as a proportion of total nitrogen deposition, as simulated for 2016. These values represent lower-bound estimates, as some nitrogen-containing organic compounds, such as amino acids and urea, are not represented in the GEOS-Chem simulations.

Appendix 3

Chapter 4 Supplemental Material

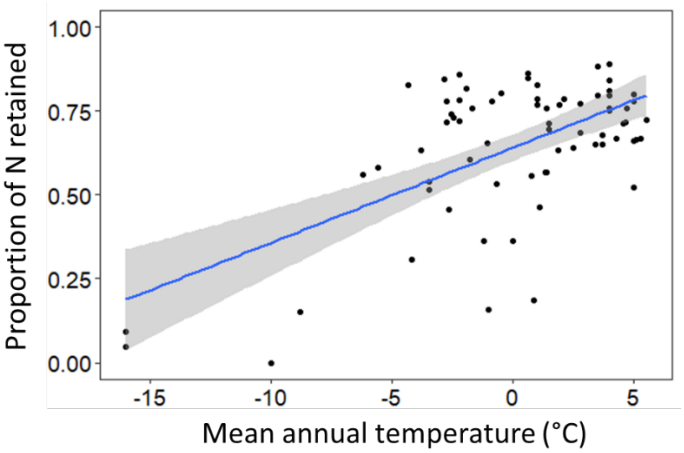

Figure S4.1. Relationship between proportion of N retained and mean annual temperature for watershed with positive net nitrogen retention value. This figure is a subset of figure 3, here detailing only watersheds with proportions of N retained greater than 0.

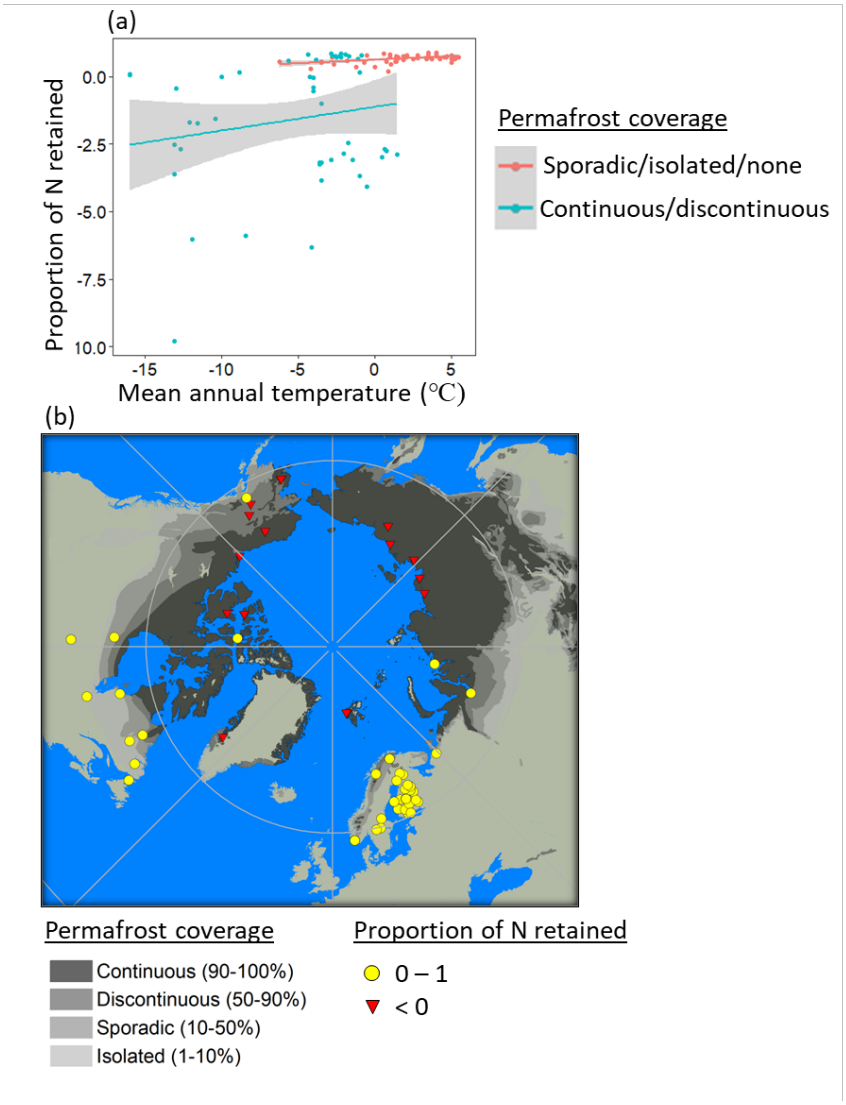

Figure S4.2. (a) Relationship between mean annual temperature and proportional N retention by permafrost coverage. Watersheds with greater permafrost coverage (continuous/discontinuous) generally retained less nitrogen. Further, temperature explained less of the variability in retention for these watersheds. (b) Map of N export measurement sites, color coded with positive versus negative retention values. Watersheds with negative retention values tended to be further north and have greater permafrost coverage.

Table S4.1. Dataset for analyzing nitrogen retention is attached as "Table S4.1.csv". Metadata and references are below.

Table S4.1 metadata.

Variable name	Description	Units (for numerical variables)
Site	Site name, as indicated in the primary literature	
Location	General location of site	
Basin_type	Categorical indicator (boreal, tundra, or glacial)	
Latitude	Latitude at site of nitrogen export measurement for each watershed	decimal degrees
Longitude	Longitude at site of nitrogen export measurement for each watershed	decimal degrees
Period	Temporal period over which quantitative variables are measured and averaged on an annual basis	Years (c.e.)
Mean_annual_temperature_C	Mean annual surface air temperature in watershed. From Matsuura and Willmott (2015a)	Degrees celcius
N_retention	Absolute area-normalized annual watershed nitrogen retention calculated as: (N_deposition) - (N_export)	kgN km^{-2} yr^{-1}
N_export	Annual area-normalized export of total nitrogen from watershed, measured at stream outlet	kgN km^{-2} yr^{-1}
N_deposition	Annual area-normalized atmospheric deposition of inorganic nitrogen in watershed. From Ackerman *et al*. 2018	kgN km^{-2} yr^{-1}
Runoff_mm	Annual watershed runoff	mm^2
Watershed_area_km2	Area of watershed	km^2
Permafrost_presence	Binary indicator of presence/absence of permafrost within watershed. From Brown *et al*. (2002)	
Permafrost_extent	Categorical indicator of permafrost extent within watershed. From Brown *et al*. (2002)	
Topsoil_organic_carbon_percent_weight	Organic carbon content for top 30 cm of soil (from Wieder *et al*. 2014)	% weight
Reference	Original source for nitrogen export data and watershed description. Full citation available in Supplemental Information file.	

Table S4.1 references:

Clair, T. A., Pollock, T. L., & Ehrman, J. M. (1994). Exports of carbon and nitrogen from river basins in Canada's Atlantic Provinces. *Global Biogeochemical Cycles*, *8*(4), 441-450.

Clair, T. A., Dennis, I. F., & Bélanger, S. (2013). Riverine nitrogen and carbon exports from the Canadian landmass to estuaries. *Biogeochemistry*, *115*(1-3), 195-211.

De March, L. (1975). Nutrient budgets for a high arctic lake (Char Lake, NWT) With 3 figures and 3 tables in the text. *Internationale Vereinigung für theoretische und angewandte Limnologie: Verhandlungen*, *19*(1), 496-503.

Dittmar, T., & Kattner, G. (2003). The biogeochemistry of the river and shelf ecosystem of the Arctic Ocean: a review. *Marine chemistry*, *83*(3-4), 103-120.

Fölster, J. (2000). The near-stream zone is a source of nitrogen in a Swedish forested catchment. *Journal of environmental quality*, *29*(3), 883-893.

Hodson, A. J., Mumford, P. N., Kohler, J., & Wynn, P. M. (2005). The High Arctic glacial ecosystem: new insights from nutrient budgets. *Biogeochemistry*, *72*(2), 233-256.

Kaste, Ø., & Skjelkvåle, B. L. (2002). Nitrogen dynamics in runoff from two small heathland catchments representing opposite extremes with respect to climate and N deposition in Norway. *Hydrology and Earth System Sciences Discussions*, *6*(3), 351-362.

Kortelainen, P., Saukkonen, S., & Mattsson, T. (1997). Leaching of nitrogen from forested catchments in Finland. *Global Biogeochemical Cycles*, *11*(4), 627-638.

Lafrenière, Melissa J., Nicole L. Louiseize, and Scott F. Lamoureux. "Active layer slope disturbances affect seasonality and composition of dissolved nitrogen export from High Arctic headwater catchments." *Arctic Science* 3.2 (2017): 429-450.

Lepistö, A., Andersson, L., Arheimer, B., & Sundblad, K. (1995). Influence of catchment characteristics, forestry activities and deposition on nitrogen export from small forested catchments. *Water, Air, and Soil Pollution*, *84*(1-2), 81-102.

Likens, G. E., Bormann, F. H., Pierce, R. S., Eaton, J. S., & Johnson, N. M. (1977). The Northern Hardwood Ecosystem at Hubbard Brook in Relation to Other Forested Ecosystems in the World. In *Biogeochemistry of a Forested Ecosystem* (pp. 103-112). Springer, New York, NY.

Lundin, L., (1994). *Impacts of forest drainage on flow regime.* Technical Report. Uppsala. Sveriges lantbruksuniversitet. Studia forestalia Suecica ; 192.

MacLean, R., Oswood, M. W., Irons, J. G., & McDowell, W. H. (1999). The effect of permafrost on stream biogeochemistry: a case study of two streams in the Alaskan (USA) taiga. *Biogeochemistry*, *47*(3), 239-267.

Mattsson, T., Finér, L., Kortelainen, P., & Sallantaus, T. (2003). Brook water quality and background leaching from unmanaged forested catchments in Finland. *Water, Air, and Soil Pollution*, *147*(1-4), 275-298.

Peterson, B. J., Hobbie, J. E., & Corliss, T. L. (1986). Carbon flow in a tundra stream ecosystem. *Canadian Journal of Fisheries and Aquatic Sciences*, *43*(6), 1259-1270.

Petrone, K. C., Jones, J. B., Hinzman, L. D., & Boone, R. D. (2006). Seasonal export of carbon, nitrogen, and major solutes from Alaskan catchments with discontinuous permafrost. *Journal of Geophysical Research: Biogeosciences*, *111*(G2).

Stottlemyer, R. (1992). Nitrogen mineralization and streamwater chemistry, Rock Creek watershed, Denali National Park, Alaska, USA. *Arctic and Alpine Research*, *24*(4), 291-303.

USGS National Water Quality Assessment Program. <https://water.usgs.gov/nawqa/>. Accessed 1 June 2017.

Wadham, J. L., Hawkings, J., Telling, J., Chandler, D., Alcock, J., Lawson, E., ... & Nienow, P. (2016). Sources, cycling and export of nitrogen on the Greenland Ice Sheet. *Biogeosciences Discussions*.

Table S4.2. Fixed effects coefficients for model of area-normalized nitrogen export. Annual runoff and a second-order coefficient for nitrogen deposition were the only factors significantly associated with export at the alpha = 0.05 level. Site was included as a random effect.

Parameter	Estimate	Standard Error	p-value
Intercept	226.688	81.110	0.007
Mean annual temperature (°C)	2.639	2.882	0.378
N deposition (kgN km^{-2} yr^{-1})	-0.474	0.240	0.072
N deposition^2	0.0004	0.0002	0.036
Annual runoff (mm)	0.058	0.024	0.033
Topsoil organic carbon content (%)	-0.15	1.551	0.920
Permafrost extent_Discontinuous	-76.374	65.564	0.249

Table S4.3. Nitrogen retention in watersheds with net nitrogen export

Of the 98 combinations of watershed and year in our overall dataset (table S1), 28 cases showed net nitrogen export, rather than retention (i.e. annual stream export of total N exceeded atmospheric inputs to the watershed). All 28 such cases were in regions of continuous or discontinuous permafrost extent. Linear mixed effects modeling (below) revealed no significant effect of mean annual temperature or permafrost extent on area-normalized nitrogen retention in these watersheds.

Parameter	Estimate	Standard Error	p-value
Intercept	-5.55	5.37	0.32
Mean annual temperature (°C)	-0.003	0.444	0.99
Permafrost extent_Discontinuous	2.57	4.47	0.56

Table S4.4. Representative rate measurements of nitrogen processes on an annual, per-area basis. Units for all three processes (N fixation, denitrification, and N deposition) have been converted to kgN km^{-2} yr^{-1}. Value ranges represent spatial variation of the measured rate within the described location.

Process	Rate	Location	Reference
N fixation	25-30	Canadian high arctic tundra	Chapin *et al*. 1991
	80 - 131	Alaskan low arctic tundra	Shaver *et al*. 2014
	25-350	Swedish boreal forest	DeLuca *et al*. 2008
	110	Frost-heave circles in Northern Sweden	Sorensen *et al*. 2018

	25	Heath vegetation Northern Sweden	Sorensen *et al*. 2018
	88	Moss bed in Northern Sweden	Sorensen *et al*. 2018
	20-200	Tundra-wide biome estimate	Stewart *et al*. 2014
	7 - 380	Alaskan high arctic tundra	Gersper *et al*. 1980, Robinson & Wookey 1997
	136 - 349	Northern Finland sub-arctic tundra	Robinson & Wookey 1997
Denitrification	2.4 - 3.4	Alaskan high arctic	Barsdate and Alexander 1975, Gersper *et al*. 1980
	100-200	Alaskan low arctic (potential rates, unlikely to occur under field conditions)	Shaver *et al*. 2014
N deposition	14 - 64	Alaskan low arctic tundra	Shaver *et al*. 2014
	200	Icelandic post-glacial lavafield	Jónsdóttir *et al*. 1995
	4 - 35	Alaskan alpine tundra	Vet *et al*. 2014
	26-37	Swedish subarctic alpine tundra	Bergstrom *et al*. 2013
	40 - 110	Swedish boreal forest	DeLuca *et al*. 2008

Table S4.4 references

Barsdate, R. J., & Alexander, V. (1975). The Nitrogen Balance of Arctic Tundra: Pathways, Rates, and Environmental Implications 1. *Journal of Environmental Quality*, *4*(1), 111-117.

Bergström, A. K., Faithfull, C., Karlsson, D., & Karlsson, J. (2013). Nitrogen deposition and warming–effects on phytoplankton nutrient limitation in subarctic lakes. *Global Change Biology*, *19*(8), 2557-2568.

Chapin, David M., L. C. Bliss, and L. J. Bledsoe. "Environmental regulation of nitrogen fixation in a high arctic lowland ecosystem." *Canadian Journal of Botany* 69.12 (1991): 2744-2755.

DeLuca, T. H., Zackrisson, O., Gundale, M. J., & Nilsson, M. C. (2008). Ecosystem feedbacks and nitrogen fixation in boreal forests. *Science*, *320*(5880), 1181-1181.

Gersper, P. L., Alexander, V., Barkley, S. A., Barsdate, R. J., & Flint, P. S. (1980). The soils and their nutrients. *An Arctic Ecosystem: The Coastal Tundra at Barrow, Alaska*, *12*.

Jónsdóttir, I. S., Callaghan, T. V., & Lee, J. A. (1995). Fate of added nitrogen in a moss-sedge Arctic community and effects of increased nitrogen deposition. *Science of the Total Environment*, *160*, 677-685.

Robinson, C. H., & Wookey, P. A. (1997). Microbial ecology, decomposition and nutrient cycling. *Ecology of Arctic Environments, ed. S. J. Woodin and Mick Marquiss, 41-68.*

Shaver, G. R., Laundre, J. A., Bret-Harte, M. S., Chapin, F. S., Mercado-Dıaz, J. A., Giblin, A. E., ... & Gould, W. A. (2014). Terrestrial ecosystems at toolik Lake, Alaska. *Alaska's changing Arctic: Ecological consequences for tundra, streams, and lakes, ed. JE Hobbie, and GW Kling*, 90-142.

Stewart, K. J., Grogan, P., Coxson, D. S., & Siciliano, S. D. (2014). Topography as a key factor driving atmospheric nitrogen exchanges in arctic terrestrial ecosystems. *Soil Biology and Biochemistry*, *70*, 96-112.

Sorensen, P. L., Jonasson, S., & Michelsen, A. (2006). Nitrogen fixation, denitrification, and ecosystem nitrogen pools in relation to vegetation development in the subarctic. *Arctic, Antarctic, and Alpine Research*, *38*(2), 263-272.

Vet, R., Artz, R. S., Carou, S., Shaw, M., Ro, C. U., Aas, W., ... & Hou, A. (2014). A global assessment of precipitation chemistry and deposition of sulfur, nitrogen, sea salt, base cations, organic acids, acidity and pH, and phosphorus. *Atmospheric Environment*, *93*, 3-100.